Contributions on Hybrid Localization Techniques For Heterogeneous Wireless Networks

Mohamed Laaraiedh

N° d'ordre : 4264 ANNÉE 2010

THÈSE / UNIVERSITÉ DE RENNES 1
sous le sceau de l'Université Européenne de Bretagne

pour le grade de

DOCTEUR DE L'UNIVERSITÉ DE RENNES 1

Mention : Traitement du Signal et Télécommunications

Ecole doctorale (MATISSE)

présentée par

Mohamed LAARAIEDH

préparée à l'unité de recherche (IETR-CPR)
(Institut d'Electronique et de Télécommunications de Rennes)
(Communication, Propagation, et Radar)

Contributions on Hybrid Localization Techniques For Heterogeneous Wireless Networks

Thèse soutenue à Rennes le 15 Décembre 2010

devant le jury composé de :

Mérouane DEBBAH
Professeur, Supélec / président

Dirk SLOCK
Professeur, Eurecom / rapporteur

Philippe BONNIFAIT
Professeur, Université de Technologie de Compiègne / rapporteur

Benoît DENIS
Docteur, CEA-Leti / examinateur

Bernard UGUEN
Professeur, Université de Rennes 1 / directeur de thèse

Stéphane AVRILLON
Maître de conférence, Université de Rennes 1 / co-directeur de thèse

PH.D Thesis

Contributions on Hybrid Localization Techniques For Heterogeneous Wireless Networks

Mohamed Laaraiedh

December 2010

Mohamed Laaraiedh

Contributions on Hybrid Localization Techniques For Heterogeneous Wireless Networks

This Ph.D. thesis was defended December 15, 2010, at University of Rennes 1.

Assessment Committee:

Prof. Mérouane DEBBAH, SUPELEC, Gif-Sur-Yvette, France
Prof. Dirck SLOCK, EURECOM, Nice, France
Prof. Philippe BONNIFAIT, UTC, Compiègne, France
PH.D. Ing. Benoît DENIS, CEA LETI, Grenoble, France

Supervisors:

Prof. Bernard UGUEN, IETR-UR1, Rennes, France
PH.D. Stéphane AVRILLON, IETR-UR1, Rennes, France

Manuscript written in LATEX

Abstract

Recent advancement in wireless networks and systems has seen the rise of localization techniques as a worthwhile and cost-effective basis for novel services. These location based services (LBSs) have been more and more beneficial and money-making for telecommunications operators and companies. Various LBSs can be offered to the user such as tracking, advertisement, security, and management. Wireless networks themselves may benefit from localization information to enhance the performances of the different network layers. Location based routing, synchronization, interference cancellation are some examples of fields where location information can be fruitful. Two main tasks a localization system must be able to do: measurement of location-dependent parameters (LDPs) (e.g. time of arrival -TOA-, time difference of arrival -TDOA-, and received signal strength indicator -RSSI-) and estimation of position using location estimation techniques. The main goal of this dissertation is the study of different location estimation techniques. Estimation and measurement of LDPs are also investigated using a provided measurements campaign in order to have a complete understanding of localization field.

Two types of location estimation techniques are addressed. The first one is based on algebraic formulation of LDPs and the second is based on the representation of LDPs in the form of geometric constraints and it is called Robust Geometric Positioning Algorithm (RGPA). Studied algebraic techniques are least-squares (LS), Maximum likelihood (ML), and Semidefinite programming (SDP). All of these techniques are developed and compared for both non-hybrid and hybrid localization schemes. Non-hybrid localization schemes are schemes which involve one type of LDPs (i.e. RSSI, TOA, or TDOA) while hybrid schemes are schemes which fuse more than one type of LDPs (i.e. RSSI+TOA, RSSI+TDOA, TOA+TDOA, and RSSI+TOA+TDOA). In addition to the comparison between the different studied algorithms, the focus is put on the importance of fusing hybrid LDPs. The dissertation proves that positioning accuracy is not only factor of involved LDPs and their precision but also factor of the used location estimation technique. Indeed, the proposed RGPA technique outperforms all algebraic methods and the ML technique is the most accurate algebraic technique. Besides, the dissertation recommends to use all available RSSIs and added necessary time-based LDPs in order to reach the requested positioning accuracy with minimum resources.

The Cramer Rao lower bound (CRLB) and the geometric dilution of precision (GDOP) are developed for all localization schemes in order to assess theoretical reachable positioning accuracies and to evaluate the effect of different radio parameters on these performances. While the GDOP is factor only of geometric configuration of the targeted device with respect to anchors, the CRLB present a weighted version of

GDOP with the involved LDPs precisions as weights. These two terms can be used as criteria for choosing LDPs and positions of associated anchors before carrying out the location estimation task itself. A proof of this suggestion is given for the (RSSI+TOA) and (RSSI+TDOA) schemes. Additional time-based LDPs and position of associated anchors must be carefully and smartly chosen based on CRLB in order to get better positioning accuracy when fused with RSSI.

In order to make the comparison between the different studied techniques and schemes as realistic as possible, statistical models of different studied LDPs are developed using a provided ultra wide-band (UWB) measurements campaign. The different necessary LDPs are extracted from these measurements based on channel impulse responses (CIR). Giving the high time precision of UWB signals, two different techniques of CIR-based TOA ranging are studied and different associated thresholds are defined and compared. These thresholds represent the quality of the radio link since they are constructed using energies carried by the whole CIR and the strongest path respectively. Then, RSSI is modeled using log normal shadowing model. Based on this model, RSSI-based ranging techniques are proposed and compared. Besides, defining a RSSI model per anchor gives better ranging accuracy. At the end of this part, a statistical model is defined for each LDP. These models are used within a generic hybrid scenario defined in order to evaluate different localization techniques and schemes.

Acknowledgments

This thesis is the result of 32 months (2 years and 8 months) of work on localization techniques in the framework of the FP7 European project ***WHERE***. On March 1^{st} 2008, I have been recruited by Professor **Bernard Uguen** and lecturer **Stéphane Avrillon** as an engineer and PH.D student in the **University of Rennes I** in the north western France in the nice Brittany. My office was in **IETR labs** where many researchers and students from various fields and various institutes are carrying out projects and researches. Respecting the definition of the *WHERE* project and the scientific background of the CPR group we have, me and my supervisors, defined the main objectives of the work and the adventure has started...

During these 32 months, a factor that made my work easier is the worm and friendly ambiance which characterized not only the office where I worked but also the academic and administrative staff of IETR. For this, I want to warmly thank professor **Bernard Uguen** and lecturer **Stéphane Avrillon** for accepting to supervise my work, for their hospitality, and for their help. I was extremely lucky cause I got very enthusiastic and serious supervisors. I want also to thank madam **Noelle Le Ber** the secretary of the CPR group not only for her help in administration issues but also for her encouragement. I would like to address many thanks also to my colleagues in the office: **Roxana**, **Nicolas**, **Lei**, and **Moussa**.

Working within an European project was very constructive for me. In fact, meetings, teleconferences, deliverables, and even e-mails were very interesting moments to discuss with high-skilled experts. These discussions helped me to criticize my work and then to improve my understanding of things. That is, I want to warmly thank **Ronald Raulefs** the coordinator of ***WHERE*** and all others participants in the project.

The nicest event during my thesis was my wedding after which I got a new breath. I'd like to address many thanks to my wife for her help and moral support. So thank you **Sana**. A special greeting to my mother, my father, and my sisters for all time we spent together. I'd like also to thank all my uncles, aunts, and cousins. A very special kisses on the cheeks of my nephew **Ali** and my niece **Ala** with whom I spent funny moments.

To
My Mother
My Father
My Wife
My Sisters
Ali and Ala

Vitae and List of Publications

Vitae

- November, 05, 1983: Born, Medenine, Tunisia.
- 2002: Bachelor Degree, Mathematics, Technical School of Medenine, Tunisia.
- 2002-2004: B.S. Mathematics and Physics, Engineering Preparatory Institute of Tunis, Tunisia.
- 2004-2007: Engineer degree, Telecommunications, SupCom, Tunis, Tunisia.
- 2006-2008: Master degree, Telecommunications, SupCom, Tunis, Tunisia and University of Poitiers, France.
- 2008-2010: Engineer and PH.D. Student, Signal Processing and Telecommunications, University of Rennes 1, IETR Labs, Rennes, France.

Journals

- M. Laaraiedh, S. Avrillon, and B. Uguen, *A Maximum Likelihood TOA Based Estimator For Localization in Heterogeneous Networks*, International Journal on Communication, Network and System Sciences (IJCNS), Jan 2010, Volume 3, N°1.
- M. Laaraiedh, *Implementation of Kalman Filter with Python Language*, Python Papers Journal, Vol 4, N°2(2009).

Conferences

- M. Laaraiedh, S. Avrillon, and B. Uguen, *Hybrid Data Fusion Techniques for Localization in UWB Networks*, In Proceedings WPNC'09 Hanover, Germany, March 2009.
- M. Laaraiedh, S. Avrillon, and B. Uguen, *Enhancing Positioning Accuracy through Direct Position Estimators based on Hybrid RSS Data Fusion*, RAS Workshop, IEEE VTC SPRING, Barcelona, Spain, April, 2009.

- S. Sand, C. Mensing, M. Laaraiedh, B. Uguen, B. Denis, S. Mayrargue, M. Garca, J. Casajs, D. Slock, T. Pedersen, X. Yin, G. Steinboeck, and B. H. Fleury, *Performance Assessment of Hybrid Data Fusion and Tracking Algorithms*, ICT Mobile Summit (ICT Summit 2009), Santander, Spain, June 2009.

- M. Laaraiedh, S.Avrillon, and B.Uguen *Enhancing positioning accuracy through RSS based ranging and weighted least square approximation*, POCA conference, Antwerp, Belgium, May, 2009.

- M. Laaraiedh, S. Avrillon, and B. Uguen, *Exploiting The Imperfect Knowledge of Reference Nodes Positions In Range Based Positioning Systems*, International Conference on Signals, Circuits & Systems (SCS09), Djerba (Tunisia), Nov 6-8 th 2009.

- M. Laaraiedh, S. Avrillon, and B.Uguen, *Overcoming Singularities In TDoA Based Location Estimation Using Total Least Square*, International Conference on Signals, Circuits & Systems (SCS09), Djerba (Tunisia), Nov 6-8 th 2009.

- C. Mensing, S. Sand, J.J. Nielsen, B. Denis, M. Maman, J. Rodriguez, S. Hadzic, J. Bastos, Z.M. He, Y. Ma, S. Zazo, V. savic, I. Arambasic, M. Laaraiedh, and B. Uguen, *Performance Assessment of Cooperative Positioning Techniques*, In Proceedings of Future Networks and Mobile Summit 2010, Florence, Italy, June 2010.

- C. Mannweiler, R. Raulefs, J. Schneider, B. Denis, A. Klein, B. Uguen, M. Laaraiedh, and H. Schotten, *A Robust Management Platform for Multi-Sensor Location Data Interpretation*, Future Networks and Mobile Summit 2010, Florence, Italy, June 2010.

WHERE Project Deliverables

- *Survey on localisation in communication networks*, D6.2, October 2008.

- *Estimation of location-dependent channel information (Preliminary Report)*, D4.4, January 2009

- *Performance assessment of hybrid data fusion and tracking algorithms*, D2.1, Dec 2008.

- *Cooperative positioning (intermediate report)*, D2.2, March 2009.

- *Fusion of Ray tracing and channel measurements*, D4.2, April 2010

- *Final report on WHERE hybrid localisation techniques*, D2.3, May 2010.

- *Performance of WHERE cooperative positioning techniques*, D2.4, May 2010.

- *Estimation of location-dependent channel information (Final Report)*, D4.6, May 2010

Presentations

- M. Laaraiedh, B. Uguen, S. Avrillon, *Advanced Techniques of Localization: Application to 3G/4G Networks and Ray Tracing Tools*, NEWCOM++ Summer School, 30-th June to 4-th July 2008, Bressanone, Italy

Supervised Projects

- A. Cheikhrouhou, L. Ben Taher, *Monitoring of RSSI in a Zigbee network for localization purposes*, Master II project, IFSIC, University of Rennes 1, 2010.
- H. Harrath, *Development of a pocket pc application to monitor RSSI in GSM, WiFi, and Bluetooth networks*, Master II project, ETSI, Tunis, Tunisia, 2010.

Contents

List of Acronyms

The following list is neither exhaustive nor exclusive, but may be helpful.

ACK	ACKnowledgment
(A)CRLB	(Average) Cramer-Rao Lower Bound
AN	Anchor Node
AOA	Angle Of Arrival
AP	Access Point
AWGN	Additive White Gaussian Noise
BPSK	Binary Phase Shift Keying
BS	Base Station
CDF	Cumulative Density Function
CDMA	Code Division Multiple Access
CIR	Channel Impulse Response
CNSS	Compass Navigation Satellite System
CLA	Constraint Layer Array
CRLB	Cramer-Rao Lower Bound
CW	Constraint Widening
DOA	Direction Of Arrival
DoD	Department of Defense
EKF	Extended Kalman Filter
ESA	European Space Agency
FI(M)	Fisher Information (Matrix)
GDOP	Geometric Dilution Of Precision

GIS	Geographic Information System
GLONASS	GLObalnaya NAvigatsionnaya Sputnikovaya Sistema
GNSS	Global Navigation Satellite Systems
GPL	General Path Loss
GPS	Global Positioning System
HDF	Hybrid Data Fusion
ICT	Information and Communication Technologies
IRNSS	Indian Regional Navigation Satellite System
KF	Kalman Filter
LBS	Location Based Service
LCS	LoCation Service
LDP(I)	Location Dependent Parameter (Information)
LMI	Linear Matrix Inequality
LoB	Line-of-Bearing
LQI	Link Quality Indicator
MAC	Medium Access Control
MEO	Medium Earth Orbit
MIMO	Mimo-Input Mimo-Output
ML	Maximum Likelihood
MS	Mobile Station
MSE	Mean Square Error
MUI	Multi-User Interferences
MVUE	Minimum Variance Unbiased Estimator
NAVSTAR	NAVigation System for Timing And Ranging
(N)LOS	(Non) Line of Sight
OCS	Operational Control Segment
OWR	One Way Ranging
PF	Positioning Accuracy

PDA	Personnel Digital Assistant
PF	Particle Filter
PL	Path Loss
pdf	probability distribution function
PHR	Physical layer HeadeR
PPS	Precise Position Service
PVT	Position, Velocity, and Time
QZSS	Quasi-Zenith Satellite System
RAT	Radio Access Technology
RDSS	Radio Determination Satellite Service
RGPA	Robust Geometric Positioning Algorithm
RNSS	Regional Navigation Satellite Systems
RPL	Anchor Path Loss
RSS(I)	Radio-Signal-Strength (Indicator)
RTT	Round-Trip Time
Rx	Receiver
SDMA	Space Division Multiple Access
SDP	Semi-Definite Programming
SFD	Start of Frame Delimiter
SHR	Synchronization HeadeR
SIVIA	Set Inversion Via Interval Analysis
SNR	Signal to Noise Ratio
SPS	Standard Position Service
SS	Space Segment
STBC	Space Time Bloc Code
STD	STandard Deviation
SVD	Singular Value Decomposition
(T)LS	(Total) Least-Squares

TOA	Time Of Arrival
TDOA	Time Difference Of Arrival
(T)WLS	(Total) Weighted Least-Squares
Tx	Transceiver/Transmitter
TWR	Two Way Ranging
UKF	Unscented Kalman Filter
US	User Segment
UWB	Ultra Wide Band
WGS	World Geodetic System
WLAN	Wireless Local Access Network
WMAN	Wireless Metropolitan Access Network
WSN	Wireless Sensor Network

List of Symbols

The following list is neither exhaustive nor exclusive, but may be helpful.

General Notations

'a', 'b', 'c', ...	Scalars and variables
'a', 'b', 'c', ...	Vectors
'A', 'B', 'C', ...	Matrices
$\|a\|$	Absolute value of a
$\hat{a}$	Estimate of a
max, min	Maximum and Minimum
$argmax$(f)	Argument that maximizes the function f
$argmin$(f)	Argument that minimizes the function f
$\sim$	Distributed according to
$\bigotimes$	Cartesian product
$\bigcap$	Intersection
$\mathbb{R}$	The set of real numbers
$\mathbb{R}^{n \times m}$	The set of $n \times m$ real matrices
log	Natural logarithm
$\log_{10}$	Common logarithm

Matrices and Vectors

$\mathbf{A^T}$, $\mathbf{a^T}$	Transpose of the matrix **A** or vector **a**
$\mathbf{A^{-1}}$	Inverse of **A**
$\|\mathbf{a}\|_\mathbf{2}$	Euclidean norm of **a**
$\|\mathbf{A}\|$	Frobenius norm of **A**

$\mathrm{tr}(\mathbf{A})$	Trace of $\mathbf{A}$
$\kappa(\mathbf{A})$	Condition number of $\mathbf{A}$
$\kappa_{lim}(\mathbf{A})$	Condition number threshold of $\mathbf{A}$
$\mathbf{A} = \mathrm{diag}(\mathbf{a})$	Diagonal matrix with entries of vector $\mathbf{a}$ along its main diagonal.
$\mathbf{A} \succeq \mathbf{0}$	$\mathbf{A}$ symmetric positive semidefinite
$\mathbf{A_{ldp}}$, $\mathbf{C_{ldp}}$, $\mathbf{b_{ldp}}$	Least-squares matrices and vector with ldp=RSSI, TOA, TDOA, and HDF

Functions and Random variables

$c(t)$	Impulse response of a multipath channel
$r(t)$	Received signal
$n(t)$	Additive white Gaussian noise
$\delta(t)$	Dirac delta function (pulse)
$\omega(t)$	Isolated ideal received pulse
L	Path loss
$\bar{L}$	Mean Path loss
X_{sh}	Shadowing Gaussian random variable

Scalar Parameters

K	Number of anchor devices or LDP
p	Number of RSSIs
$q - p$	Number of TOAs
$K - q - 1$	Number of TDOAs
L	Length of simulated area
c	Speed of light
λ	Wavelength
β	Effective signal bandwidth
f_c	Carrier Frequency
a_n	Amplitude of n^{th} path

τ_n	time delay of n^{th} path
T	Signal Duration
T_p	Pulse Duration
T_s	Sample Duration
N_0	Noise spectral density
$E_r(\tau)$	Cumulative energy at time τ of the received signal $r(t)$
$E_c(\tau)$	Cumulative energy at time τ of the impulse response $c(t)$
$E_n(\tau)$	Cumulative energy at time τ of the noise component $n(t)$
E_T	Energy carried by the CIR
E_M	Energy carried by the strongest path
E_{0-M}	Cumulative energy carried until the strongest path
τ_0	Real time of arrival
γ_{th}	Threshold for thresholding ranging technique
γ_{cum}	Threshold for cumulative thresholding ranging technique
κ_{th}	Unit-less constant for thresholding ranging technique
κ_{cum}	Unit-less constant for cumulative thresholding ranging technique
$R_{1,2}$	Correlation between two signals
P_r	Received Power
P_t	Transmitted Power
G_r	Rx antenna gain
G_t	Tx antenna gain
n_p	Propagation constant
d_0	RSSI reference distance
$\sigma_{sh\,k}$	Standard deviation of shadowing
S_k, M_k	RSSI parameters

Location-dependent parameters

τ_{stg}	TOA of the strongest path
τ_{th}	TOA obtained with thresholding technique
τ_{cum}	TOA obtained with cumulative thresholding technique
τ_k	TOA between the MS and the k^{th} anchor
σ_k	Standard deviation of measured TOA between the MS and the k^{th} anchor
d_k	True distance between the MS and the k^{th} anchor
P_k	Measured power (RSSI) between the MS and the k^{th} anchor
P_0	Measured power (RSSI) at $d = 0$
r_k	RSSI based range between the MS and the k^{th} anchor
σ_k	Standard deviation of RSSI based range between the MS and the k^{th} anchor
$\hat{d}_{est}$	Estimated Distance between the MS and the k^{th} anchor using different RSSI ranging techniques (est= mean, median, or mode)
τ_{kl}	TDOA between the MS and the k^{th} anchor with reference to the l^{th} anchor
σ_{kl}	Standard Deviation of measured TDOA between the MS and the k^{th} anchor with reference to the l^{th} anchor
d_{kl}	True distance difference between the MS and the k^{th} anchor with reference to the l^{th} anchor

Intervals and Boxes

$\underline{x}$, $\overline{x}$	endpoints of the interval $[x]$
$\mathbb{S}_k$	Feasible set of the k^{th} constraint, $[\mathbb{S}_k]$ the associated box
$\mathbb{S}$	Feasible set of the localization problem, $[\mathbb{S}]$ the associated box

List of Figures

List of Tables

1 Introduction

Security, emergency, management, and entertainment are some, but not all, of fields where the location information is being more and more demanded. Nowadays, most of fields use location information in order to perform tasks and to offer valued services. Moreover, the location information becomes even requested by telecommunication networks themselves in order to enhance their functionalities and performances. In this context, this dissemination is dedicated to the study of localization techniques within future wireless networks. This work is done in the framework of the FP7 European project WHERE which aims to use location information in order to enhance higher network layers (especially Data-link, Network, and Transport layers).

Although GPS and other GNSS systems have offered up to now localization and navigation services, they can perform localization only if the GPS receiver is in visibility with at least four satellites. In indoor and dense urban environments, this condition is not usually guaranteed. Even if in some countries GPS repeaters are allowed to overcome this problem, the cost of such an approach is still very high and the used repeaters may cause interferences between GPS receivers. In addition to this drawback, the positioning precision offered by GNSS systems is from few meters to some tens of meters. Such a positioning error may not be adequate for many applications and services which request centimetric precision in order to be executed.

Wireless communications are, by any measure, the fastest growing segment of the communications industry. Today's wireless applications like cellular phone services or television broadcast are a part of the day to day life of many people. Wireless communication has evolved immensely from the time it was first implemented. The ease of setting up a wireless network, tetherless communication, and low cost of deployment are some of the key reasons for its popularity. Also, the reliability of wireless communication has improved significantly and is reflected in its application to a wide variety of civilian and military fields. The today's landscape of wireless communications is mainly characterized by the coexistence of different technologies (e.g. Bluetooth, WiFi, Zigbee, UWB, Cellular, WiMax, etc). The widespread implementation of these heterogeneous

wireless networks make wireless localization a service that is available "anytime" and "anywhere".

A device's position is usually estimated by monitoring a location dependent parameter (LDP) such as received signal strength indicator (RSSI), time of arrival (TOA), time difference of arrival (TDOA), etc, from another device whose location is known. The localization is done by computing distances from these LDPs and then applying estimation techniques to find the device's position. Different techniques of estimation are defined such as least-squares, maximum likelihood, and convex optimization. The localization accuracy is mainly factor of the LDP measurement nature and accuracy, the wireless standard, and the estimation technique itself. Since each location based service, before being proposed to users, require a minimal positioning accuracy, the localization system should choose the best standards, the best LDPs, and the best estimators, able to perform accurately the requested service.

The expansion, the heterogeneity, and the coexistence of wireless networks are the motivations make it possible for localization systems to implement novel techniques of localization. These techniques use more than one LDP type (for example RSSI + TOA or RSSI + TDOA) and we call them "Hybrid Localization Techniques". This thesis is a contribution to the study of these hybrid localization techniques. We propose to study two different approaches of these hybrid techniques: algebraic and geometric approaches. Therefore, we organize this manuscript as follows:

Document Overview

After this introduction, the second chapter presents the state of the art on existing localization techniques and systems. A classification of location-based services into user-oriented and network-oriented services is given. The principles techniques of localization are briefly described and most of existing localization systems are presented. The focus is then put on the heterogeneous aspects of existing and future wireless networks and standards. This is the line of research that the present study pursues. This chapter gives, at the end, some aspects of hybrid localization in heterogeneous networks which are more developed in following chapters.

The third chapter treats the techniques of estimation and measurements of location dependent parameters. The focus is put on RSSI, TOA, and TDOA. For each of these LDPs, the existing techniques of measurement are described within various wireless standards and some estimation techniques are proposed and described. The main goal of this chapter is to extract statistical models of LDPs in order to be used in evaluation of the performances of proposed algebraic and geometric hybrid localization techniques. For that, the carried measurements campaign is described and the LDPs database constructed from this campaign is presented. The effects of radio channel on these LDPs are also discussed.

The fourth chapter presents the algebraic localization techniques. Three techniques are investigated: least-squares, maximum-likelihood, and semidefinite programming. For each technique, non-hybrid and hybrid estimation algorithms are presented using RSSI, TOA, and TDOA. The theoretical performances are then assessed using Fisher information matrices, Cramer Rao lower bounds, and geometric dilution of precision. A generic scenario is defined using statistical models extracted in the third chapter. The performances of different studied schemes are evaluated within this scenario. This

chapter shows the importance of the fusion of LDPs in enhancing localization accuracies.

The fifth chapter present a generic localization algorithm based on the exchange of geometric constraints. The LDPs are represented as geometric sets of points and fused together by intersection of these different volumes. The importance of such an algorithm is shown and compared to algebraic techniques using the same scenario defined in the fourth chapter. The proposed algorithm would make the fusion of LDPs easier and faster.

In addition to these four main chapters, the introduction, and the conclusion, four abstracts are put in the end of the dissertation. The first and the second appendixes present two master projects supervised during the thesis during which we have developed two applications to monitor RSSI in GSM, WIFI, Bluetooth, and Zigbee. The two other appendixes detail some calculations which has not been developed in the main body of the dissertation.

2

State of The Art on Localization Services, Techniques, and Systems

As its title shows, this second chapter aims to present the state of the art of the localization services, techniques, and systems. Therefore, two sections of this chapter are dedicated to survey this state of the art. In the first section (2.1), location based services (LBSs) are addressed. First, the definition, a brief history, and the different components of LBSs are given. The knowledge of all the components and infrastructure elements necessary to achieve a LBS is quite important in order to define the most suitable localization technique that can offer this LBS with the required quality. Second, a classification of LBSs into user-oriented and network-oriented services is proposed. For each class of LBSs, different examples are given and discussed.

In the second section (2.2) of this chapter, we address the localization techniques and systems. First of all, we start by reviewing the different architectures currently used to implement localization systems. So, we present centralized versus distributed, satellite versus terrestrial, outdoor versus indoor, and static versus dynamic systems. Second, we present the different localization techniques namely angle-, range-, fingerprinting-, and Bayesian- based techniques. Performances of these different techniques are evaluated based on different metrics which will be defined also in the section 2.2.2.5. Then, two more subsections are dedicated respectively to satellite- and terrestrial- based localization systems where the different past and current systems are briefly presented in order to give the reader a complete vision about the localization landscape.

Finally, a short third section (2.3) is dedicated to introduce our work during this thesis. In this section, we start by presenting the B3G networks which are more and more expanded and implemented as a future communication system which will agglomerate and fuse most of current communication systems. The new challenges the B3G localization systems may face are given and our vision of these future localization systems is presented and argued.

2.1 Location-Based Services

2.1.1 Definition and Components of LBS

Location-based services (LBSs) are services accessible with mobile devices through the mobile network and utilizing the ability to make use of the location of the mobile device [1]. Hence, a service is called location-based if it cannot be performed without the knowledge of the position. The most basic LBS is called location service (LCS) and consists in giving the position or the target of the mobile user and making this location data available for other actors (other users or network). The LBS adds a value to location data provided by the LCS. It uses this knowledge to offer a valued service to the mobile user or to a third party.

From a historical point of view, location-based services are not a new thing which came up with the invention of mobile phones. Espinoza emphasizes, in [2], that position specific information is also transported on one hand in a person-to-person communication by post-it notes and graffiti. On the other hand, methods to locally inform a mass-audience are posters (e.g. of concerts in the town) or simply traffic signs, which submit navigational information.

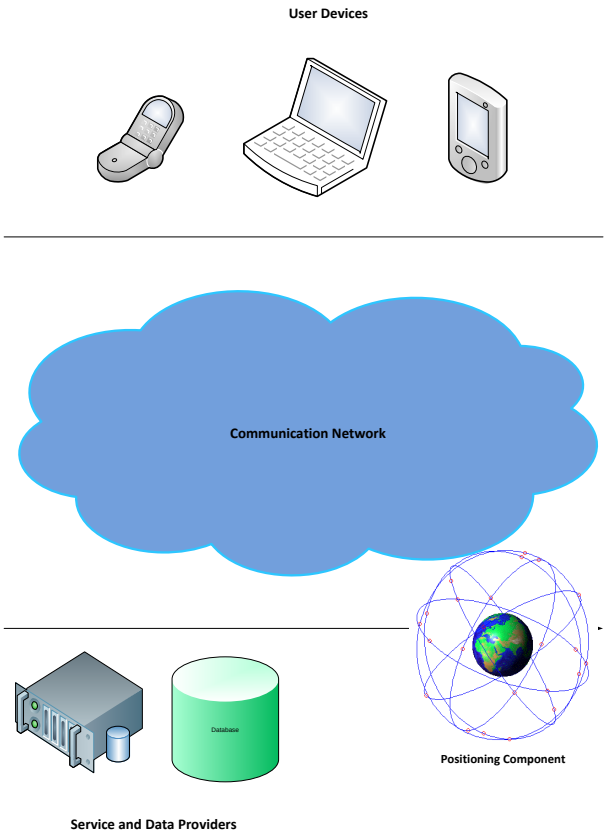

Figure 2.1: Different components of location-based services.

In order to perform a location-based service, different infrastructure elements are necessary. These components are represented in Figure 2.1 and are respectively:

- User device: This is a tool for the user to request and to display the needed information. This information may be a picture, a sound, or a text. Devices can be personal digital assistants (PDAs), mobile phones, laptops, GPS receivers, etc. The position may be determined automatically without the user request.

- Communication network: This component connects the user to the service providers or other users. It transfers user data and requests from user to the providers and the requested data back to the user.

- Positioning component: It includes all the devices involved in the localization process. It can be, for outdoor cases, the mobile network with its fixed base stations (BSs) and mobile stations (MSs) or the global positioning system (GPS). For indoor cases, wireless access points (APs), active badges, and radio beacons may be used to perform positioning.

- Service and application provider: The service provider offers a number of different services to the user and is responsible for the service request processing. Such services offer the calculation of the position, finding a route, searching yellow pages with respect to the position or searching specific information on objects of user interest and so forth.

- Data and content provider: Service providers do usually not store and maintain all the information that can be requested by users. Therefore, geographic-based data and location information data are usually requested from the maintaining authority (e.g. mapping agencies) or business and industry partners (e.g. yellow pages, traffic companies).

2.1.2 User versus Network Oriented LBS

Location-based services can be classified in two different groups: user-oriented LBS (U-LBS) and network-oriented LBS (N-LBS). U-LBS are services which exploit the position of the user in order to give him information about his location or the location of another person or thing. This information may be given in order to assist, guide, and/or inform the user or a third party about the user vicinity and/or his target. N-LBS are services which exploit the location information in order to enhance the performances of the different network layers. These services concern mainly the three first layers: physical layer, data-link layer, and the network layer.

2.1.2.1 User-oriented LBS

We distinguish different types of U-LBS that can be classified in five categories:

1. Emergency and Security

   Emergency and security have been a part of civilization since time began. Such activities have evolved from simple precautions into more sophisticated emergency and security systems including preparedness, response, mitigation, and recovery strategies. Radio, TV, and Internet were been used in the twentieth century to deliver warnings and real time information to people [3]. Over the

past few years, mobile phone messaging systems have been exploited to complement traditional emergency and security systems. Since that, the accuracy and robustness of delivered emergency and security services are rising because of the development of new and sophisticated localization techniques based on mobile radio networks.
The most famous emergency services are E911 in the United States and E112 in the European Union. The user, in the form of a mobile phone call or a distress short message service (SMS), initiates these services. Then service providers are obliged to give information about the location of user with accuracies within 50 to 150 meters [4]. Many other location-based emergency systems have been developed in last years in order to provide information and guarantee security in the case of natural disasters, accidents or fires.
After the Tsunami disaster in Sri Lanka, Dialog GSM, a mobile service provider, used location-based cell broadcasting technology to provide ongoing updates and emergency information to its subscribers along the coasts of Sri Lanka. The information included coming waves, brief news reports, hospital help lines, and supply distribution centers. Both Japan and South Korea have launched a satellite-based alert system. The system provides both countries with instant warnings of natural disasters. Many other examples of location-based emergency systems are presented in [5].

2. Management and Assistance

   These services aim mainly to control facilities, infrastructures, and environment and to assist users about available resources or facilities. Controlling public buildings, hospitals, parks, roads, and means of transport is determinant in order to ensure their good functioning. Location information may be valuable, in this case, in order to detect and localize possible problems and hitches. Many environmental applications used to use location information. Satellite signals for example are usually used to forecast weather, to study the icebergs and tectonic movements, and to collect data about environment.

3. Navigation and Tracking

   Navigation services are based on mobile users who need directions within their current geographical location. The ability of a mobile network to locate the exact position of a mobile user can be manifested in a series of navigation-based services. The most popular location-based navigation service is GPS which is a global navigation satellite system (GNSS) developed by the United States department of defense (DoD). Many other GNSS systems are being deployed like GALILEO in Europe, GLONASS in Russia, and COMPASS in China. These systems will be further described in section 2.2.3.
   Tracking consists in following user in space and in time. This means that the position is determined at each time step fixed by the user or the system. One popular example refers to tracking postal packages so that companies know where their goods are at any time. Vehicle tracking can also be applied to locating and dispatching an ambulance that is nearest to a given call. A similar application allows companies to locate their field personnel (for example, salespeople and

repair engineers) so that they are able, for example, to dispatch the nearest engineer and provide their customers with accurate personnel arrival times.

4. Information and advertising

   This category refers to services that disseminate contents to mobile users correlated with his location, context, and profile. Finding the nearest service, accessing traffic news, getting help with navigating in an unfamiliar city, obtaining a local street map are just a few of the many location-based informative services that can be offered to the user. Disseminated contents may be adverts about restaurants, supermarkets, cinema, etc.

5. Games, Leisure and Billing

   Leisure and games are ones of the most attracting fields for users especially for young and teen peoples. Location-based leisure activities like body finder or instant messaging are very interesting and may make interesting incomes for services providers. Mobile games and geocaching, too, are using to be more and more required. On the other hand, location sensitive billing refers to the ability of a mobile location service provider to dynamically charge users of a particular service depending on their location when using or accessing the service.

2.1.2.2 Network-oriented LBS

1. Physical Layer Enhancements

   Physical layer enhancements based on position information are investigated in all different components of a cellular wireless communication chain [6, 7]. Different location based technologies are proposed in order to enhance the functionalities of the physical layer. Some of these technologies are:

   - Location-based synchronization: the location information can be valuable here in order to estimate the arrival times of the signals received from neighboring base stations. These signal arriving times can be predicted using the signal traveling distances to the respective base stations. These distances can be calculated from the geographic positions of the mobile terminal and the received base stations. The idea of this approach is to timely relate synchronization signals coming from different base stations, which allows exploiting additional signal energy for synchronization and, therefore, turning interference into useful signal [8].
   - Channel estimation: channel fingerprinting and predictive channel estimation would benefit from positioning data input, which provides MS movement history, making possible to predict the likely evolution of the channel. The improved channel prediction capabilities lead to an increased data throughput even for high speeds [9].
   - Adaptive MIMO (multiple-input multiple-output): according to MS's relative position regarding other MSs in the cellular coverage area, it is possible to choose, and adapt, the most appropriate MIMO technique (i.e. space

time bloc code -STBC-, beam-forming, or space division multiple access -SDMA-) [8, 10].

- Interference cancellation: location information can be exploited in order to coordinate inter-cell interference, enhance interference cancellation algorithms, and perform better FDMA scheduling [11].

2. Cross Layer Optimization for PHY/MAC Layers

   In non cooperative networks, Radio Resource Management (RRM) strategies can be enhanced by positioning data input, applied to better physic layer realization, namely SDMA by exploiting positioning to identify spatially separable users and allowing them to transmit or receive simultaneously. In cooperative networks, enhanced RRM [12] and physic layer strategies through positioning data input, using cooperating nodes may improve communication performances. Virtual MIMO is one implementation that can be considered to take advantage of the positional data input [13, 14].

3. Relaying and Cooperative Communications

   Cooperative communication turns out to be a promising technique to improve the efficiency and reliability of wireless networks [15, 16]. Both WLAN and cellular network management can establish relayed or cooperative communication if it is the better way to connect with the MS. Exploiting positioning data would improve the degree of cooperation between nodes allowing better QoS at lower complexity [17].

2.2 A Survey of Wireless Localization Systems and Techniques

2.2.1 Architectures and Implementation of Localization Systems

A localization system is a set of technologies implemented and used in order to perform the task of positioning. Localization systems basically involve the presence of a number of anchor nodes (AN) at fixed and precisely known locations in a coordinate reference frame and of a terminal to be located (often a mobile station).

2.2.1.1 Centralized versus distributed systems

A localization system is centralized when a central entity is implemented in order to perform positioning of all the network users [18, 19]. The job of the targeted MS is restricted to send information (signals) necessary to perform its positioning. In different manner, if each MS performs locally the positioning task based on the electromagnetic signals transmitted by the reference stations, the system is called distributed or decentralized [20]. Semi-centralized (or semi-distributed) approaches are defined when different small entities, implemented in different areas, perform localization for the MSs which lie in each area [21].

2.2.1.2 Satellite versus terrestrial systems

Satellite systems rely on a constellation of artificial satellites rotating in well-known orbits and continuously transmitting signals used by the mobile terminals to perform ranging measurements. They are inherently navigation systems, while most recent terrestrial systems are intended for positioning only. The well-known global positioning system GPS is nowadays the primary satellite-based system [22, 23].

Terrestrial systems rely on wireless networks infrastructures to perform localization. Because of the variety of wireless terrestrial systems and modulations formats, many different approaches have been proposed so far to enable positioning in personal handsets and portable devices. These approaches include terminal-centered and network-centered procedures for cellular networks, for which the very first proposals were studied more than fifteen years ago, procedures tailored to the modulations and protocols for WLANs and WMANs, approaches to exploit the peculiarities of an innovative modulation scheme such as ultra-wide band (UWB) and those of a novel network concept such as that supporting the wireless sensor networks (WSNs).

2.2.1.3 Outdoor versus indoor systems

Because of the particularities of each environment (indoor and outdoor), different techniques and systems are defined for each environment. GPS is the system used to offer localization in outdoor environment with good precision (up to 10 m) [22, 23]. Nevertheless, it cannot perform localization in indoor environment because of the non-visibility of satellites in this type of environment. Cellular based localization techniques are defined especially for outdoor scenarios but they are still applicable for indoor localization [24, 25]. In indoor environments, WLAN and UWB technologies are the main systems used for localization [25–27]. WSN are used for both indoor and outdoor environments but especially for short-range localization [28, 29].

2.2.1.4 Static versus dynamic systems

By static localization, we mean instantaneous localization at a precise time and position. By contrast, dynamic localization consists in tracking the position of the terminal when moving. Dynamic localization imposes additional constraints, namely mobility and radio-channel variability. Bayesian techniques are used in such applications and systems. The Kalman filter (KF) [30], its variants (extended KF [31] and unscented KF [32]), and particle filters (PF) [33, 34] are the mostly used Bayesian techniques in this context.

2.2.2 Localization Techniques

2.2.2.1 Direction finding based techniques

Direction finding based techniques estimate position using angle of arrival (AOA) of signals arriving to the measuring device. The signal source is on the straight line passing through the measurement device with the estimated AOA [35]. This line is called the line of bearing (LOB). The intersection of, at least, two independent LOBs gives the estimated 2D-position (Figure 2.2). Three independent LOBs give the

estimated position in 3D-scenarios. In practice, noise and multipath force the use of more than two AOA measurements. AOA technique is also called direction of arrival (DOA) and direction finding (DF).

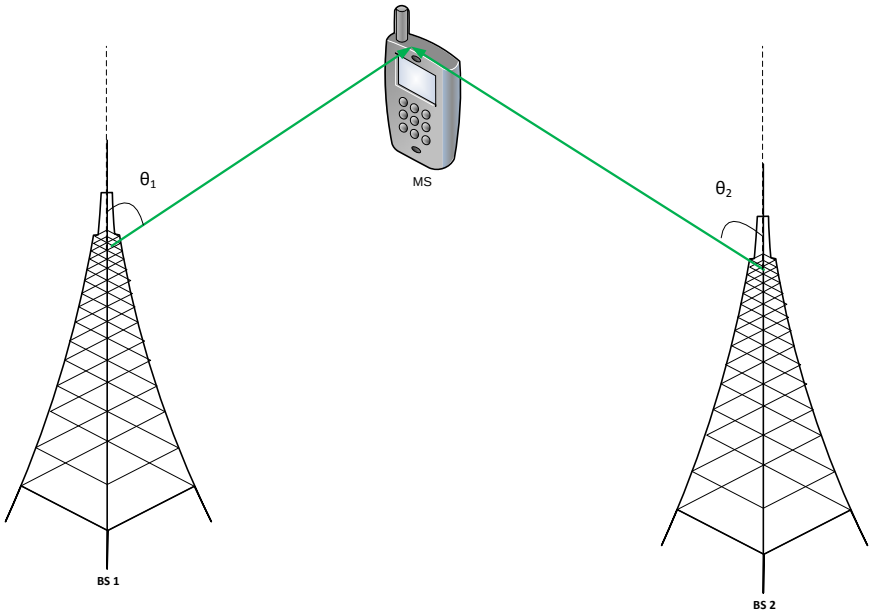

Figure 2.2: AOA based positioning technique.

The main advantage of AOA technique is that few number of measurements (two in 2D and three in 3D) are needed to estimate position, and that no time synchronization between the measuring units is required. The main disadvantages of AOA technique are relatively large and complex hardware requirements and location estimate degradation as the mobile moves farther from the measuring units. Furthermore, shadowing and multipath reflections limit the accuracy of AOA-based location estimation [25, 36, 37].

2.2.2.2 Range based techniques

Range-based techniques are based on the measurement of distances (ranges) between the targeted MS to be located and the anchors. Three major range-based techniques are used in localization systems [25, 38]. At this stage of this dissemination, we give simple definitions of these techniques. More investigations will be given later in next chapters.

Time of arrival (TOA): It is defined as the time spent by signals between the MS and each anchor. In this case, ranges are obtained simply as the products of measured TOAs by the speed of light, c. This technique is called spherical localization. Indeed, the location is given as the intersection between a set of spheres in 3D (or circles in 2D), each centered on a signal source with radius equal to the measured range (see Figure 2.3).

Radio signal strength indicator (RSSI): It is defined as an indicator of the power received by the end side of the radio link between the MS and each anchor node. The received power and the power attenuation are the main used RSSI. Using a path loss

model (PL model), which rely the distance to the power attenuation or the received power, ranges can be estimated and the position is calculated as the intersection between different spheres (see Figure 2.3).

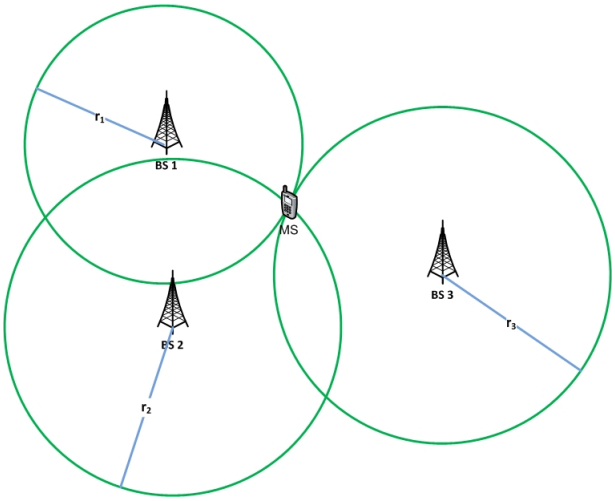

Figure 2.3: Lateration technique with three BSs based on either TOA or RSSI.

Time difference of arrival (TDOA): It is a hyperbolic method. The TDOA measures the difference of ranges between Tx-Rx pairs. For each TDOA measurement, the MS lies on a hyperboloid. The position is then given as the intersection of these hyperboloids (see Figure 2.4).

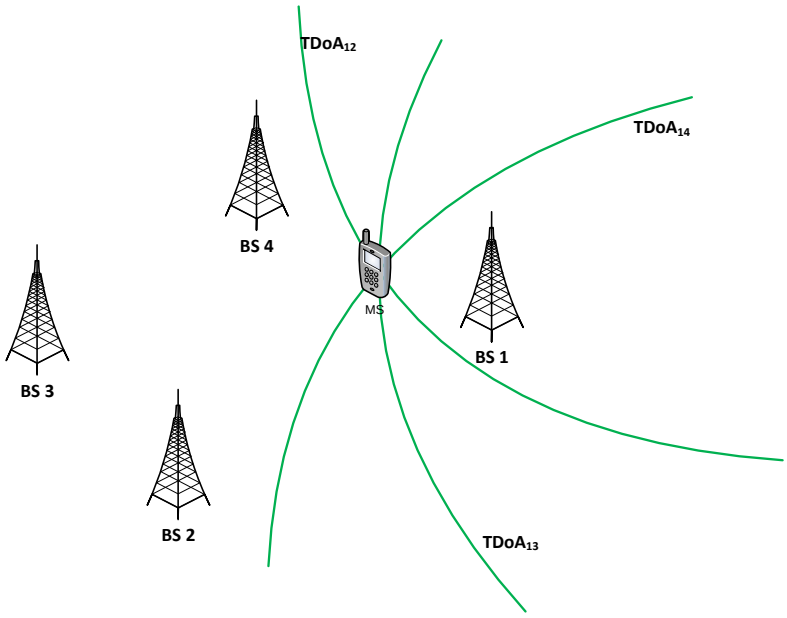

Figure 2.4: Lateration technique with four BSs based on TDOA.

2.2.2.3 Fingerprinting based techniques

Fingerprinting techniques (or mapping techniques) use the information from a database that consists of previously estimated or/and measured location-dependent parameters (LDPs) corresponding to known MS locations [25, 39]. The database is usually obtained by a training phase (off-line phase) before the real-time positioning (on-line phase) starts.

In the off-line phase, LDPs are measured using a set of anchor nodes. Measurements are done in carefully chosen points [40]. Some important considerations are made while selecting these points. They must be in an area of high interest (where position is likely to be sought). They are evenly spread out in the area of interest, so that they provide a good reference when determining position. Also, they have to be at such a location that their positions can be easily determined (like at an intersection). Their number is balanced between level of accuracy and labor burden in fabricating a database [41, 42]. In the on-line phase, the MS acquires the vector of LDPs, measured with the set of ANs, in the place where it requires its position. Then, it compares the measured vector to the database using appropriate algorithms [43, 44]. The result is the most likely location of the MS.

The technique of fingerprinting, compared to geometrical techniques, requires huge amount of resources and time especially to establish and to stock the database [45]. Once the database is constructed, the technique consists then in comparing actual measurement to the database. Nevertheless, any change in the environment requires the update of the database which may increase the cost of the localization systems.

2.2.2.4 Bayesian filtering techniques

Bayesian filters probabilistically estimate a dynamic system's state from noisy observations. In wireless location estimation, the state is a MS's location, and location ANs provide observations about the state. The state could be a simple 2D position or a complex vector including 3D position, pitch, roll, yaw, and linear and rotational velocities [37].

Kalman filter (KF) remains one of the Bayesian techniques widely used because of its computational efficiency. The traditional Kalman filter yields the optimal minimum mean squared error (MMSE) estimate when assuming Gaussian noises and linear measurement and state equations [46]. However, the location estimation in wireless communication systems may be a nonlinear problem because of the nonlinear relationship between measurements and position. The most common application of the KF to nonlinear estimation problems is in the form of the suboptimal extended Kalman filter (EKF), which consists of a simpler linearization of the prediction and measurement functions, based on a series expansion, maintaining the computational efficiency, and supposes that the Gaussian properties are preserved after being propagated. The main drawback of the EKF is that the convergence is not guaranteed in the case that the propagation error can not be properly approximated by a linear function. The unscented Kalman filter (UKF) was developed as a derivative-free optimization to address the limitations of the EKF in nonlinear estimation and to avoid the complexity of the Monte Carlo method by applying the unscented transform (UT) [32]. UT is a method of propagating mean and covariance through nonlinear transformations.

Particle filters approximate the optimal solution numerically. When the measurement equation is non-linear or when noises are not Gaussian, the particle filter is particularly promising. The key idea is based on Monte Carlo methods and consists in representing the required posterior density function by a set of random samples with associated importance weights, and to compute estimates based on these samples and weights [33, 34]. In sampling problems where the target distribution changes over time, the sample weights can be updated directly to reflect the new distribution [47]. The particle filter approaches the optimal Bayesian estimate as the number of samples becomes large, at the price of computational intensity.

2.2.2.5 Performance metrics of localization techniques

Various factors may affect the choice of the appropriate localization technique for the requested application or service. In fact, the constraints are different from one application to another, namely from typical commercial to business or military applications. In this section, we survey the principal factors that affect the choice of localization techniques.

1. Positioning accuracy

   The accuracy of the positioning technique depends of many factors: used location-dependent parameters, the localization algorithm, the computational capacity of the localization system, the geometric configuration of the reference system with respect to the targeted MS, the radio propagation conditions, and the used system RAT. Generally, time based LDPs, namely TOA and TDOA, are more precise than RSSI because of the strong variations of RSSI parameters. Hence, the use of TOA or TDOA may enhance the accuracy of the localization system. Furthermore, the used RAT technology may affect the precision of measured LDPs and thus the positioning accuracy. For example, UWB ranging [48] is more precise than WLAN ranging based on round-trip time (RTT) [49].
   The geometric configuration of the anchors affects the accuracy of the position estimation. The geometrical dilution of precision (GDOP) is defined as the optimum accuracy that can be performed for each configuration of ANs with respect to the targeted MS [50]. The radio propagation phenomena such as multipath and shadowing affect more or less the precision of measurement of the LDPs and, thus, the positioning accuracy. Finally, the LBS accuracy requirement may define one or more of these factors in order to achieve the requested quality of LBS.

2. Robustness

   The robustness of a positioning technique measures its capability of functioning with particular and sudden changes of the radio channel or the available information. This is the case when some signals are no longer available or new signals appear. Indeed, sometimes the signal from the transmitter is totally or partially blocked so that the signal cannot be measured. Besides, sometimes some anchor nodes are no longer seen by the MS (dead nodes or discharged battery). In this case, a robust localization technique should be able to offer the same (or close) accuracy with the available signals.

3. Resources and computation requirements

   Resources and computation requirements depend essentially on two factors: the type of the network and the complexity of the localization technique. Resource requirements vary considerably depending on the type of the network where the localization is deployed. For example, the localization technique deployed in sensor networks should have low complexity and low consumption of energy, since the available resources are generally poor. Cellular networks have generally more resources and computation capabilities than sensor networks especially at BS and network core levels. The available resources may affect the performances of the localization technique. In [51], the authors combine the result of multiple location estimation techniques to improve accuracy. It shows that if Bluetooth and 802.11 networks are available, then the accuracy of the location estimates can be improved by considering both technologies for localization. An improvement of 40% to 70% is reported when two Bluetooth and two 802.11 APs are used instead of four 802.11 AP.
   The computation requirements depend also on the localization technique. A simple RSSI based localization technique with least-squares (LS) approximation is less greedy than iterative-based or fingerprinting-based techniques. Hence, the choice of the localization technique to be deployed in a network depend conjointly on the computation requirements of the technique itself and the available resources that can be accorded to it by the network. This trade-off should be imperatively addressed before the deployment of localization systems in order to reduce the congestion and to preserve resources for other applications and other parts of the network.

4. Cost of deployment

   This is the most important factor for commercial and enterprise deployments of LBS. It includes the cost of initial deployment and the cost of maintenance and upgrade. For a low cost deployment, it may be interesting to overlay the localization technique over an already existing network. This avoids the cost of the implementation of a dedicated localization system. The localization technique, itself, may increase or decrease this cost. The RSSI based technique may be favorable compared to TOA or TDOA based techniques. Indeed, these two time-based techniques require ranging between network units, which may consume much energy.

5. Effect of the network system

   The underlying communication network may incur some overhead cost due to localization. This is not a serious issue when dedicated schemes such as GPS are utilized. However, it has to be considered for other localization schemes that are deployed over the existing communication networks. The additional latency, data traffic and processing for localization may affect the performance of the underlying network. It may reduce throughput, disrupt client connection, limit user mobility, or induce delay in user connectivity. Such effects should be understood before selecting a localization scheme. For example, in military

application, this factor would be of high importance, due to the critical nature of communications and the mobile operation requirements.

6. Security and privacy

   An attacker or intruder in a system would try to gain access to restricted network resources in order to disrupt the system or obtain confidential data. Since anonymity is highly desirable in his case, an attacker would try to disrupt the localization scheme or spoof his location. Similarly he may try to fool the localization scheme to access some location based services. Location based service such as accessing high security (proprietary) data within a room, may be deployed in an enterprise. Secure localization would provide an additional level of security that would prevent malicious users (who may have compromised the authentication scheme) from accessing the data. Similarly, in [52], authors describe the use of localization for authentication issues where the user is granted network access within a predefined area only. Depending on the level of security required, secure localization schemes may be selected [53, 54].
   Privacy is an important issue while localizing users. However, requirement for security and privacy lead to conflicting design issues. The users may not like to disclose their location to the network or other users. Since localization is carried out by measuring physical layer parameters, user (location) privacy may be compromised even for a secure encrypted network. For example, packet transmissions in 802.11*i* are encrypted but the MAC addresses of the source are openly transmitted. The MAC address may be used along with a RSSI based scheme to determine the location of a user without his consent. For a military deployment, where privacy may be a very important issue, localization scheme may be deployed using spread spectrum technology. These signals would appear as noise for all receivers except intended recipients.

2.2.3 Satellite-based localization systems

Satellite navigation systems are based on the measurement of the TOAs of a set of electromagnetic signals transmitted by the satellites (ranging signals, one signal per satellite). The receiver determines its own position by evaluating the time the signals needed to travel from the satellites to the receiver itself. This is possible thanks to the presence of very accurate atomic clocks on boards of the satellites, all synchronized among them. On the contrary, the receiver clock is by no means synchronized with the satellite time when it starts receiving the signals, but synchronization can be achieved after signal acquisition and tracking, once the so-called navigation message, carried by the satellite signal, has been decoded and the contained information facilitates the synchronization. The position of satellites is precisely known and transmitted within the navigation message.

In addition, the time at which the signal left the satellite is embedded in the navigation message, so that the receiver can easily compute the propagation time of the ranging signal. Multiplying this by the speed of light, the receiver is then able to determine the user-to-satellite range. As a result, the user determines its possible positions as a sphere centered on the satellite, with radius equal to the user-to-satellite range.

Ideally, the analytical intersection of three spheres returns two points whose only one is a feasible solution for the user's position, if the user is near the Earth (solution below the plane of the satellites).

However, the lack of synchronization between the system time and the receiver clock introduces a further uncertainty, whose resolution requires the addition of a fourth ranging measurement, in order to resolve the three-dimensional user's position and the receiver clock offset with respect to the system time. Therefore, for the complete determination of the user's position, at least four satellites in view are necessary [22, 55]. Several other causes of errors are present in the range measurements, yielding to the need of taking measurements from as much satellites as possible. These causes of errors are [22, 55]:

- Control system: ephemeris, clocks, codes, measurement errors;
- Ionospheric delay: the propagation delay depends on the frequency and on the density of electrons along the path;
- Tropospheric delay and atmospheric attenuation: the propagation delay and attenuation depend on the pressure, temperature, humidity of the air;
- Multipath from reflective surfaces and scattering points close to the receiver;
- Receiver noise and clock errors;
- Uncompensated relativistic effects.

The satellite-based systems that cover all the globe are called global navigation satellite systems (GNSS). Actually, the main commercialized GNSS are GPS, Galileo, GLONASS, and Compass. In next paragraphs, we describe briefly their fundamental system components and techniques and we underline their current status and their future directions. After that, we introduce the regional navigation satellite systems (RNSS), which nearly have the same philosophy of GNSS but their coverage are limited to a country-size region.

2.2.3.1 The GPS system

The NAVSTAR-GPS (NAVigation system for timing and ranging - global positioning system) project was officially launched in 1973 by the U.S. department of defense (DoD) to give birth to a positioning service with global coverage and continuous-time availability. The GPS was originally developed for authorized (military) use only and subsequently made available to civil users in 1983 [22]. GPS provides two services: the standard position service (SPS) and the precise position service (PPS). The SPS is designed for the civil community; whereas the PPS is slated for the United States authorized military and selected government agency users. The GPS system is composed of three segments [22]:

- Satellite constellation (the space segment (SS)): the current (2009) GPS constellation consists of 31 satellites, positioned on six earth-centered orbital planes with five to six satellites on each plane.

- Ground control/monitoring network (the operational control segment (OCS)): the OCS monitors satellite health and signal integrity and maintains the orbital configuration of the spread spectrum/space segment. Furthermore, the OCS updates the satellite clock corrections and ephemerids, as well as other fundamental parameters.

- User receiver equipment (the user segment (US)): the US is typically the user receiver equipment, that processes the GPS signals to determine user's PVT (position, velocity, and time).

The current constellation is composed of satellites from Block IIA, launched between 1990 and 1997, during which the system was declared fully operational, Block IIR (1997-2004) and Block IIR-M (2004-present). Ten prototype satellites (called Block I) have been launched to test and validate the system concepts between 1978 and 1985 whereas Block II was launched from 1989 and 1990. Next-generation satellites (Block IIF) are scheduled to be launched in the near future, whereas Block III satellites are planned to be employed for a post-2010 deployment. The nominal orbital period of a GPS is one-half of a sidereal day (approximately 11 h 58 min). The orbits are nearly circular and equally spaced about the equator at a 60° separation with an inclination relative to the equator of nominally 50°, whereas the orbital radius is approximately 26,600 km. The GPS constellation provides a 24-hr global user navigation and time determination capability.

2.2.3.2 Enhancements of the GPS system

The localization precision obtainable with GNSS systems is often accurate enough for most civil services (e.g., car, ship and aircraft navigation in open space), but it necessitates to be strongly improved for professional, security or critical services, e.g., guidance in harbor entry and in airport, indoor navigation where the GNSS precision is poor due to the wall attenuation and multipath propagation, or even high-precision machine control. In these situations, where sub-meter level accuracy is required or poor visibility has to be overcome, improvement of GNSS position estimates can be achieved basically in three different ways [55], globally called augmentation systems:

1. Mitigation of measurement errors: enabled by the availability of information about the corrections to be applied when resolving the PVT solution. Since only a differential information can be obtained, i.e. an information extracted from GNSS measurements in a precisely known location (reference station) nearby the terminal, this approach is known as Differential GPS (DGPS). Differential corrections are provided by most augmentation systems: Satellite-Based Augmentation Systems (SBASs), Real-Time Kinematic (RTK), Assisted-GPS (AGPS).

2. Improvement of the satellite geometry: obtained through the use of additional satellites or terrestrial pseudo-satellites (the so-called pseudo-lites), which transmit GNSS-like ranging signals with the aim of adding new ranging information for terminals with reduced visibility of the core constellation. This method is realized by SBAS systems and pseudo-lites.

3. Use of coarse positioning or timing information provided by independent systems: This is the case of the AGPS, where the cellular communication network the terminal is connected to provide an assistance message containing coarse information of the mobile handset position and timing, computed on the basis of measurements obtained by the network infrastructure itself.

Differential GPS

DGPS uses a network of fixed and ground-based reference stations to broadcast the difference between the positions indicated by the satellite systems and the known fixed positions. These stations broadcast the difference between the measured satellite pseudo-ranges and actual (internally computed) pseudo-ranges, so that the user terminal receiver may correct their pseudo-ranges by the same amount. The underlying hypothesis of DGPS is that any two receivers that are relatively close together experience quite the same atmospheric errors. The first GPS receiver, called reference station or beacon, must be set up in a fixed, known and perfectly geo-referenced location. The reference station receiver calculates its position based on satellite signals and compares this estimate to its true position. The difference vector represents the differential error which is transmitted to the second GPS receiver, i.e. the user terminal, commonly indicated as the roving receiver, which applies these corrections to its own GPS data. Thus, differential correction techniques are then used to enhance the quality of location data gathered using GPS.

The corrected information can be applied to data from the roving receiver in real time in the field or through post processing after data storage using special processing software and proper DGPS data-bases [55]. In real-time DGPS, the reference station calculates and broadcasts corrections for each satellite, using a forward radio link to the roving receivers. Thereby, the roving GPS receiver is enabled to provide a differentially corrected position, by correcting the computed pseudo-ranges with the data received by the beacon. Although real-time and post-processing methods are based on the same underlying principles, each accesses different data sources and achieves different levels of accuracy.

DGPS can provide meter- to decimeter-level accuracy [56]. Its performance inherently decreases with the increasing distance between the user terminal and the reference station, and with the increasing delay between the time the corrections are computed at the reference station and the time they are applied to the terminal. Real-time differential corrections allow one to two meters navigation accuracy, depending on the service and the GPS receiver. Clearly, the cost for implementing a DGPS service is the cost for installing a network of reference stations, sufficient to guarantee good correction accuracy, i.e. distanced a few hundreds kilometers apart. Furthermore, the DGPS-enabled UT receivers must be equipped with a radio receiver, aside from the conventional GPS receiver, and specific procedures to decode and apply the differential corrections, through a proper interface with the GPS receiver.

Satellite-based augmentation systems

SBASs are similar in principle to the DGPS, from which they are derived. Instead

of a ground station, the correction data are sent via GEO satellites equipped with transponders (but not by signal generators) transmitting in the same band and with the same modulation as the core constellation [57]. Because of the direct derivation of these satellite-based systems from DGPS, SBAS is often called wide area differential GPS (WADGPS). The intended coverage of SBASs is worldwide, through the cooperation of different regional systems aiming at augmenting not only GPS, but GNSS systems in general.

SBASs use GEO satellites to broadcast ranging, integrity and correction information to GNSS users, with the aim of increasing accuracy, reliability, and availability of GNSS positioning. Unlike the standard DGPS, a SBAS satellite does not directly send corrections to the pseudo-range data, because of the too wide coverage of a GEO satellite. Instead, SBAS estimates the effect of the individual sources of error and sends corrections for each one of them, for each satellite; i.e. it sends clock corrections, ephemeris corrections, and ionospheric corrections [57]. Tropospheric corrections cannot be broadcast, because of the localized nature of this error, but the local receiver can apply its own corrections based on a proper atmospheric model, parameterized on the current receiver location [57].

SBASs are safety-critical systems, consisting of a ground network of reference sites that monitor satellite integrity to assess current GNSS performance. Moreover, differently than DGPS, the space segment provides further GNSS user support through the transmission of additional ranging signals. Note that there is no correction done by the GEO satellite; the master ground station will even correct errors produced by the GEO satellite itself. Seven major elements can be recognized in a SBAS system [57]:

1. The navigation satellites, i.e. the core constellation;
2. The reference stations, or ranging and integrity monitoring stations (RIMS) precisely geo-referenced on the Earth surface;
3. The communications network, created among the reference stations to monitor satellite signals;
4. The master station(s), which gathers and processes data from the reference stations and generates SBAS signals;
5. The uplink center(s), which transmits the augmentation messages to the geostationary satellites (Cband is used);
6. The correction satellite(s), i.e. the GEO satellites transmitting the additional information. Every SBAS satellite is assigned with a different spreading code, which belongs to the same family (Gold codes) of the ones used by the GNSS core constellation (but is obviously different);
7. The user terminal (UT), carrying the GNSS receiver with SBAS capabilities.

Several commercial SBAS systems are providing services to users, including OmniSTAR (Fugro, The Netherlands), Starfire (NavCom Technology, United States), and Veripos (Subsea 7, United Kingdom). Besides, four non-commercial SBASs are currently under development:

- Wide area augmentation system (WAAS) (United States), commissioned for initial safety-of-life use in 2003;
- European geostationary navigation overlay system (EGNOS) (Europe), whose initial operations started in 2005;
- Multi-functional satellite augmentation system (MSAS) (Japan), for which two multi-functional transport satellite (MTSAT) satellites were launched in 2005-2006;
- GPS aided GEO augmented navigation (GAGAN) (India), scheduled for completion by the end of 2008.

Pseudo-lites

Pseudo-lites (pseudo satellites) are ground-based transmitters that generate and transmit GNSS compatible signals [58]. Pseudo-lites can be placed in locations that have poor satellites visibility to improve availability and accuracy of GNSS based positioning. In an indoor space where the GNSS signals are heavily attenuated, a set of pseudo-lites can be even used to replace the whole GNSS constellation.

Pseudo-lites have several positive qualities: their signals can be received without hardware modifications to common GNSS receivers and only minor firmware adjustments [59]. Their number and locations can be optimized for a given environment, in order to maximize the accuracy offered by the augmented system. Furthermore, pseudo-lite signals are not impaired by ionospheric delays, since their propagation is fully tropospheric. Nonetheless, pseudo-lites are not the answer to any problem: one major limitation they experience is the so-called near-far problem. It is generated by the decrease of the received pseudo-lite signal power with the increase of the distance between the pseudo-lite and the receiver. While the power received from a satellite is nearly constant over wide areas, apart for small-scale fading effects, the power received from a very near pseudo-lite can be significantly higher than that received from other pseudo-lites, as well as from GNSS satellites. Therefore this pseudo-lite can act as a strong jammer [60].

Furthermore, the pseudo-lite position must be known with extreme precision with respect to the GNSS coordinate reference frame. However, this precision might be hard to reach in case of indoor or underground installations, or when a quick deployment is necessary (e.g., emergency interventions). In any case, one of the most critical impairments of any wireless location method, i.e. multipath effect, is not solved by pseudo-lites; on the contrary, because of the nearly-horizontal propagation from the transmitter to the GNSS receiver, pseudo-lite signals may be even more multipath-prone than satellite ones.

The signal power transmitted by pseudo-lites is generally low, in order to limit the multipath and near-far effect and not to harm GNSS receiver. This entails a reduced coverage and therefore the necessity to deploy several pseudo-lites to serve a few square-kilometer areas. In these conditions, a master station is required to maintain accurate clock synchronization of all the pseudo-lites, whose internal clock are generally low-performance devices so as to limit the deployment costs. The use of a carefully

deployed pseudo-lite system allows achieving real-time positioning even at centimeter-level [60]. Automating the heavy and expensive mining machines in open-pit mining has been one of the major applications [58].

Network RTK

RTK is a method enabling an opportunely equipped GNSS receiver to achieve centimeter-level accuracy positioning in real-time [61]. The first RTK concepts were developed in the 90's and involved a reference receiver, located in a fixed and perfectly Geo-referenced location, transmitting its raw GPS measurements or observation corrections to a rover receiver via some sort of data communication link (e.g., VHF or UHF radio, cellular communication networks) [62]. The rover equipment must be in turn constituted by a GPS receiver, a radio link with the reference station and a software/firmware able to interpret the RTK data from the reference station. The data processing at the rover site includes ambiguity resolution of the differenced carrier phase data and coordinate estimation of the rover position.

Network RTK is today a widely used technology to provide precise outdoor positioning to authorized/paying mobile terminals over large territories (e.g., countries). To give a few examples, today the entire Greek territory (mainland and most islands) is covered by a RTK network, maintained by a governmental entity, for geodetic purposes; the 99-stations network has been designed and deployed in years 2005-2006 and has recently become operative. Another example is the deployment of a network of stations in the Kingdom of Bahrain territory.

Generally, RTK networks are managed by one or more network processing centers, which gather the information from the reference stations and pre-process them, in order to continuously monitor the network status and some positioning parameter, first of all the carrier phase, to guarantee its reliable real-time ambiguity resolution. The information pre-processed by the network center is then circulated along the stations network for the rovers' necessities. RTK is a technology essentially implemented with proprietary solutions [62].

Assisted GPS

Assisted-GPS is a network-assisted method that integrates GPS with information provided by the cellular network in the aim of reducing the so-called time-to-first-fix (TTFF), i.e. the time necessary to the GPS receiver to produce the first estimate of its current position, and, at the same time, increasing the sensitivity of the GPS receiver [63].

Indeed, a GPS receiver needs to correctly demodulate the whole navigation message to determine the satellite ephemeris, prior to resolve the PVT solution. This could take several seconds even in ideal acquisition and tracking conditions, which easily become some minutes in normal conditions. The idea behind AGPS is to use the cellular network to communicate a copy of the navigation message of each visible satellite to the GPS receiver, which, therefore, does not need to wait for the complete signal tracking and data demodulation before producing its position estimate. This reduced TTFF is clearly essential, for example, in emergency calls.

Network assistance is also fundamental in case of critical receiving conditions, e.g., in dense scattering environments or indoor, when deep fades in the satellite propagation channel, originated tightly near the receiver, prevent the continuous tracking of the signal, and so the demodulation of the complete navigation message [64]. GPS receiver sensitivity can be enhanced by reducing the acquisition search space in both Doppler shift and code phase domains, thanks to a rough information about the most probable Doppler shift and code phase computed and transmitted by the cellular network to the UT. The architecture of an AGPS service comprises [64]:

1. The GPS satellite constellation;
2. The wide area reference network (WARN), a network of reference receivers, co-located with the cellular base stations, which collects the navigation messages of all the satellites in view and simultaneously computes differential corrections;
3. The location server, or AGPS server which collects and stores data from the WARN, produces the assistance messages for the UTs, then sends these messages to the UT using the conventional cellular communication link; in case of UT request, it can also compute and transmit the user's position solution;
4. The MSs, i.e. the user terminals to be located, equipped with a GPS receiver and an AGPS enabled cellular network receiver.

2.2.3.3 The GALILEO system

Galileo is the European GNSS providing a global positioning service under civilian control. It has to be inter-operable with GPS and GLONASS, the American and Russian GNSSs, respectively. The first stage of the Galileo program was agreed upon officially on May 26, 2003 by the EU and the European Space Agency (ESA). Galileo is based on a constellation of medium earth orbit (MEO) satellites and ground stations providing information concerning the positioning of users in many sectors such as transport (e.g., vehicle location, route searching, speed control, guidance systems), social services (e.g., aid for the disabled and for the elderly), services for the justice system and customs procedures (e.g., location of suspects, border controls), public works (e.g., geographical information systems), search and rescue (SAR), and leisure (e.g., direction-finding at the sea or in the mountains) [65]. The fully deployed Galileo system will consist of 30 satellites (27 operational and 3 spares), positioned in three circular MEO planes at a nominal average orbit semi-major axis of $29,601.297$ km, and at an inclination of the orbital planes of $56°$ with reference to the equatorial plane [66]. Five different services are expected from Galileo [66]:

- An open service (OS) providing all information such as positioning, navigation and timing services, free of charge, for mass market navigation applications, interoperable with other GNSSs, and competitive to the GPS standard positioning services;
- A safety-of-life (SOL), compliant to the needs of safety critical users such as civil aviation, maritime and rail domain. The SOL includes high integrity and authentication capability, although the activation of these possibilities will depend on the user communities. Furthermore, the SOL service includes service guarantees;

- A commercial service (CS), generating commercial revenue by providing added value over the OS, such as by dissemination of encrypted navigation related data, ranging and timing for professional use, with service guarantees, high integrity level, precise timing services, high data rate broadcasting, provision of ionospheric delay modes, local differential correction signals and controlled access;

- A public regulated service (PRS), for application devoted to European and member states, for critical applications and activities of strategic importance. It makes use of a robust signal and is controlled by member states. This service provides service guarantees, high integrity, full range of value added features and an access controlled by encryption;

- A search and rescue (SAR) service, providing assistance to the COSPAS-SARSAT2 system by detecting emergency beacons and forwarding return link messages to the emergency beacons. It is a service for SAR applications by providing near real time reception of distress message and precise location of alert.

2.2.3.4 The GLONASS system

GLONASS ("GLObal'naya NAvigatsionnaya Sputnikovaya Sistema") is a navigation satellite system developed by the former Soviet Union in response to the GPS. Like GPS, GLONASS was initially targeted to the URSS Army needs: navigating and ballistic missile targeting with world coverage. The setting-up of the system started in 1976 to reach full deployment in 1995 [67].

At that time, the constellation comprehended 24 satellites and transmitted on the L1 band using a frequency division multiple access (FDMA). In the following years the lack of funding, due to collapse of the Russian economy, deeply damaged the system efficiency. However, the strategic importance of the satellite navigation was worldwide affirmed: European Union started the Galileo project and the United States the GPS modernization. Therefore, in 1999 GLONASS became officially a dual-use system, by a Presidential decree and, at the beginning of the new century the GLONASS reconstruction was boosted by the Russian extra-gain due to the oil and gas export. Now, the GLONASS system is under a deep modernization, with the civil side managed by the Russian Space Agency. New satellites were launched in the last years: six in 2007 and six in 2008 [67]. Since 2004, Russia involved India in the GLONASS system upgrade, but the details of the Indian involvement are not public. According to the Russian Government program, the full GLONASS constellation with 24 healthy satellites would be operative in 2009 but the system should reach the GPS/Galileo performance only in 2011 [67]. These goals were unreachable since till now (September 19^{th} 2010) only 21 satellites was been launched.

2.2.3.5 The COMPASS system

Compass is the incoming Chinese GNSS. China has started the development of an indigenous navigation satellite system technology since the 60's of the last century but only during the 80's the research become really effective. In 1994, China approved a new satellite system for navigation purposes based on the radio determination satellite

service (RDSS), a different technology in comparison to the GPS [68]. The first Chinese system was named Beidou, from the Chinese name of the Northern Star, the brightest star of the Ursa Minor constellation. Beidou was born like a regional dual system, both military and civil, to provide navigation and timing to China and surrounding areas. China considers the GNSS technology fundamental for its military and economical safety sharing the European vision of an unreliable American GPS [68].

The evolution of the Beidou system is usually called Beidou-2 or, more usually, Compass. The first satellite of the Compass navigation satellite system (CNSS), which is a MEO satellite, was launched on April 2007 [68]. The system is expected to cover China and parts of neighboring countries by 2012 and then develop into a global constellation step by step.

2.2.3.6 Regional systems

Regional systems provide additional signals from satellites operating over a given geographical area that are compatible with one or more GNSS systems. Currently there are two main regional navigation satellite systems (RNSS):

- The Indian regional navigation satellite system (IRNSS), which includes three satellites in geostationary orbit and four satellites in geosynchronous orbit, transmitting L-band and S-band signals and providing coverage primarily for the Indian land mass [69]. The first satellite is planned for launch in the last quarter of 2011 and a complete constellation is currently scheduled to be in place by 2014 [70];

- The Japanese quasi-zenith satellite system (QZSS), which is based on three inclined geosynchronous orbit (IGSO) satellites operating over Japan and surrounding areas and transmitting signals that are compatible and inter-operable with existing and future modernized GPS signals. The first satellite "Michibiki" was launched on 11 September 2010. After three years of experiment, the satellite positioning service is expected to start in 2013 [71].

2.2.4 Terrestrial-based localization systems

By contrast to satellite-based systems, terrestrial network-based positioning systems were born with the main objective to build communication systems. After that, they have been used as a support to develop positioning applications. At the contrary, the satellite based systems was designed with the primary objective to obtain a positioning system with a global coverage. Therefore, since many years much scientific research has been focused on wireless terrestrial networks to build the basis for positioning and navigation systems.

The principal terrestrial communication systems for which position location capabilities have been deployed are cellular networks, WLANs, wireless networks based on UWB technology, and WSNs. Some of these wireless technologies have common LDPs estimation techniques, such as RSSI, TOA, TDOA, AOA, and position estimation techniques, such as geometric, fingerprinting methods, and tracking algorithm (see section 2.2.2). However, the final location accuracy depends on different aspects, but

in particular it is strongly related to the signal format, bandwidth, and propagation properties of the wireless technology used by the location system. In this section, we present localization systems based on cellular networks (namely GSM and UMTS), WLAN networks, UWB networks, and WSN networks.

2.2.4.1 Localization with cellular systems

Localization with GSM

The applications of location using the GSM network have emerged in the early 2000s with the E-911 service in Japan and the United States [72]. Since that, the GSM network based localization systems are studied and proposed. Studies have shown that operators can generate interesting incomes when offering location-based services through GSM networks [73]. In GSM networks, as originally planned, base stations are not synchronized between them. As some time based localization techniques need synchronization between BSs, new units, namely LMU (location measurement unit), are integrated in GSM core networks in order to provide the required synchronization (Figure 2.5). Nevertheless, GSM network is still inappropriate for some applications, which require high accuracy (a few meters) such as E-112. Indeed, in rural environments where only few BSs are available, the reachable accuracy may be very inaccurate. If only a single base station is available, the best location accuracy is about the cell, or the sector, covered by the BS. UMTS may offer better performances because localization is an integral part of this standard associated with third generation networks.

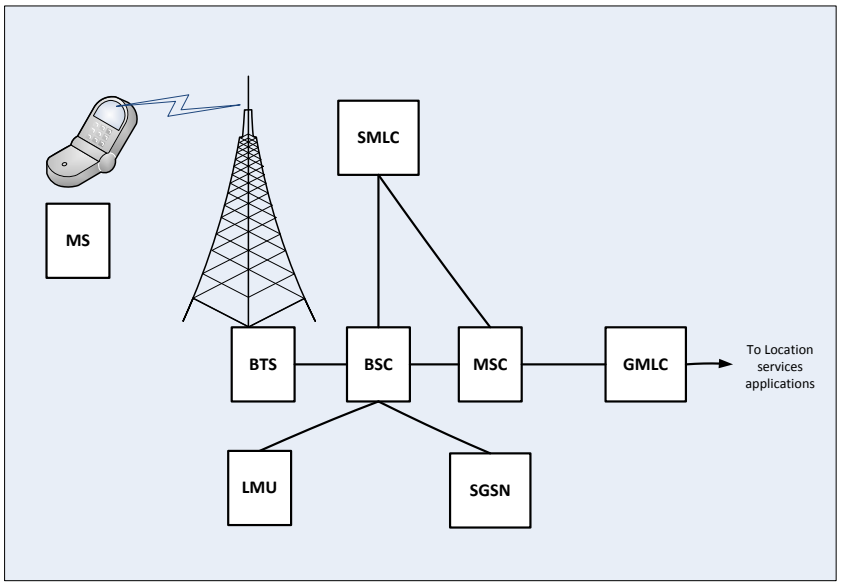

Figure 2.5: Adaptation of GSM networks for localization.

Localization with UMTS

Localization techniques are included in the UMTS standard as defined by the 3GPP. The 3GPP defined a set of methods for estimating the location of the MS using the network infrastructure. Then, operators and suppliers services should use the estimated value of the position of the MS to develop and customize their own location based services.

Unlike the GSM network, the UMTS core network includes units dedicated to perform localization. The typical structure for the UMTS network is given in Figure 2.6. The network elements involved in localization are [74]:

- The serving radio network controller (SRNC): it performs the estimation of the MS's position. Unlike GSM networks, the SMLC functions in the UMTS are directly integrated in the SRNC.

- The gateway mobile location center (GMLC): represents the entry node to the PLMN (public land mobile network) service, which provides the estimation of the terminals positions. In collaboration with the HLR (home location register), it performs the authorization and authentication of the external servers requesting information related to the position of the subscriber. These Servers are called LCS clients. The GMLC has to forward the QoS required by the LCS client to the concerned network elements. Depending on the requested QoS, the computational and material capabilities of the terminal, the SMLC selects the best technique among those supported by the network.

- The location measurement unit (LMU): it supports the SMLC by performing the radio measurements required by the localization technique. These measurements are principally the RTD (round time difference) and the RTT (round trip time).

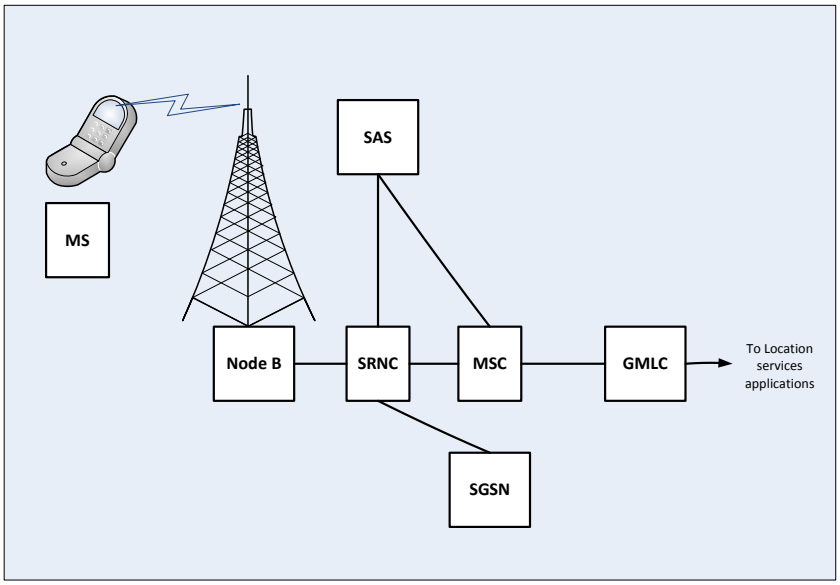

Figure 2.6: UMTS network structure as defined by 3GPP.

Localization Techniques used in cellular systems

Several localization techniques are used in GSM and UMTS networks. The easiest method is based on the identification of the cell in which the mobile lies. This method is called Cell ID method or Cell Identification. More developed methods based on time measurements, namely TOA and TDOA, and direction finding, namely AOA, are proposed. Finally, fingerprinting methods are also used in cellular systems. The TOA, AOA, and fingerprinting techniques are already described in section 2.2.2. The other localization techniques used in cellular networks are developed in this section.

- Cell-id: This method is the simplest and cheapest method compatible with all existing cellular MSs. It requires only the broadcast of one signal between the network core and the user MS. The mobile phone is located by identifying the cell to which belongs the antenna through which the communication is transmitted. The time required by this technique is very short and is equal to the search time in the database using the cell-identifiers. The accuracy of this method depends principally on the size of the cell. It is generally equal to the cell radius. Better accuracies may be possible when using sector antennas for the BS. In this case, it is possible to identify the sector in which the mobile lies. Despite its lack of precision, the majority of operators have chosen this technique for the E-112 because of its low cost of implementation.

- Uplink-TDOA (U-TDOA): this method is used because it does not require synchronization between the MS and the BSs. The MS broadcasts frames with slots dedicated for localization. This method is only applicable for mobiles located near the base stations. The localization is done in two steps. The first step consists in estimating the TDOAs. The MS emits a signal that arrives at different times at each BS. A central server collects these signals from the BSs and determines the difference arrival time between signals by subtracting the times of arrivals of different BSs or by applying a correlation of the received signals. The second step consists in the resolution of the mathematical problem related to this situation. Different methods of resolution are presented in [75] and [76]. This technique is centralized so that the complexity is placed at the network level, and its implementation depends only on the operator. Thus, if improvements or modifications are required, the operator does not need to update all MSs. Operators should not neglect such a constraint.

- Enhanced Observed Time Difference (E-OTD): Unlike the U-TDOA technique, where the mobile emits signals and the network performs localization, in the E-OTD technique, the MS itself estimates its position from signals received from different BSs. The E-OTD technique requires synchronization between the BSs implied in localization process. The LMU is an additional hardware added to the GSM network to perform precise TDOAs measurements. The same technique exists for UMTS networks, but it is known under the acronym OTDOA (Observed Time Difference Of Arrival).

2.2.4.2 Localization with WLAN

Within the WLAN-based positioning systems the most used signal parameters are RSSI, TOA and TDOA. But, RSSI is still the mostly used location-dependent parameter. Geometric lateration and mapping (fingerprinting) are the principles techniques used within WLAN positioning systems. Different localization systems based on WLANs are commercialized. Brief descriptions of some of these systems are given.

AeroScout Wi-Fi RFID Tags

AeroScout tags and software are fully integrated with the standard wireless networking equipment from multiple leading vendors. Through these partnerships, the vendors' APs can now act like RFID readers, picking up transmissions from AeroScout tags and other Wi-Fi devices, without interrupting their normal operations and without adding additional network hardware. This joint solution enables low-cost, highly reliable location-based applications, enabling hospitals, manufacturers, and other enterprises to use a single, unified wireless network for data, voice, and visibility services. Location is determined by either the AeroScout Engine or the networking vendor's location appliance, and AeroScout MobileView provides the enterprise software layer to deliver business value from Wi-Fi RFID asset location and status. The end result is that users benefit from a high return on investment, as well as a system flexible enough for numerous environments and multiple visibility applications [77].

Ekahau Positioning Engine

Ekahau positioning engine (EPE) is completely a software-only solution that utilizes the existing WLAN infrastructure. The EPE uses its predictive capabilities to determine location based on the process of site calibration that builds a signal strength model of the environment. Clients will retrieve received signal strength values and return the values to the engine for location calculations. The EPE exposes location information in the form of (x, y, floor) and logical area. The accuracy of the system is about one meter if there is a minimum of seven access points in sight but in a long term the accuracy decreases due to fluctuations in signal strength. The error in EPE can range from 1.5 meters when no one is in the room to 3.0 meters when the room is half filled with people [78].

Navizon Virtual GPS

Navizon is a positioning system that combines GPS, WLAN, and Cellular Network geometric techniques. The Navizon positioning engine (NPE) calculates the geographic location of a wireless device by analyzing the signals from nearby WLAN BSs and cellular towers, comparing them against the Navizon Network Database (NDD) of known data points. Navizon is an open system with a collaborative approach: it uses the data collected by users with a GPS device to improve the coverage and accuracy of the system when used in WLAN or Cellular positioning modes. It can be used as an Assisted GPS by switching to WLAN or Cellular positioning modes when GPS

signals are weak or unavailable such as in indoor environments. It can also be used as an alternative positioning system on devices without a GPS receiver but with a WLAN or Cellular radio. It can also be used to improve the time of acquisition of a position fix which can take up to 5 minutes with a standard GPS and less than one second with WLAN or Cellular triangulation. NAVIZON achieves 20-40m positioning accuracy using just WLAN signals [79].

Skyhook Wireless

This US company based in Boston (Massachusetts) offers a hybrid positioning system to geo-locate MS equipped with a WLAN, GSM, UMTS and/or GPS interfaces. The main attraction of the company's solution is the WLAN Positioning System (WPS) uses WLAN MAC addresses of nearby BSs (access points) and their RSS (received signal strength) as the underlying reference system. Skyhook has built a database of major North America, Europe and Asia cities with WLAN signals from public and private BSs, their locations and has identified them via their MAC address. The client scans the area every 0.1 seconds for BSs, reads each BS MAC address and compares it to the database by using a proprietary algorithm that gives more weight to stronger signals. WPS calculates the MS location each second. They claim an accuracy of within 10m to 20m and the process takes roughly 100-150 milliseconds (4 seconds from cold start) [80].

2.2.4.3 Localization with UWB

Ultra wide band is a viable technology for short-range wireless indoor communication with a number of attractive features: high-rate transmission, low complexity, low cost, and low-power consumption. This technology has generated considerable and increasing interest by many manufacturers since February 2002, when the Federal Communication Commission (FCC) opened up 7.5 GHz of spectrum (from 3.1 GHz to 10.6 GHz) for use by UWB devices. The traditional design approach for a UWB communication system uses narrow time-domain pulses of very short duration, typically on the order of a nanosecond, thereby spreading the energy of the radio signal quite uniformly over a wide frequency band ranging from extremely low frequencies to a few gigahertz [48, 81]. This method is usually called impulse radio UWB (IR-UWB). A great advantage of the short pulse modulation is the possibility to estimate the TOA with a fine resolution, which translates in ranging estimation with a less than one meter accuracy.

In March 2004, a technical group called Task Group TG4a was established. Its mission was to define an alternative physical layer, based on the UWB characteristics, for the IEEE 802.15.4 standard, the most used by wireless sensor networks (WSNs). In particular IEEE 802.15.4 specifies both the physical layer (PHY) and medium access control layer (MAC) for low-rate wireless personal area networks (LR-WPANs) while the new standard IEEE 802.15.4a based on UWB aims to propose only the physical layer with low cost and low power properties [82]. In March 2005, two optional PHYs respectively based on IR-UWB (operating in unlicensed UWB spectrum) and chirp spread spectrum (CSS) (operating in unlicensed 2.4 GHz spectrum) schemes were selected with 100% approval. Compared to the existing IEEE 802.15.4 standard, the

main interest was in high precision ranging (lower than meter accuracy) and ultra low power consumption. The two design goals low cost and low power, are achieved by the new PHY based on UWB through simple demodulation schemes, low bit rates, and low transmitted power. Low power consumption is also achieved through low duty cycle operations [48, 82].

UWB systems employ pulses of very short durations (sub-nanosecond) with very low power spectral densities. UWB signals are robust to channel fading and have very good time-domain resolution allowing for many location and tracking applications. In addition, they can facilitate design of low-complexity and low-cost transceivers. Giving these interesting characteristics, UWB systems are able to perform high accurate measurements of TOA through ranging techniques. The two principle ranging techniques defined for UWB are One Way Ranging (OWR) and Two Way Ranging (TWR). These techniques will be investigated in section 3.1.2 of chapter 3.

The AOA approach is not suited to UWB positioning for the following reasons. First, use of antenna arrays increases the system cost, annulling the main advantage of a UWB radio equipped with low-cost transceivers. More importantly, due to the large bandwidth of a UWB signal, the number of paths may be very large, especially in indoor environments. Therefore, accurate angle estimation becomes very challenging due to scattering from objects in the environment. Moreover, as we will see later, time-based approaches can provide very precise location estimates, and therefore they are better motivated for UWB over the more costly AOA-based techniques [83]. The RSSI-based approach itself cannot achieve better accuracy than other WLAN based systems since the unique characteristic of a UWB signal, namely the very large bandwidth, is not exploited to increase the best achievable accuracy [83].

For positioning systems employing UWB radios, time-based schemes provide very good accuracy due to the high time resolution (large bandwidth) of UWB signals. Moreover, they are less costly than the AOA-based schemes, the latter of which is less effective for typical UWB signals experiencing strong scattering. Although it is easier to estimate RSSI than TOA, the range information obtained from RSSI measurements is very coarse compared to that obtained from the TOA measurements [83].

2.2.4.4 Localization with sensor networks

WSN are particularly interesting in hazardous or remote environments, or when a large number of sensor nodes have to be deployed. The localization issue is important where there is an uncertainty about some positioning. If the sensor network is used for monitoring the temperature in a building, it is likely that we can know the exact position of each node. On the contrary, if the sensor network is used for monitoring the temperature in a remote forest, nodes may be deployed from an airplane and the precise location of most sensor may be unknown. An effective localization algorithm can then use all the available information from the motes to compute all the positions. Thus, most WSN applications are useless if no information about node locations is available. The IEEE 802.15.4a Zigbee and UWB physical layers are the most commonly used physical layer technologies in WSNs today. ZigBee is a communication technology intended for WSN applications that have relatively low requirements on throughput and latency [84–86]. The key features of ZigBee are low complexity, low power consumption,

and low data rate transmissions, to be supported by low-cost stationary or moving devices.

The positioning problem in WSNs can vary widely in character from network to network, and from application to application. Depending on the available hardware, the available measurement data, and the application requirements, different positioning approaches for sensor nodes may be more or less appropriate. In some cases fixed infrastructure can be installed throughout the network deployment area in order to aid in the positioning of mobile sensor nodes [87]. This infrastructure may include anchor nodes at known location, or central processing stations with extended resources in terms of computational power and/or energy supply. In other networks, for instance networks of mobile nodes that move in an unpredictable fashion over large remote areas, basing the positioning scheme on fixed infrastructure may not be feasible. If this is the case, then the sensor nodes themselves are the only resources available to the positioning algorithm.

The expected size of the network, i.e. the node density and coverage area of the network, also plays an important role in the design process. Some WSN applications that have been envisioned in the literature involve thousands of sensor nodes, densely spread out over very large areas. In such large networks, it is of paramount importance that the complexity of the positioning algorithm is not a rapidly increasing function of the number of nodes and/or connectivity level of the network, i.e. algorithm scalability is often an important factor to consider. Other factors that influence the choice and design of a WSN positioning algorithm include whether the sensor nodes are individually identified by their own identifier (ID), and what measurement capabilities individual nodes have in terms of measuring the range to neighboring nodes, measuring the angle of arrival of received signals, etc.

2.3 Beyond 3G Networks and New Challenges

2.3.1 Vision of Beyond 3G networks

The current wireless landscape over the different regions is characterized by the presence of distinct wireless standards (e.g. GSM, UMTS, EDGE, HSPA, WLAN, DVB, Bluetooth, etc). In the future, it is expected that this landscape will further be enriched by new higher data rate standard (e.g. LTE, LTE-Advanced, Wimax). Moreover, there are additional emerging cognitive standards (e.g. IEEE 802.22, IEEE SCC41) as well as provision of self-organization by standardized interfaces.

There is no doubt that one key capability of a future wireless Radio Access Technology (RAT) is that it should provide truly mobile broadband, i.e. the combination of high capacity and close to full mobility and coverage. The development of the future mobile systems, with the introduction of higher data rate RATs can be approached in two distinct ways: Both an evolutionary as well as a revolutionary approach are envisaged [88]. In the revolutionary scenario, the new high data rate RAT (e.g. 4G) is foreseen to replace all existing standards, enhancing the mobile data rate and satisfying the set of requirements of the mobile user as well as of wirelessly interaction machine to machine systems. In the evolutionary case, any new high data rate RAT is seen as one new component enriching the mobile/wireless environment, thus complementing

all other existing technologies. In the latter case the key challenges are in facilitating dependable and seamless interoperation and interoperability between standards. The high-level system view of Figure 2.7 depicts one potential vision for this evolutionary wireless telecommunications future, the user being at the center and the overall set of radio access technologies allowing a seamless and efficient end-to-end connectivity. Following this vision, the evolution towards 4G will encompass the introduction of new technology segments, including potential new releases of legacy radio access technologies or/and introduction of radically new radio access systems [88].

The wireless community strives towards offering all users broadband everywhere at all times. Mobile broadband has already taken off and will continue to grow. The trend of the mobile wireless access technologies is to achieve higher data rates and still supporting full mobility. Also the nomadic wireless access technologies target the high data rates and have the potential to cover large areas even though mobility is not supported. One common objective can however be identified for both technology tracks, namely to offer broadband access to users independently of time and position, enabling in this case to offer the best seamless experience to the users.

From a localization vision, the main characteristics of B3G/4G networks are heterogeneity, density, and connectivity. By heterogeneity we mean the various and different RATs to which a mobile device can be conjointly connected. B3G/4G networks are very dense at both infrastructure level and users level. This density may offer a seamless connectivity to MSs. The challenges which may be imposed by these characteristics and our vision of B3G localization systems which respond to these challenges are presented briefly in next two subsections, namely 2.3.2 and 2.3.3. These topics are the materials of the rest of this dissemination.

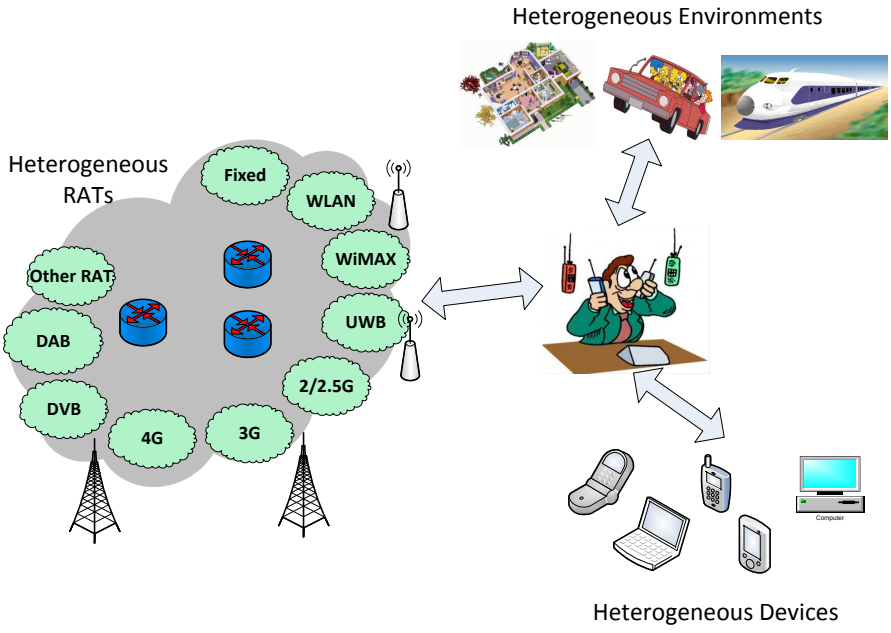

Figure 2.7: Heterogeneous B3G/4G landscape.

2.3.2 New challenges for Localization in Beyond 3G

In B3G networks, the MS may be able to support conjointly two or more radio access technologies. Indeed, currently developed mobile terminals are mostly able to connect to 2G, 3G, WLAN, Bluetooth, and Infrared networks conjointly. This fact has its advantages but imposes new constraints to B3G localization systems. The advantages are:

- Availability of location-dependent parameters: Despite the fact that RSSI measurements are usually available with no additional cost, in B3G networks other location-dependent measurements are usually available thanks to different technologies supported by terminals. In lateration based techniques, the minimum numbers of measurements necessary to perform localization are three in 2D and four in 3D. Hence, getting the necessary amount of TOA or TDOA, for example, is not usually possible in one RAT based networks especially in indoor and personal networks (WLAN, UWB, Bluetooth, etc) where the environment can be sufficiently covered by only one or two access points. This constraint is reduced, and generally omitted, in B3G networks.

- Larger choice from localization techniques and schemes: When various LDPs are available, the system may have the ability to choose from different localization techniques and schemes depending on the required accuracy, the available measurements, and the computational capabilities and resources of the MS and the localization system.

- Fusion of nature- and source- different parameters: In B3G, available LDPs may be different in source (i.e. RAT) and in nature (time-based, power-based). One interesting localization technique consists in the fusion of these different parameters in order to enhance positioning accuracy.

The principle constraints, which should be taken into consideration in order to conceive B3G localization systems, are:

- Different natures of LDPs: The question here is how to fuse measurements different in nature. How can power-based parameters (RSSI) be fused with time-based parameters (TOA and TDOA) to enhance positioning accuracy?

- Different sources of LDPs: This constraint is imposed mainly when synchronization is needed to perform LDPs measurement especially in the case of TOA or TDOA. In such cases, the synchronization of anchors from different RATs is difficult or even impossible.

- Different accuracies of LDPs: These differences of accuracies can be either between parameters different in nature or different in sources. For example, the cellular RSSI measurements have not the same accuracy as Indoor RSSI; The UWB ranging is generally more accurate than WLAN ranging. The question here is about the effect of imprecise LDPs on localization accuracy and whether such imprecise LDPs should be used or discarded.

- Complexity and computation resources: These characteristics of B3G localization systems may introduce additional complexity and consume more resources in order to perform fusion of LDPs and the computation of the position. The question here is how can the system offer the requested accuracy using the minimum resources?

- Overhead and latency: The use of ranging techniques, the higher amount of LDPs, and the requested higher positioning accuracies which characterize heterogeneous localization systems may incur some overhead cost. The additional latency, data traffic, and processing for localization may affect the performance of the underlying network. Such effects should be understood before selecting a localization scheme or/and technique.

- Architecture and design of localization systems: Since B3G networks are seen as a network of networks, the design and architecture may not be easily decided.

2.3.3 Our vision of B3G localization systems

In this work, our vision of B3G localization system is based on these different realistic assumptions:

- The development of hardware technologies increases more and more the capabilities and capacities of mobile terminals. Furthermore, user terminals are able to support different RATs. Hence, we assume that localization is done locally in the user terminal. Nevertheless, the user terminal can request the help of the infrastructure if it has not the ability to reach the required accuracy of localization. It is anticipated that the scope of action the MS can achieve will strongly depends on the context and circumstances which will affect strongly the number of available neighbor devices (see Figure 2.8) [89]. Three cases can be distinguished:

    1. A low number of neighbors are available: in this case the only solution is to rely on the infrastructure and possibly on fingerprinting techniques if available based on prior information stored in a database of the association between a given position in the radio scene, (possibly in a geographical database) and a set of LDPs gathered by the MS.
    2. A medium number of neighbors are available: in this case the number of neighbor devices is assumed to be sufficient to provide the required positioning accuracy through triangulation and/or trilateration. The goal is to carefully complement the LDPs available by default (e.g. cellular or indoor RSSI measurements) by the least number of additional observables (e.g. shorter TOA or TDOA measurements). The assumption made here is that the system will try to reduce the number of ranging procedures to preserve resources. The question addressed is how to choose the best set of neighbors which can achieve requested PA with the minimum of resources.
    3. A high number of neighbors are available: in this case there is such a high density of available nodes that the knowledge of their short-range connectivity (e.g. the relative distances measured between them through TOA or

RSSI estimation) may enable to access directly to precise positional information either based on centralized or distributed localization approaches.

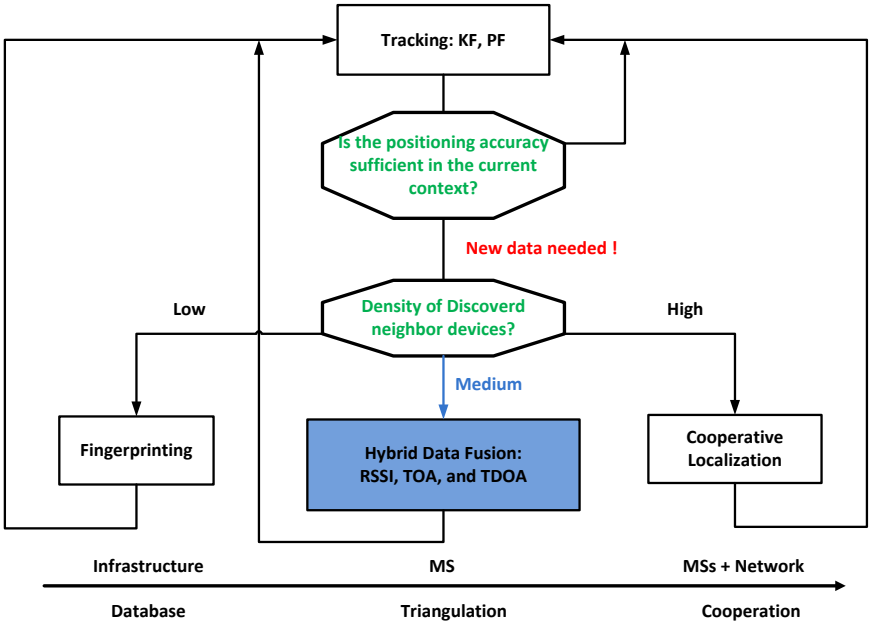

Figure 2.8: Different localization schemes.

- Since RSSI measurements are usually available, we assume here that the localization is preferably done with only RSSI measurements. Other parameters, namely time-based, can be measured in order to be fused with RSSI and achieve the required accuracy. The goal is to reduce as possible the use of time-based parameters because they demand more resources and induce more complexity.

- Before performing the localization task, sophisticated criteria should be defined in order to choose the best localization scheme (i.e. the number, the nature, and the position of LDPs which should be gathered). The application of these criteria may reserve resources and time while keeping a good positioning accuracy.

Hence, our objectives in this thesis are:

1. To study principle LDPs (i.e. RSSI, TOA, and TDOA) and to propose simple statistical models for them. These models will be Gaussian and extracted from real measurements campaign. To perform this task, techniques of extracting these LDPs from measurements campaigns will be studied and proposed. From this measurements campaign available during this thesis, we have to construct a location-dependent database which will serves to evaluate the proposed models and localization techniques;

2. To study non-hybrid and hybrid localization schemes based on RSSI, TOA, and TDOA. We will propose techniques of position estimation from these LDPs. These schemes and techniques have to consider the constraints and properties

of B3G described above. The localization techniques will be classified into algebraic and geometric techniques. On the one hand, algebraic techniques are based on mathematical and analytical formulations of the localization problems. Once the localization problem is formulated mathematically, solvers should be proposed in order to resolve it and estimate the targeted position. On the other hand, a natural approach is proposed during this thesis and consists in expressing each LDP as a geometric constraint and then use appropriate techniques to find the intersection of all constraints that represent a localization problem and hence estimate the targeted position.

3. To assess the performances of these localization techniques theoretically using Cramer-Rao Lower Bounds (CRLBs) and empirically using measurements campaigns. The definition of CRLB as a prior information about the best reachable positioning accuracy makes it a good candidate to be a criterion for the choice of appropriate localization schemes in order to achieve the best requested positioning accuracy.

2.4 Conclusion

The purposes of this chapter were twofold. First, it has surveyed the whole location based services, techniques, and systems. Second, it has exposed our vision of localization for future B3G networks. On the one hand, we have shown that LBSs are very various and more and more requested by both human users and network operators in order to make benefits, facilitate the life, but also in order to enhance the communications systems which is the first goal of network-oriented LBSs. Moreover, different are the localization techniques and systems. This variety is due to that of LBSs, communications standards, and localization applications. Thus, for each service, for each system, and for each application, a suitable localization system should be implemented and a suitable localization technique should be chosen.

On the other hand, this chapter has presented the characteristics of B3G networks which may affect localization systems and techniques. This characteristics are mainly heterogeneity of radio access technologies, density of devices, and seamless connectivity. Then, the main features of our vision of B3G localization techniques and systems have been explained. This vision, which will be argued and demonstrated in the next chapters, is mainly based on the fusion of LDPs in an opportunistic way in order to reduce complexity and cost and which aims to guarantee an optimal use of available resources and a preservation of throughput.

3

Measurement and modeling of Location-Dependent Parameters

After giving a state of the art about different localization fields in the second chapter, we get on the road of our contribution by presenting in this third chapter the considered location-dependent parameters. Like the second chapter, this chapter is organized into three sections. The first section (3.1) reviews LDPs measurement techniques in different wireless standards with a special focus on TOA based ranging techniques for UWB standard. The second section (3.2) describes the measurements campaign done within the framework of FP7 European WHERE project. This measurements campaign is based on UWB technology and it is done in an indoor environment. From this campaign, a database of LDPs is extracted and serves first to model LDPs and second to evaluate and study the proposed localization techniques. The different models extracted from this database are then described in the third section (3.3) where we evaluate mainly the TOA- and RSSI- based ranging techniques and path-loss models.

3.1 Review of Location-Dependent Parameters Measurement techniques

3.1.1 RSSI Measurement Techniques

RSSI based localization methods were first introduced in 1969 [90]. RSSI is used to be the easiest and cheapest modality for wireless localization because RSSI information can be obtained at no additional cost with each radio message sent or received [41]. RSS is the power (i.e. the magnitude of electrical field) being received by an antenna. Generally, the higher the level of RSS is the stronger is the signal. Different RSS indicators (RSSI) can be defined to describe this received power. RSSI can be the value of RSS itself, the attenuation experienced by the power during the propagation,

or others.

The attenuation is known as path loss (PL) and it is equal to the difference between the transmitted and received power. RSS and PL are usually expressed in decibels above a reference level of one milliwatt (dBm). The power attenuation is mainly the result of the propagation, the fading, and channel fluctuations. First, the power is attenuated as a function of the distance. This attenuation is caused by the natural expansion of the radio wave front in free space. Fading may either be due to multipath propagation, referred to as multipath induced fading, or due to shadowing from obstacles affecting the wave propagation, referred as shadow fading or shadowing [91]. These propagation phenomena make difficult the prediction of RSSI in radio propagation channels. Hence, different path loss models are proposed. These PL models are very interesting for localization issues since they relate RSSI to the distance (so to the location of the device). Using these PL models, RSSI and ranges can be easily estimated in each point of space. Nevertheless, the accuracy of RSSI estimation depends strongly on the accuracy of the used PL model.

The RSSI information is made available with no additional cost with novel mobile embedded technologies. Indeed, MSs based on android, windows mobile, or even J2ME provide a number of methods that claim to return the received signal strength. The most known methods are:

- *SystemState.PhoneSignalStrength()* for Windows Mobile 6
- *RIL_GetCellTowerInfo()* for Windows Compact Edition
- *android.telephony.NeighboringCellInfo.getRssi()* for Android

This "free" availability of RSSI is a concrete justification for our vision which proposes the use of available RSSI and try to reach the required accuracy while minimizing the number of additional time-based LDPs (i.e. TOA and TDOA). An example of application developed during the thesis is presented in Appendix A. This application is developed using *C#* language and aims to get RSSI from Bluetooth, WLAN, and GSM networks.

3.1.2 TOA Ranging Techniques

In this subsection, we start by presenting the famous TOA based ranging techniques (one-way ranging -OWR- and two-way ranging -TWR-). Then, we survey the techniques implemented within wireless standards, namely WLAN and UWB. Finally, we present the techniques based on the UWB channel impulse response (CIR).

3.1.2.1 OWR and TWR ranging techniques

The one-way ranging technique (see Figure 3.1) is based on one transmission of a signal between the Tx and the Rx. This technique supposes that the two sides of the link are synchronized. The TOA is then measured as the difference between the time of reception at the Rx and the time of transmission at the Tx. By contrast to the OWR technique, the two-way ranging technique (see Figure 3.2) is based on two transmissions of a signal between the Tx and the Rx. These two transmissions

overcome the constraint of synchronization. A short time of signal reply must be taken into consideration in this technique. This time is the time spent by the Rx to resend the received signal. The TOA is then measured as the half of the difference between the time spent by the Tx to receive the signal and the time of reply.

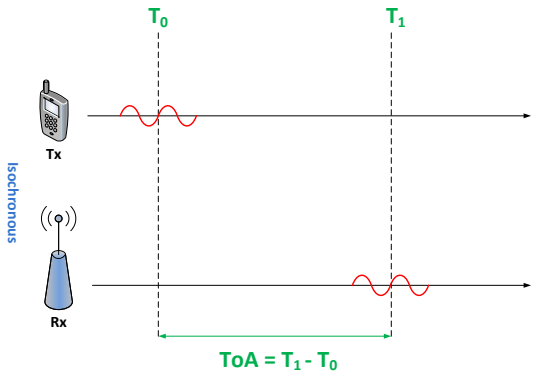

Figure 3.1: One Way Ranging.

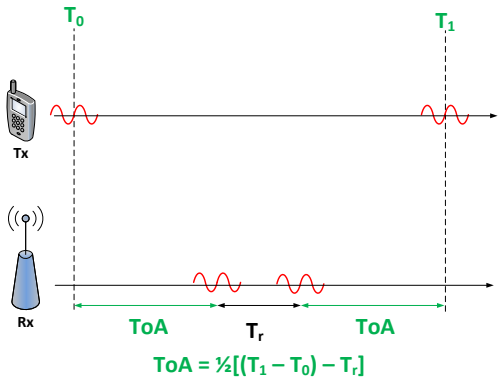

Figure 3.2: Two Way Ranging.

3.1.2.2 TOA ranging techniques in Wireless Standards

TOA ranging techniques in UWB standard

The impulse radio (IR) UWB system defined by the IEEE 802.15.4a standard, specifies an optional ranging capability [86]. According to this standard, the ranging capable device implementing the ranging support is called RDEV, the ranging frame is called RFRAME. The RFRAME is indicated by setting a ranging bit in the PHY header of the IEEE.802.15.4a packet [86]. A range between two RDEVs is determined typically via two-way ranging technique based on the exchange of a RFRAME and tracking its arrival time as illustrated in Figure 3.2. This is called two-way time-of-arrival (TW-TOA).

For a single path additive white Gaussian noise (AWGN) channel, the Cramer-Rao lower bound for the TOA estimate is expressed as [48]:

$$\sqrt{\mathrm{Var}(\mathrm{TOA})} \geq \frac{1}{2\sqrt{2}\pi\sqrt{\mathrm{SNR}}\beta} \tag{3.1}$$

where SNR is the signal-to-noise ratio and β is the effective signal bandwidth. Apparently, high SNR and/or wider bandwidth help reduce the ranging error.

UWB signals have relative bandwidths of more than 20% or absolute bandwidths of at least 500 MHz [92]. This large bandwidth provides high time resolution and facilitates better detection of leading signal edge. Also, the probability of some frequency components penetrating through or going around an obstacle increases. Therefore, it becomes more likely to encounter a line-of-sight (LOS) signal [48]. In other words, both high resolution and penetration capability make UWB signals suitable for ranging purposes. Nevertheless, this accuracy may be reduced by multipath propagation, NLOS, and multi-user interferences (MUI). In the IEEE 802.15.4a standard, the packet

preamble is designed in consideration of multipath channels to make first path detection easier [48].

The IEEE 802.15.4a packet consists of a synchronization header (SHR) preamble, a physical layer header (PHR) and a data field. The SHR preamble is composed of the (ranging) preamble and the start of frame delimiter (SFD) [93]. The number of symbols in the ranging preamble are specified according to application requirements. There can be 16, 64, 1024 or 4096 symbols in the preamble depending on the channel power delay profile, the SNR of the link and capabilities of RDEVs. The longer lengths, 1024 and 4096, are preferred for non-coherent receivers to help them improve the SNR via processing gain. Hence, they can have a reasonably accurate TOA estimate [93]. The SFD signals the end of the preamble and the beginning of the PHY header. In other words, it is used to establish frame timing; and its detection is important for accurate counting of the reply time. It can consist of 8 or 64 symbols [93].

The standard adopts a slightly modified version of the conventional two way ranging protocol as mandatory. Moreover, by symmetric double-sided RFRAME two-way signal exchanges, it is also possible to eliminate clock offset differences between the RDEVs. Both these protocols estimate the range without a common timing reference. In some applications, the range information is a critical deliverable. Therefore, the standard also supports private ranging to safeguard the integrity of the ranging traffic itself. Further descriptions of ranging in UWB are given in [48] and [93].

TOA ranging techniques in WLAN standard

In order to avoid the synchronization between the MS and the APs, TOA can be estimated from round-trip time (RTT) technique. RTT is the time a signal takes to travel from a transmitter to a receiver and back again. As can be seen in Figure 3.3, RTT is estimated by measuring the time elapsed between two consecutive frames under IEEE 802.11 standard: a link layer data frame sent by the transmitter (the MS) and the reception of the corresponding link layer acknowledgment ACK from the receiver (the AP).

The RTS and CTS frames of the 802.11 standard can be also used to estimate RTT. As described in Figure 3.4, the receiver replies with the ACK message after waiting for a short inter frame spacing (SIFS) duration. Since the waiting time SIFS is the shortest waiting time and other stations can only access the medium after a longer waiting period DCF inter-frame spacing (DIFS), no other stations can access the medium in the meantime to cause a collision. The other stations must wait for DIFS plus their backoff time in the contention period. In other words, the ACK message has the highest priority. This mechanism ensures the proper transmission and reception of the ACK message.

In [49], the authors proposed to measure the RTT by using the internal clock module ($f_c = 44$ MHz) of a WLAN card. The module starts counting cycles when it detects the end of transmission of a data frame, and it stops when the corresponding ACK frame arrives. Due to the variability of the radio channel multi-path, the clock quantification error, delays due to electronics of the hardware module and the relative clock drift, the RTT is time-variant. In order to mitigate these errors, RTT is estimated as the average value of different RTT samples [49].

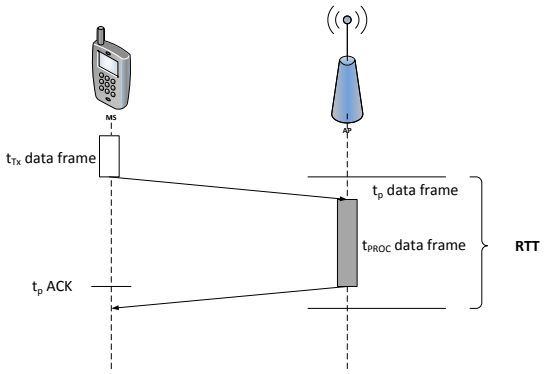

Figure 3.3: RTT measurement using IEEE 802.11 data/ACK frames.

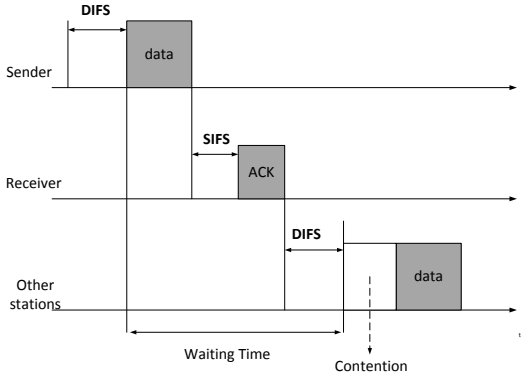

Figure 3.4: Unicast data transfer mode for IEEE 802.11.

3.1.2.3 CIR-based ranging techniques

Different techniques have been proposed for estimating TOA using channel impulse responses. The simplest and easiest technique considers that the strongest path is the first path. That is, the TOA is the time of arrival of the strongest path. However, this assumption is not usually applicable in multipath conditions. In these conditions, the first path may not be the strongest path. In this section we present two techniques of CIR-based ranging. These techniques are based on the choice of a threshold to detect the first path. The first technique is classic and widely used for UWB ranging [94–98]. The second technique is novel and is presented in this section. Notice that the two techniques are being applied on the squared CIR.

Channel IR model

To proceed, we consider a multipath channel with an impulse response expressed as follows:

$$c(t) = \sum_{n=1}^{N} a_n \delta(t - \tau_n) \tag{3.2}$$

where a_n and τ_n are, respectively, the amplitudes and time-delays of the N propagation paths. τ_1 is the time of arrival of the first path (i.e. The TOA) which we search to find out.

The received signal can then be expressed as:

$$r(t) = \sum_{n=1}^{N} a_n \omega(t - \tau_n) + n(t) = s(t - \tau_1) + n(t) \tag{3.3}$$

where $\omega(t)$ is the isolated ideal received pulse with duration T_p (i.e. in the absence of multipath and noise) and $n(t)$ is the additive white Gaussian noise (AWGN) with zero mean and spectral density $\frac{N_0}{2}$. In all the rest of this chapter, we use the sampled form of $r(t)$ with a sample rate $\frac{1}{T_s}$ where T_s is the sample duration. Let M be the number of samples which compose $r(t)$. Hence, if the received signal is observed in

the interval $[0, T]$, we get $T = M.Ts$. The m^{th} sample occurs at the time $t_m = m.Ts$ $(m \in (1, ..., M))$.

Given a channel impulse response modeled by (3.3), the goal is to estimate τ_1, i.e. the TOA of the first path. In LOS situations, there is no difficulty to estimate the TOA. In this case, the best estimate is the delay of the strongest received path. In NLOS+DP (i.e. non line of sight but with existence of direct path, DP) and NLOS-DP (i.e. without DP), usually the first path is not the strongest path. Hence, we need more elaborated techniques than the strongest path based method to estimate TOA.

Thresholding the CIR (Th-TOA)

The Th-TOA ranging approach is the most natural and has been described in [99]. This approach consists in defining a threshold above the noise level such as limiting as much as possible false alarm on noise peak while maintaining a sufficient level of detection. This technique involves the following steps:

- Consider the squared CIR $r^2(t)$;
- Compare the actual value of $r^2(t)$ to the appropriate threshold;
- Search the first crossing point and let m be the corresponding sample. The TOA estimate $\hat{\tau}_{th}$ is then given by $m.Ts$.

Thresholding the normalized cumulative CIR (Cum-TOA)

We define the cumulative energy $E_r(\tau)$ at time τ of the CIR $r(t)$ as follows:

$$E_r(\tau) = \int_0^\tau r^2(t)dt = \int_{\tau_1}^\tau s^2(t-\tau_1)dt + \int_0^\tau n^2(t)dt + 2\int_{\tau_1}^\tau s(t-\tau_1)n(t)dt \tag{3.4}$$

$$E_r(\tau) = E_s(\tau) + E_n(\tau) + 2\int_{\tau_1}^\tau s(t-\tau_1)n(t)dt \tag{3.5}$$

where $E_s(\tau)$ and $E_n(\tau)$ are the integrated energy of respectively the useful signal $c(t)$ and the noise $n(t)$ until time τ. The last integral $\int_{\tau_1}^\tau s(t-\tau_1)n(t)d\tau$ can be neglected assuming independence between signal and centered noise. This leads to the following expression:

$$E_r(\tau) \approx E_s(\tau) + E_n(\tau) \tag{3.6}$$

The Cum-TOA ranging technique apply the same steps of Th-TOA technique when replacing $r^2(t)$ by the cumulative CIR $E_r(t)$ defined by:

$$E_r(t) = E_s(t) + E_n(t),\ t \in [0, T] \tag{3.7}$$

Figure 3.5 presents examples of respectively CIR and cumulative CIR with different chosen thresholds.

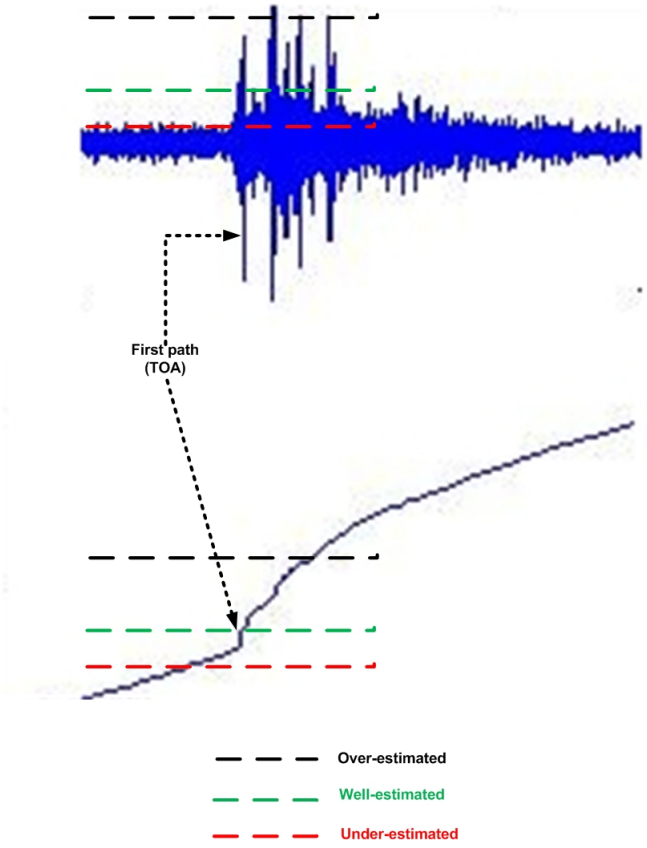

Figure 3.5: Choice of thresholds in both CIR and cumulative CIR cases.

The choice of thresholds

The critical issue with these two techniques is the choice of appropriate thresholds. With a small threshold, the probability of detecting noise peaks (false alarm) is high. Whereas, with a large threshold, it is the probability of skipping the direct path which is higher (see Figure 3.5). To optimize threshold, we consider the CIR dynamics. The threshold is defined relatively to the maximum value of the signal in order to reduce estimation error. Let γ_{th} and γ_{cum} the appropriate thresholds for respectively Th-TOA and Cum-TOA ranging techniques. We get γ_{th} and γ_{cum} respectively by:

$$\gamma_{th} = \kappa_{th} E_M \tag{3.8}$$

$$\gamma_{cum} = \kappa_{cum} E_{0-M} \tag{3.9}$$

where E_M and E_{0-M} are respectively the energy carried by the strongest path and the cumulative energy carried until the strongest path and it is given by $E_{0-M} = E_r(\tau_M)$ with τ_M is the time of arrival of the strongest path.

In the first method (Th-TOA), the threshold should be set between zero and E_M in order to estimate the TOA. For this, κ_{th} should be set in $]0, 1[$. Moreover, κ_{th} should be chosen representative of the channel dynamics. Since in UWB the detection of strongest path is made easier thanks to high time precision, the strongest path energy

E_M and the total received energy E_T are the easiest parameters which can be extracted. Using these two parameters and respecting the above constraints, three different κ_{th} can be defined:

$$\kappa_{th} = \begin{cases} \frac{\sqrt{E_T}-\sqrt{E_M}}{\sqrt{E_T}+\sqrt{E_M}} \\ \text{or} \\ \frac{\sqrt{E_T}-\sqrt{E_M}}{\sqrt{E_T}} \\ \text{or} \\ \sqrt{\frac{E_M}{E_T}} \end{cases} \tag{3.10}$$

These three different quantities can be easily obtained from the CIR and they have the property of being in $]0,1[$. Hence, γ_{th} is chosen from values in $]0, E_M[$.

Equivalently to κ_{th}, κ_{cum} should have the same properties when replacing E_M by E_{0-M}. Hence, different possible values of κ_{cum} are:

$$\kappa_{cum} = \begin{cases} \frac{\sqrt{E_T}-\sqrt{E_{0-M}}}{\sqrt{E_T}+\sqrt{E_{0-M}}} \\ \text{or} \\ \frac{\sqrt{E_T}-\sqrt{E_{0-M}}}{\sqrt{E_T}} \\ \text{or} \\ \sqrt{\frac{E_{0-M}}{E_T}} \end{cases} \tag{3.11}$$

The comparison of these different thresholds and the choice of the adequate threshold for each ranging technique are done statistically based on UWB measurements campaign in section 3.2.2.

3.1.3 TDOA Ranging Techniques

3.1.3.1 Cross Correlation

A straightforward method for estimating the TDOA is to cross-correlate the signals arriving at a pair of anchor nodes (ANs). The cross-correlation of two signals $r_1(t)$ and $r_2(t)$, received from RN_1 and RN_2 respectively, is given by [100]:

$$R_{1,2}(\tau) = \frac{1}{T}\int_0^T r_1(t)\, r_2(t+\tau)\, dt \tag{3.12}$$

and it has a peak for t equal to the exact TDOA, in the absence of errors. This method is widely used especially in cellular systems [100].

3.1.3.2 TDOA ranging techniques in WLAN and UWB

In [101], authors presented a method to estimate the TDOA by using the IEEE 802.11 link layer frames without the need to have the APs synchronized. Suppose to have three APs (AP_0, AP_1, and AP_2) at known locations. Firstly, the AP_0 sends a data frame to the MS at time t_0, then the MS replies with an ACK message after it receives the data. Meanwhile AP_1 and AP_2, monitors the communication between AP_0 and

MS and measures the time delays between the arriving time of the data frame and the ACK message, i.e. τ_{11} and τ_{21} as shown in Figure 3.6 and Figure 3.7.

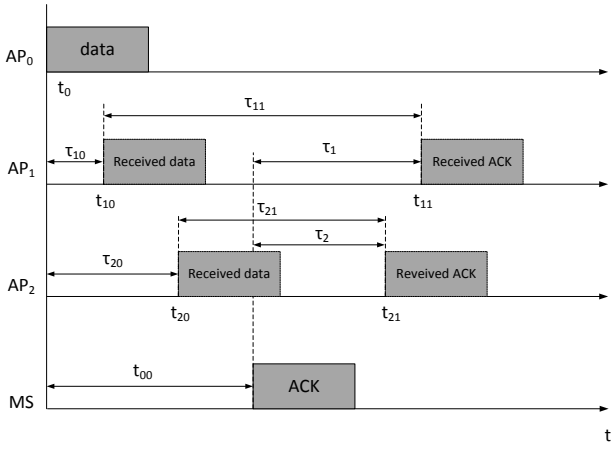

Figure 3.6: TDOA ranging method for 802.11 WLAN networks.

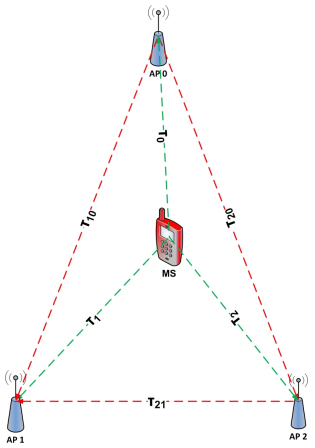

Figure 3.7: Sample Scenario.

AP_1 and AP_2 receive the data frame at τ_{10} and τ_{20}, and ACK message at $\tau_{11} + \tau_{10}$ and $\tau_{21} + \tau_{20}$, respectively. The delays τ_{10} and τ_{20} are TOAs from AP_0 to AP_1, and to AP_2, respectively, while the delays τ_1 and τ_2 are TOAs from MS to AP_1 and to AP_2, respectively. Since the distances from AP_0 to AP_1 and to AP_2 are known, the TOAs τ_{10} and τ_{20} can be accurately estimated. Therefore, the TDOA from MS to AP_1 and AP_2 can be obtained as follows:

$$\begin{aligned} TDOA_{12} &= \tau_2 - \tau_1 \\ &= [(\tau_{20} + \tau_{21}) - \tau_{00}] - [(\tau_{10} + \tau_{11}) - \tau_{00}] \\ &= (\tau_{20} + \tau_{21}) - (\tau_{10} + \tau_{11}) \end{aligned} \tag{3.13}$$

Using this method, AP_1 and AP_2 have only to measure time delays τ_{11} and τ_{21}, respectively, i.e. the delay between arriving times of data frame and ACK message. The same principle of TDOA measuring method can be used for systems using the optional RTS/CTS mechanism. Since this measurement is a time delay, it is not necessary to have AP_1 and AP_2 synchronized to a common reference time. However, it should be noted that to measure the time delay accurately, a high-precision timer is needed at each AP. In fact, since the chipping rate is 11 MHz for 802.11 WLAN systems, an alignment of the received PN code with the local PN code by using the conventional correlation techniques is not sufficient for ranging.

In [102], authors proposed a similar technique for UWB networks. In UWB, TDOA measurements may be more accurate because of the high time precision due to large-bandwidth allocated to UWB communications. The localization by TDOA is based on the perfect synchronization between anchor nodes.

3.2 Measurements Campaign and Location Dependent Parameters Database

In order to model location-dependent parameters and to evaluate the localization techniques proposed during this thesis, we have used a measurements campaign done jointly by the CEA-LETI and SIRADEL companies in the framework of FP7 WHERE project [103]. This measurements campaign is based on UWB standard. This campaign of measurements would allow us to better evaluate localization techniques in realistic conditions and environments. A database of location-dependent parameters is then constructed from these measurements. This database will be used for the evaluation of localization techniques, the modeling of location-dependent parameters, and the comparison of measurements and simulations results.

3.2.1 UWB Measurements campaign

The measurements campaign have been done in the framework of the FP7 WHERE project. It has been carried out by the CEA-LETI in the SIRADEL headquarter building in Rennes, France (Figure 3.8). The goal was to collect UWB impulse responses in a same local area. In order to assess small-scale fading, impulse response measurements are made on several square grids. The investigated area is limited to a few rooms and offices on the first floor of the SIRADEL building (Figure 3.9).

In Figure 3.9, the most important pieces of furniture (metallic cupboards and tables) are plotted. These pieces should be taken into consideration when modeling the channel propagation and extracting location-dependent parameters in order to better understand the effects of radio propagation, channel characteristics, and environment components on extracted parameters. Nevertheless, many other small pieces of furniture (chairs, printers, refrigerator, etc) are present when performing measurements but not presented in the figure for simplicity.

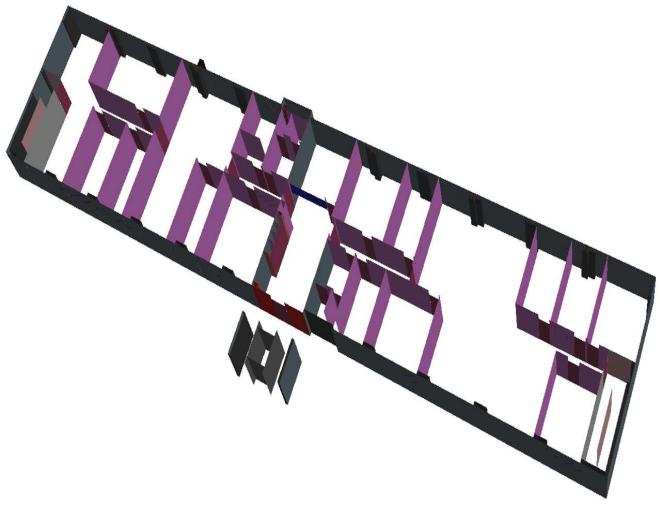

Figure 3.8: Top view of Siradel building (Ray tracing model).

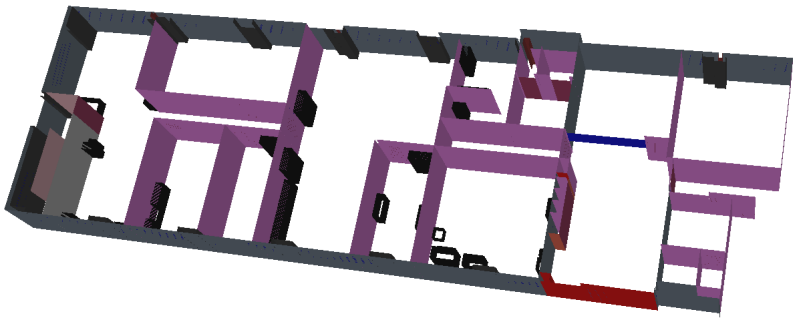

Figure 3.9: Top view of investigated rooms in the first floor of Siradel building (Ray tracing model).

The time-domain channel sounder is mainly composed of a pulse pattern generator, a wideband digital oscilloscope, and UWB antennas. The whole measurement setup is illustrated in Figure 3.10 [104]. On the transmitter side, a Pulse Generator (**Picosecond Pulse Lab 4050B**) with two additional impulse forming networks and a power amplifier fit the desired UWB impulse shape in the $3-7$ GHz bandwidth (see Figure 3.11). On the receiver side, a wide-band Digital Oscilloscope (*Tektronix TDS 6124C*) is used with a sampling rate of 20 Gsps in real-time. In order to improve the time precision, a *sinc* interpolation is used in order to get a final time step of 5ps. Moreover, the signal is averaged over 16 snapshots for increasing the signal-to-noise ratio (SNR). For dynamic range consideration, it is also necessary to use Low Noise Amplifiers in front of oscilloscope input channels. On both Tx and Rx sides the same kind of antenna is used. The radiation pattern is omni-directional in azimuth with a dipolar radiation pattern in elevation [103].

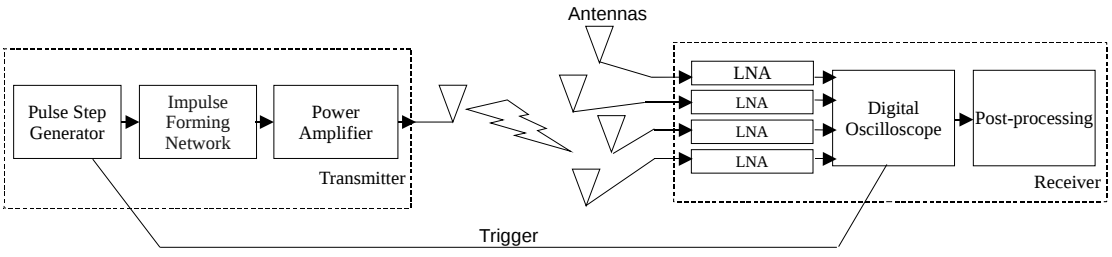

Figure 3.10: Overall measurement chain.

During the campaign, four fixed receiver positions were defined and 302 measurement points were selected for the transmitter positions [103]. Then, two measurement configurations were performed:

- Static small-scale measurements with the transmitter and the four receivers at the same height (120cm between the floor and the antenna ground plan).
- Static small-scale measurements with the four receivers at the same height (120cm between the floor and the antenna ground plan) and transmitter at 150cm.

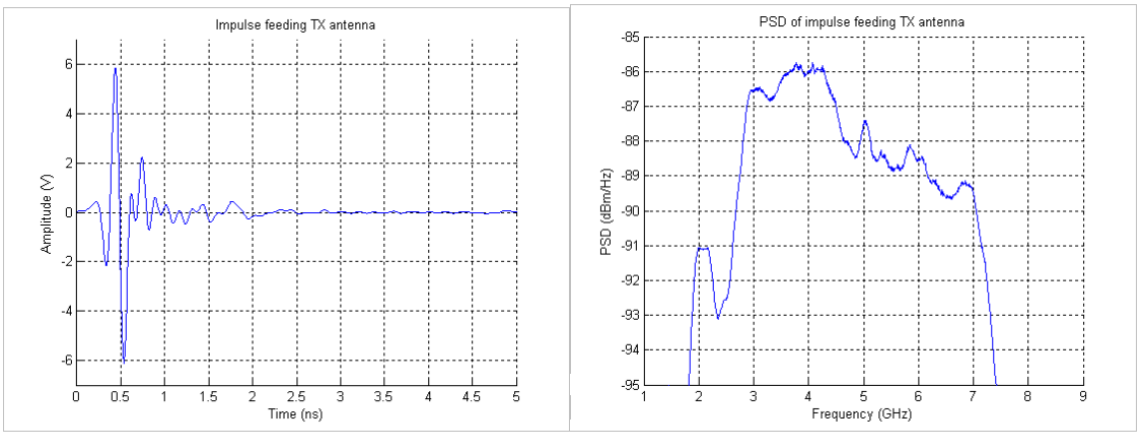

Figure 3.11: UWB impulse feeding the Tx antenna.

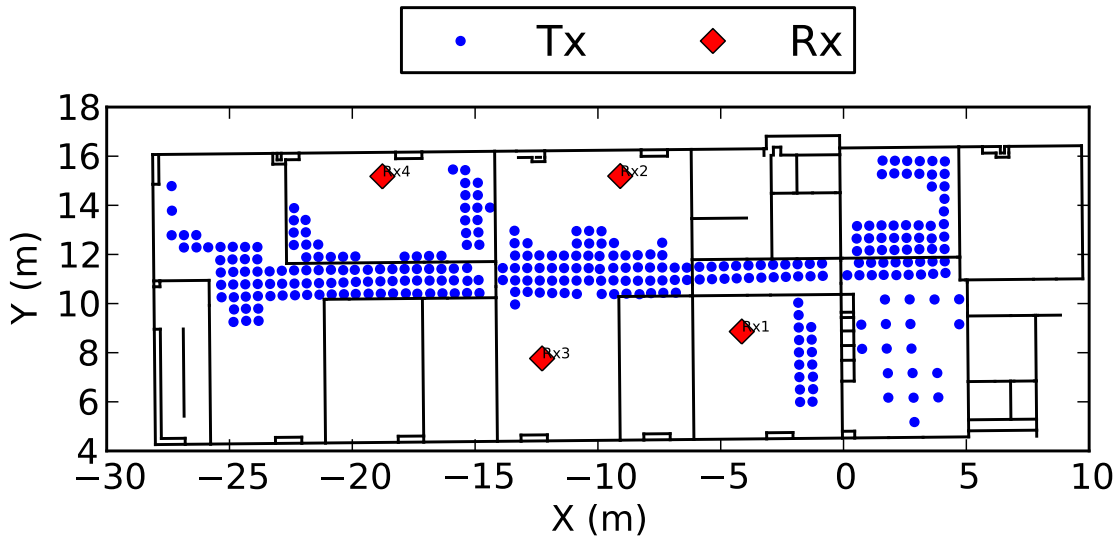

Figure 3.12: Rx and Tx locations.

When performing channel sounding, it is necessary to extract exclusively the channel behavior (with or without antennas) by using appropriate calibration procedures based on deconvolution tools [105]. This calibration procedure aims to eliminate the effects of all the elements involved in the link like PA, cable, and LNAs. In results, an overall number of collected profiles has been calculated and saved: 302 (Tx positions) x 4 (Rx positions) x 2 (Tx heights) = 2416 profiles. In each profile, the CIR measured by the sounder is stored directly in a Matlab binary file. In addition to the CIR, different parameters are saved in each profile mainly Tx and Rx positions, date, and time [103]. The Tx and Rx locations (2D) are given in Figure 3.12. In the rest of this report, we consider the measurements campaign done at equal height of receivers and transmitters. Hence, the number of considered profiles is 1208.

3.2.2 Location-dependent parameters database

In order to extract the different parameters relevant to localization (location-dependent parameters), we have post processed the 1208 measured profiles and we have constructed a location-dependent parameters database. The objective is to store, for each couple Tx-Rx, relevant location-dependent parameters which will be necessary to statistically produce LDP models and to evaluate localization techniques and metrics presented in next chapters. For each profile, we extract parameters given in Table 3.1.

Table 3.1: Extracted parameters from UWB measurements.

Parameter		Definition
Identity	Id	An identity is given for each Tx in order to differentiate them
Position	(x, y, z) (m)	Cartesian coordinates of the Tx
Distance	d	The distance between Tx and Rx
RSSI	E_T (dB_{nJ})	The Total energy integrated over the CIR
	E_M (dB_{nJ})	The energy integrated over the Strongest received path
TOA	τ_{stg} (ns)	The TOA of the strongest path
	τ_{th} (ns)	The TOA estimated by thresholding the CIR
	τ_{cum} (ns)	The TOA estimated by thresholding the cumulative CIR
TDOA	τ_{ij}	The TDOA estimated using cross correlation
Visibility	Vis	LOS, NLOS+DP, or NLOS-DP
Link Quality	LQI (dB)	The ratio between the maximum signal amplitude and the maximum noise amplitude estimated during the first five nanoseconds corresponding to a common time slot without any signal

LQI

The LQI gives an indication about the SNR of the received signal. The extracted models for RSSI, TOA, and TDOA presented and used in the rest of this dissertation are extracted using only signals with a LQI higher or equal to 10dB. Signals which have a LQI lower than 10.0dB need to be used carefully, because the SNR is expected to be very low [103].

RSSIs

Consider the received signal $r_{ij}(t)$ at the Rx j from the Tx i defined as in 3.3. Two RSSIs are defined: E_T and E_M. Their mathematical formulations are respectively given for (i, j) by:

$$E_T = 10 \log_{10} \int_{\tau_1}^{T} r_{ij}^2(t) dt \tag{3.14}$$

$$E_M = 10 \log_{10} \int_{\tau_M - \alpha T_s}^{\tau_M + (1-\alpha) T_s} r_{ij}^2(t) dt \tag{3.15}$$

τ_1 is the time of flight of the signal at the receiver j. It is equal to d/c where d is the true distance between i and j and c is the speed of light. τ_M is time of arrival of the strongest path. T_s is the sampling time and it is equal to 0.225ns. α is a constant used to define the time interval where the energy is integrated. This interval is equal to T_s and centered on τ_M when α is set to 0.5. For all the rest, α is set to 0.25 respecting the shape of transmitted pulse. Indeed, the maximum of the pulse occurs at 0.5ns and the significant part of the pulse is of a length equal to 2ns which results in $\alpha = 0.25$. The motivation behind extracting E_M is the time precision of UWB signals. Because of the large used bandwidth, the strongest path can be identified and hence the energy that it carried can be evaluated.

TOAs

While τ_{stg} is easily extracted as the time of arrival of the strongest path, τ_{th} and τ_{cum} are respectively estimated using respectively Th-TOA and Cum-TOA techniques presented in section 3.1.2.3. Three different thresholds have been defined for each of these two techniques. In Figure 3.13 and Figure 3.14, we plot the ranging error versus the used threshold for respectively Th-TOA and Cum-TOA.

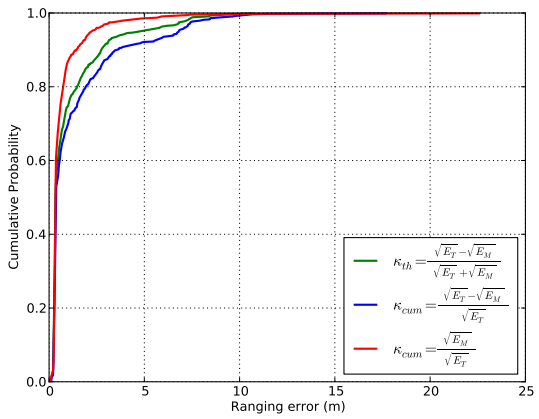

Figure 3.13: Th-TOA ranging error for different thresholds.

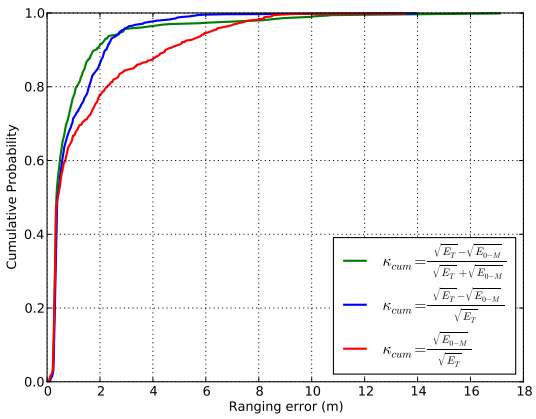

Figure 3.14: Cum-TOA ranging error for different thresholds.

These figures show that different thresholds give different ranging accuracies for each ranging technique. These two figures suggest the choice of following κ_{th} and κ_{cum} as thresholds for respectively Th-TOA and Cum-TOA techniques.

$$\kappa_{th} = \frac{\sqrt{E_M}}{\sqrt{E_T}} \tag{3.16}$$

$$\kappa_{cum} = \frac{\sqrt{E_T} - \sqrt{E_{0-M}}}{\sqrt{E_T}} \tag{3.17}$$

3.3 Modeling of Location Dependent Parameters

3.3.1 Modeling of RSSI

3.3.1.1 Log-Normal Shadowing Model

For all the rest of this report, log-normal shadowing model [91] is considered. This model is widely used in radio and localization applications because it set a simple linear relation between the path loss and the logarithm of the distance. In free space, the Friis formula expresses the received power P_r at a distance d as [106]:

$$P_r = P_t \frac{G_r G_t \lambda^2}{(4\pi d)^2} \tag{3.18}$$

where P_t is the transmitted power, G_r and G_t are the antenna gain at respectively the reception and the transmission sides, and λ is the wavelength. The linear path loss is defined as the ratio of transmitted power to received power without considering gains of antennas:

$$L = \frac{P_t}{P_r} = (\frac{4\pi d}{\lambda})^2 \tag{3.19}$$

We define the path loss as the dB value of the linear path loss, which is equal to the difference in dB between the transmitted and the received power. The free-space path loss model is then given by:

$$L\,(dB) = -20log_{10}\left(\frac{\lambda}{4\pi d}\right) \tag{3.20}$$

In fact, the simple analysis often used in coexistence studies limits the propagation characteristics to the large scale of the signal at given distances (pathloss). In mathematical terms, the mean received power (around which there will still be shadowing and multipath) varies with distance with an exponential law. The total pathloss $\bar{L}$ at a distance d is often modeled, in dB, as [106]:

$$\bar{L} = L_0 + 10n_p log_{10}\left(\frac{d}{d_0}\right) \tag{3.21}$$

L_0 is the path loss at a reference distance, d_0, which is usually taken equal to 1 meter [106]. n_p is the propagation constant. L_0 is given by:

$$L_0 = 20log_{10}\left(\frac{4\pi d_0}{\lambda}\right) \tag{3.22}$$

Alternatively, L_0 can be determined by measurement at d_0 or optimized (alone or together with n_p) to minimize the mean square error (MSE) between the model and the empirical measurements [107]. The value of n_p depends on the propagation environment: for propagation that approximately follows a free-space model, n_p is equal to 2. The value of n_p for more complex environments can be obtained via a minimum mean square error (MMSE) fit to empirical measurements. Alternatively, n_p can be obtained from an empirically-based model that takes into account frequency and antenna height [91].

In fact, this expression of $\bar{L}$ represents only the mean loss of the power. The measured loss varies around this mean according to a zero-mean Gaussian random variable, X_{sh}, with a standard deviation σ_{sh}. X_{sh} models the shadowing caused by obstacles between the transmitter and receiver that attenuate signal power through absorption, reflection, scattering, and diffraction [91, 106]. The complete path loss L, expressed in dB, is then given by:

$$L = L_0 + 10n_p log_{10}\left(\frac{d}{d_0}\right) + X_{sh} \tag{3.23}$$

Equivalently, the received power can be expressed as:

$$P_r = P_0 - 10n_p log_{10}\left(\frac{d}{d_0}\right) + X_{sh} \tag{3.24}$$

where P_0 is the received power at d_0.

Since we use the received energies E_T and E_M as RSSI, we define the path loss model in energy as follows:

$$E_r(dB_{nJ}) = E_0 - 10n_p log_{10}\left(\frac{d}{d_0}\right) + X_{sh} \tag{3.25}$$

where E_r is the received energy (i.e. E_T or E_M) and E_0 is the received energy at d_0. In all the rest of this report, the mathematical formulation given by equation (3.25) is used.

Notice that it is also possible, if we have the duration T_p of transmitted pulses, to compute the received power P_r in dB_m as follows:

$$P_r(dB_m) = E_r(dB_{nJ}) - 10log_{10}(T_p) - 60 \tag{3.26}$$

where 60 results from the conversion of E_r from dB_{nJ} to dB_{mJ}. Notice also that since energy and power are equivalent, the use of one of them will not affect the RSSI-based ranging or localization performances.

3.3.1.2 Extracted RSSI Models

A log-normal shadowing model is defined by three parameters: E_0, n_p, and σ_{sh}. Using linear regression techniques applied on extracted LDPs, namely distance d and RSSIs E_T and E_M, in the database, we get PL models described in Table 3.2 for $d_0 = 1$m. These models are made using all profiles having a LQI higher than 10dB chosen from the initially available 1208 profiles. Hence, we call them general path loss models (GPL). As shown in this table, a GPL model is defined per RSSI type. As presented before, for each RSSI type E_0 and n_p define the mean RSSI value over which the RSSI values vary according to a zero-mean Gaussian r.v with a standard deviation σ_{sh}. Although the mean RSSI presents a straightforward relation between signal strength and distance (i.e. position), the shadowing term X_{sh} introduces a considerable difficulty for the estimation of distance and position from RSSI. Obviously, the smaller is the shadowing variance the better is the distance (and hence position) estimation.

In order to show the dependency of RSSI on distance d, we plot in Figure 3.15 the RSSI values with respect to distance d between the Rx and the Tx for respectively E_T

and E_M. We plot also, the linear fitting of these RSSI values to the distance d. In fact, the fitting curves (black lines) represent the different GPL models presented in Table 3.2. The slope of each line gives the parameter n_p for each RSSI respectively. Table 3.2 and Figure 3.15 show that E_T and E_M have obviously different models. In the two cases, E_0 values are very close since they approximate the same quantity which is the energy received at distance $d_0 = 1$m from the Tx antenna. Indeed, at this short distance E_T and E_M are very close and they approach E_0 since few multipaths and radio phenomena occur at this distance from the Tx. The second and third GPL parameters (i.e. n_p and σ_{sh}) are higher in the case of E_M.

Table 3.2: Extracted GPL model parameters from UWB measurements.

RSSI	PL Parameters		
	$E_0(dB_{nJ})$	n_p	$\sigma_{sh}(dB_{nJ})$
E_T	-36.03	2.386	3.98
E_M	-40.91	3.10	6.63

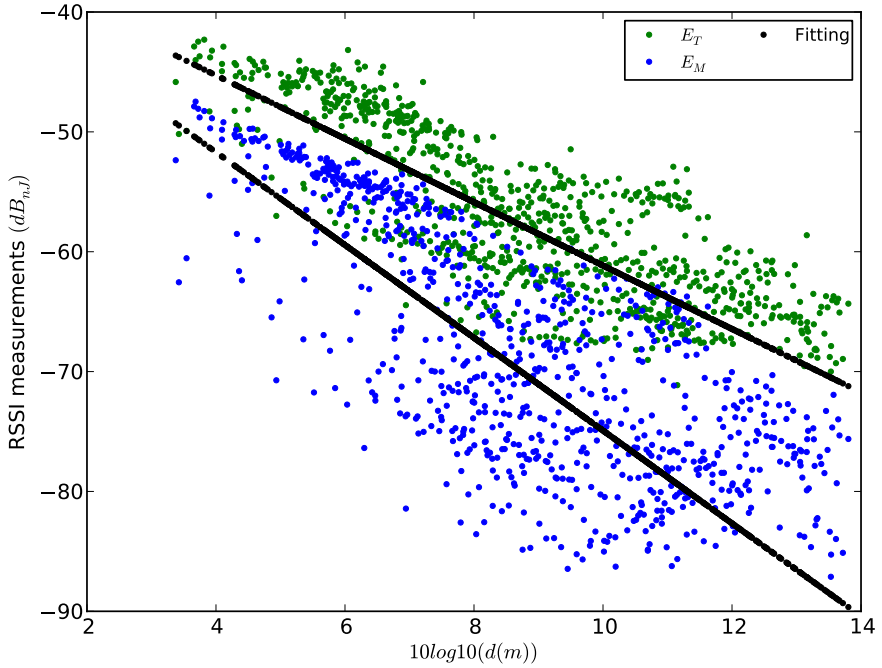

Figure 3.15: RSSI values with respect to distance d.

These path loss models are very interesting because they make easier the estimation of RSSI at each point of the studied environment. Actually, a calibration procedure is essential to the model to be reliable. This calibration is done based on measurements campaign and aims to select the PL parameters, namely E_0, n_p, and σ_{sh}, which represent the best the signal attenuation in the considered environment. For illustration, in Figure 3.16 and Figure 3.17 we plot measured versus simulated RSSIs for each receiver using the GPL models for both E_T and E_M respectively.

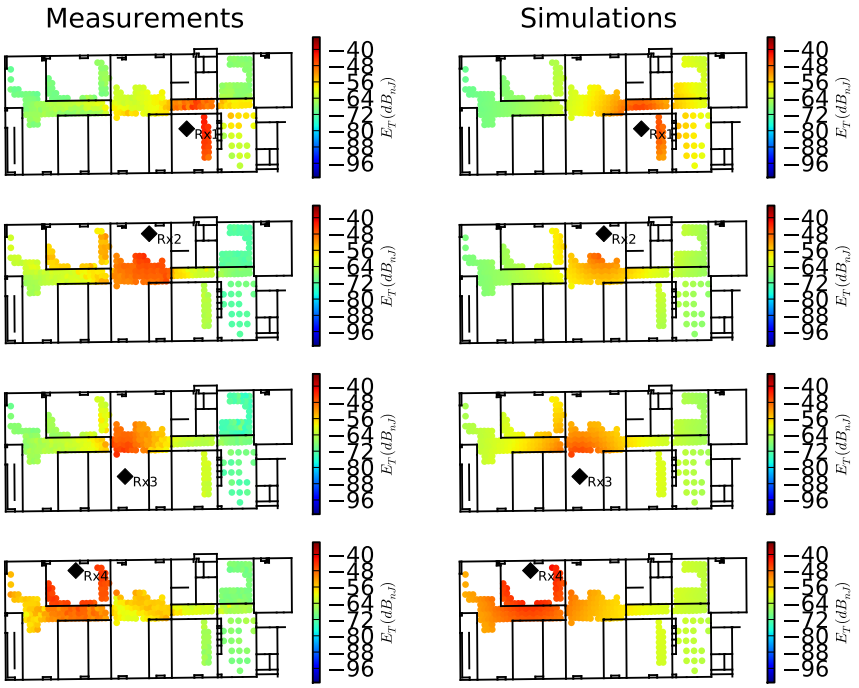

Figure 3.16: Measured (left) versus (*b*) Simulated (right) E_T using GPL.

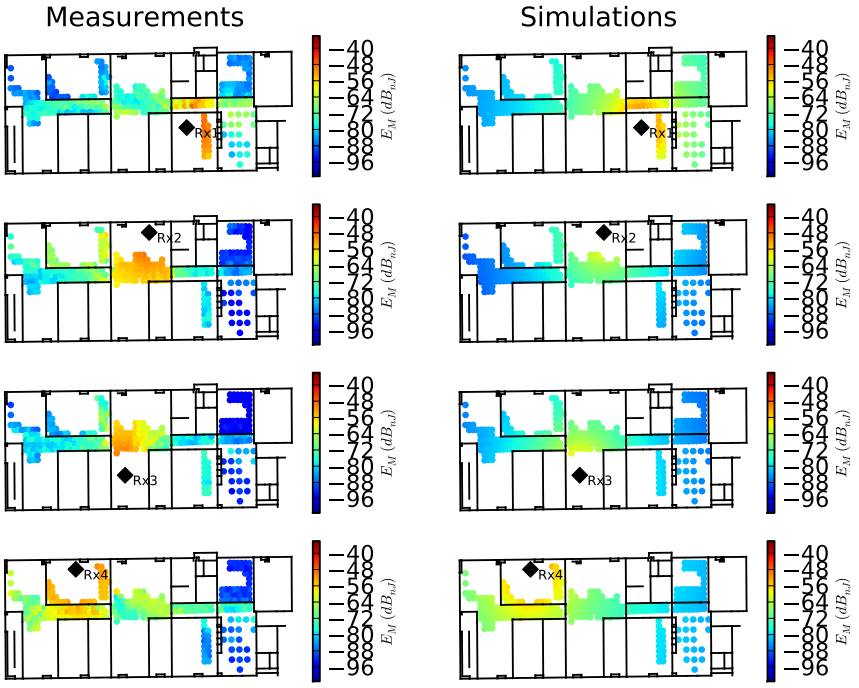

Figure 3.17: Measured (left) versus (*b*) Simulated (right) E_M using GPL.

Equivalently, one can define a PL model per anchor device (APL). These APLs are given in Table 3.3. The RSSI-distance dependencies are plotted in Figure 3.18. These results reveal that each receiver can get more or less different APL models compared to GPL models. In general, each anchor device (e.g. BS, AP, femtocells) can gather RSSI measurements when communicating with mobiles and update in an on-line manner its APL model based on an estimation of distance which can be made using already collected RSSI or TOA based ranging techniques. In that way, each APL model represents a specific vision of radio propagation channel. In fact, these APL models would be more accurate than GPL models since they are able together to better characterize the propagation phenomena. Later in this chapter, we will demonstrate this enhancement on the RSSI based ranging techniques (see section 3.3.1.3).

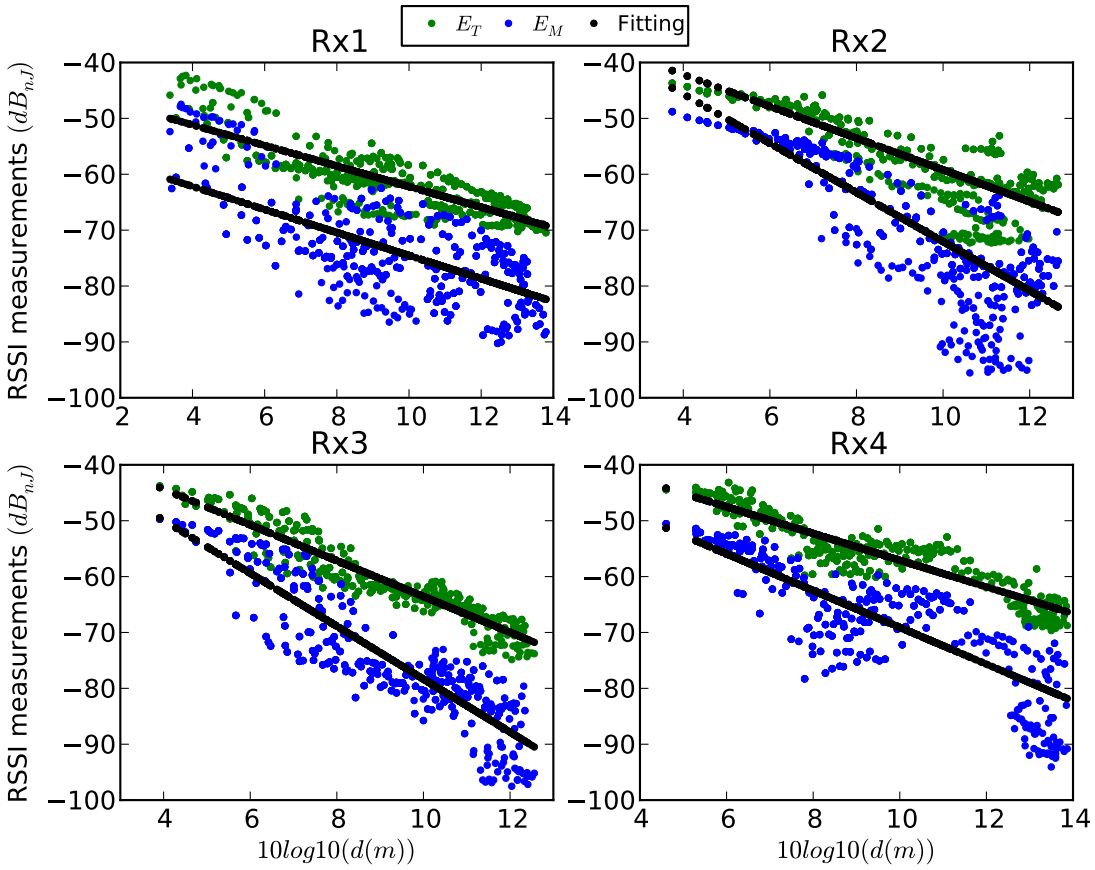

Figure 3.18: RSSI values with respect to distance d for different receivers.

In Figure 3.19, the CDFs of absolute RSSI estimation error are plotted for both E_T and E_M when using GPL and APL respectively. The absolute RSSI estimation error is the absolute value of the difference between the actual measured and simulated values of RSSI. The figure reveals that RSSI estimation error is lower when using APL models for both RSSIs. Thus, applying APL models allows achieving higher RSSI estimation accuracies. Moreover, the figure shows that E_T offers better performances than E_M.

Table 3.3: Extracted path loss model parameters from UWB measurements for different receivers.

Receiver	RSSI	Parameter		
		$E_0(dB_{nJ})$	n_p	$\sigma_{sh}(dB_{nJ})$
Rx1	E_T	-43.8	1.84	2.85
	E_M	-53.93	2.06	5.85
Rx2	E_T	-30.81	2.84	3.56
	E_M	-28.07	4.39	5.78
Rx3	E_T	-31.53	3.20	2.47
	E_M	-30.97	4.74	5.07
Rx4	E_T	-33.19	2.38	2.59
	E_M	-36.15	3.29	5.41

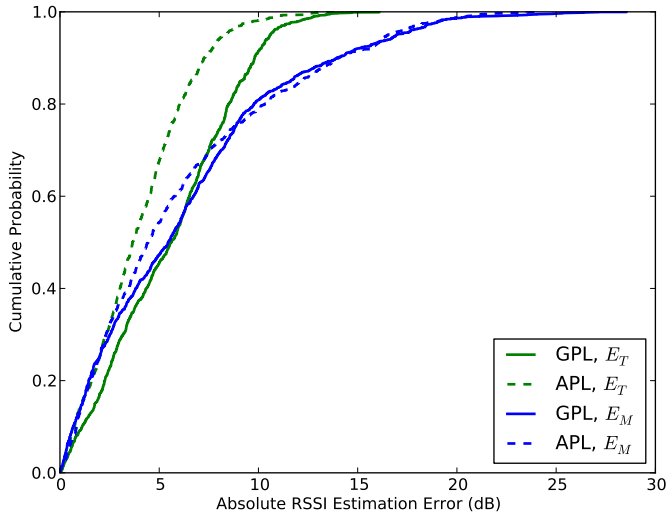

Figure 3.19: Absolute RSSI simulation error using both GPL and APL models for both E_T and E_M.

3.3.1.3 RSSI Based Ranging Techniques

Since log-normal shadowing model links RSSI to distance, RSSI-based ranging is made possible. Let's consider the log normal shadowing model described by the equation (3.24) where we assume that the shadowing term X_{sh} is zero-mean Gaussian:

$$X_{sh} \sim \mathcal{N}(0, \sigma_{sh}^2) \tag{3.27}$$

From (3.24) and (3.27), we derive the fact that the distance d follows a log-normal distribution:

$$p_d(d, L) = \frac{1}{\sqrt{2\pi} dS} e^{\frac{-(\ln d - M)^2}{2S^2}} \tag{3.28}$$

where S and M are given respectively by:

$$S = \frac{\sigma_{sh} \ln 10}{-10 n_p} \tag{3.29}$$

$$M = \frac{(P_0 - P) \ln 10}{10 n_p} + \ln d_0 \tag{3.30}$$

As the probability density function (pdf) of d follows a log-normal distribution, the estimated distance $\hat{d}$ can be given by the mean, median, or the mode of the pdf (see Figure 3.20). Based on [108], these estimates are given respectively by:

$$\hat{d}_{mean} = e^{M + \frac{S^2}{2}} \tag{3.31}$$

$$\hat{d}_{median} = e^{M} \tag{3.32}$$

$$\hat{d}_{mode} = e^{M - S^2} \tag{3.33}$$

From equations (3.31) to (3.33), one can notice that the only estimator that does not consider the knowledge of shadowing, given by the term S, is the median. Thus, this estimator may be practical when no information about shadowing is available. Once the MS get this knowledge, the best estimator will be the mode which is the best estimator in the maximum likelihood (ML) sense [109]. The mean estimator is not a good choice since it over-estimates the distance, and it is very inaccurate especially for strong values of S.

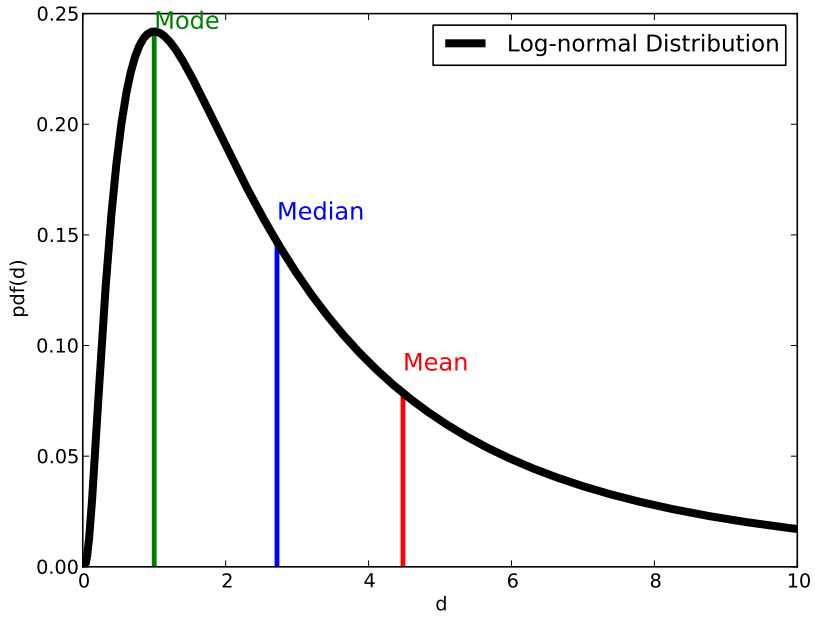

Figure 3.20: Log-normal Distribution and different estimators.

To better evaluate the performances of these different estimators, we derived for each estimator its variance. These variances (developed in Annex C) are given respectively by [109]:

$$\hat{\sigma}^2_{mean} = e^{2M+3S^2}(e^{S^2} - 1) \tag{3.34}$$

$$\hat{\sigma}^2_{median} = e^{2M+S^2}(e^{S^2} - 1) \tag{3.35}$$

$$\hat{\sigma}^2_{mode} = e^{2M-2S^2}(1 - e^{-S^2}) \tag{3.36}$$

In Figure 3.21, we plot the different CDF of RSSI based ranging error for different RSSI and different range estimators. This figure reveals that ranging based on E_T is more accurate and that the mode estimator is the most suitable for RSSI based ranging. Table 3.4 summarizes the statistical parameters of RSSI based ranging errors for both RSSI types and different ranging estimators. This table emphasizes that for both RSSI types, $\hat{d}_{mode}$ is the most accurate estimator which gives the lowest RSSI based ranging error. In addition, $\hat{d}_{median}$ is more accurate than $\hat{d}_{mean}$. Hence, when no information about shadowing variance is available (i.e. σ_{sh} is unknown) the median estimator is the best estimator in ML sense. Once, the system or/and the mobile can get this information about shadowing, the mode estimator becomes more adequate than median estimator.

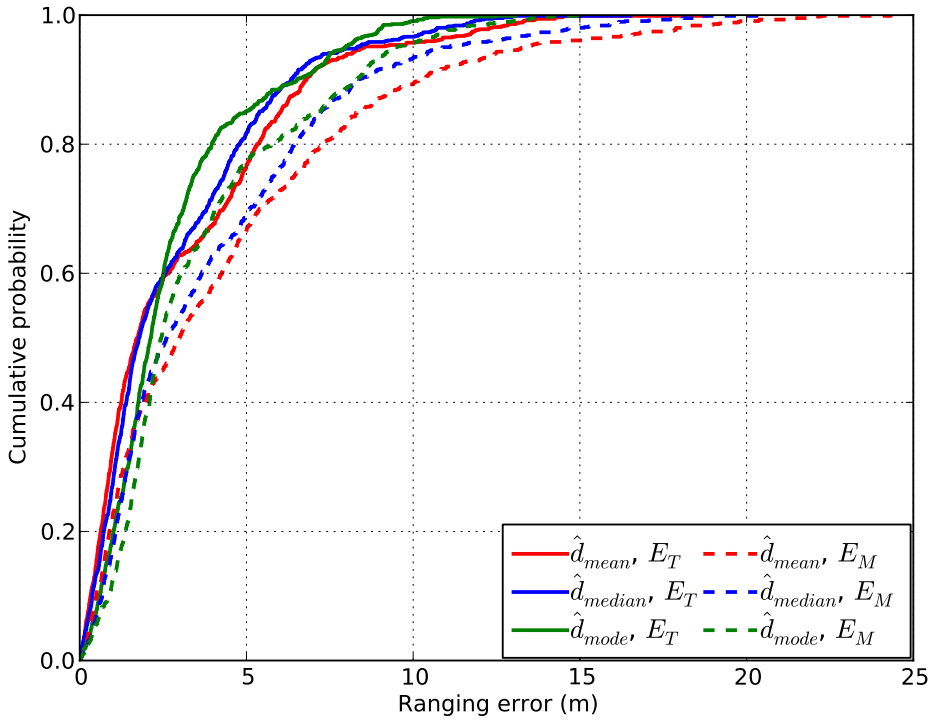

Figure 3.21: CDF of RSSI-based ranging error using GPL models.

Using E_T and $\hat{d}_{mode}$, we compare in Figure 3.22 the ranging capabilities of different receivers first using the GPL model and then using the appropriate APL model for each receiver. This figure shows that different receivers have different ranging accuracies and that using APL models instead of GPL models enhances the ranging accuracies. This is justified because each receiver has a different vision of the channel and then constructs an appropriate APL model which is different from the others.

Table 3.4: Statistical RSSI based ranging models extracted from UWB measurements.

RSSI	Ranging estimator	Statistical parameters			
		Mean (m)	Std (m)	Min (m)	Max (m)
E_T	$\hat{d}_{mode}$	2.766	2.276	0.015	13.066
	$\hat{d}_{median}$	2.829	2.658	0.002	16.538
	$\hat{d}_{mean}$	3.016	3.033	0.000081	18.811
E_M	$\hat{d}_{mode}$	3.550	2.918	0.00098	14.924
	$\hat{d}_{median}$	3.908	3.596	0.0055	20.547
	$\hat{d}_{mean}$	4.400	4.374	0.0088	24.328

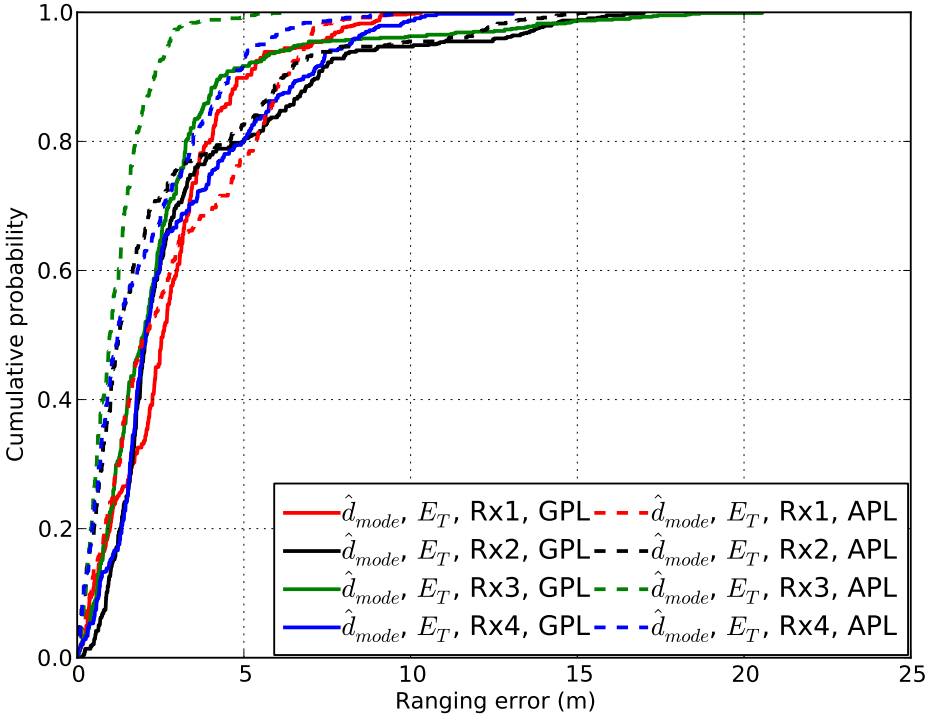

Figure 3.22: CDF of RSSI-based ranging error using E_T and mode estimator for different receivers when using GPL and APL models.

As visibility conditions affect the RSSI, they obviously affect also RSSI-based ranging accuracies. This fact is shown by Figure 3.23 where the CDF are plotted for different RSSI-based ranging techniques using the mode estimator. This figure shows clearly that the NLOS situations make difficult the estimation of distance from RSSI. This is mainly because the shadowing in NLOS situations has greater variances than LOS conditions where the first path has the strongest energy and then the estimation of distance can be easily done.

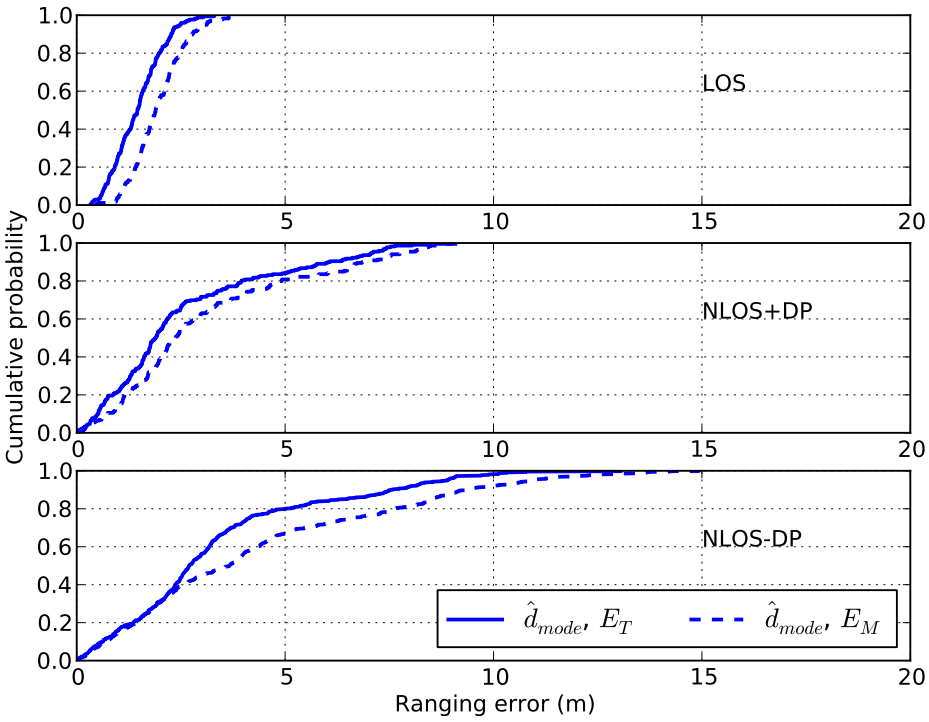

Figure 3.23: CDF of RSSI-based ranging error using mode estimator for different visibility conditions when using GPL model.

3.3.1.4 Joint localization and Path Loss Modeling

When communicating, devices exchange signals and thus the knowledge of RSSI is made available with each message transmitted or received. Based on this exchange, we propose here a scheme for conjoint localization and path-loss modeling. This scheme is given in Figure 3.24. Each BS receives and sends signals from/to the MSs which lie in its coverage area. At time t_k, the anchor-based path loss model of the BS is noted $\text{APL}^{(k)}$. This model is constructed using the RSSI measurements available up to time t_k. When at time t_{k+1} the BS collects new measurements from MSs, it should apply some linear regression techniques in order to get the new path loss model ($\text{APL}^{(k+1)}$). This regression supposes the knowledge of the distance (or an estimate of it) between the MS and the BS. This distance can be either estimated using the previous APL model $\text{APL}^{(k)}$ or using other information if available (e.g. TOA, TDOA, etc).

The new APL model is then broadcast to the other components of the infrastructure and also to all MSs lying in the BS coverage. This new model is hence used for RSSI based ranging and localization techniques. The interest of such models is mainly to keep an updated knowledge about the channel changes. For this, old measurements should be eliminated. Depending on the environment type, the MS density, the coverage size, the frequency of measurements, the standard, and many other factors the quantity of used amount of RSSI measurements necessary to estimate the PL model. These measurements can be stocked in a FIFO queue of a chosen length.

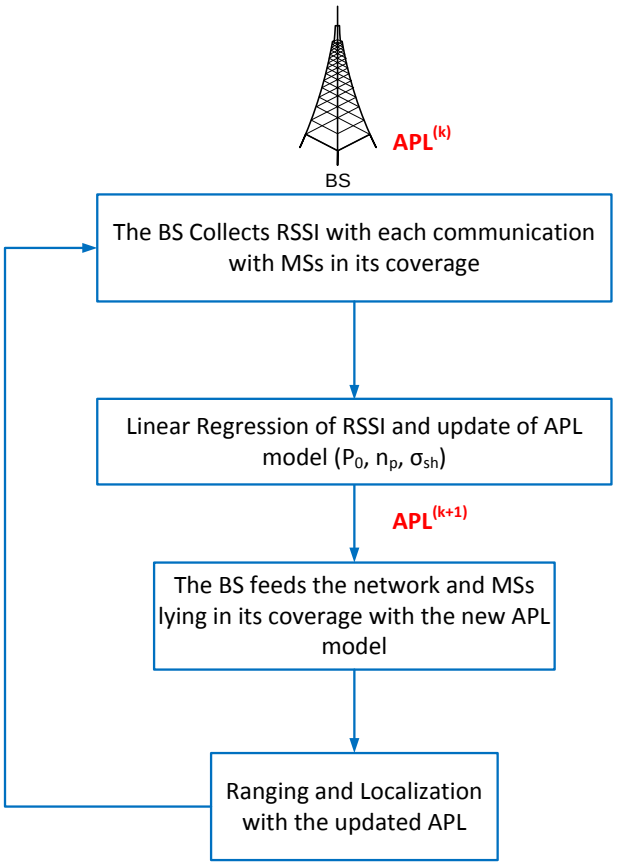

Figure 3.24: On-line path loss model learning.

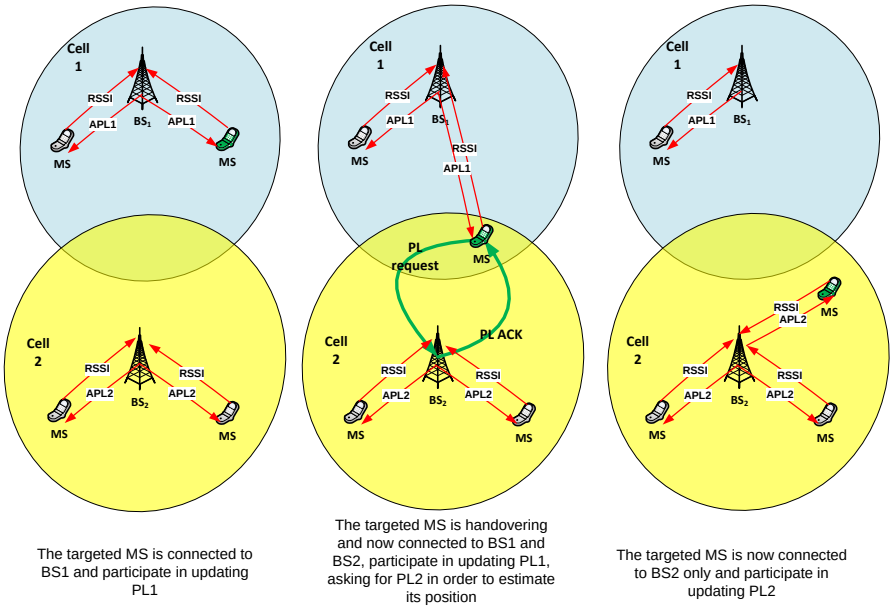

Figure 3.25: A scenario of on-line PL model learning while handovering.

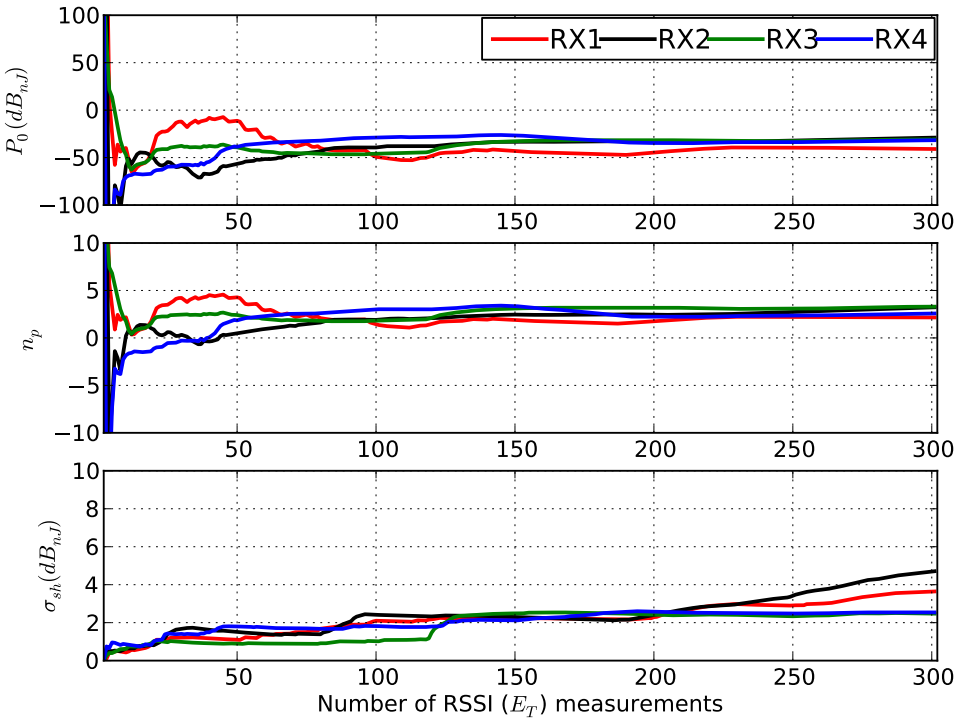

Figure 3.26: Evolution of estimated APL parameters with respect to the number of used RSSI.

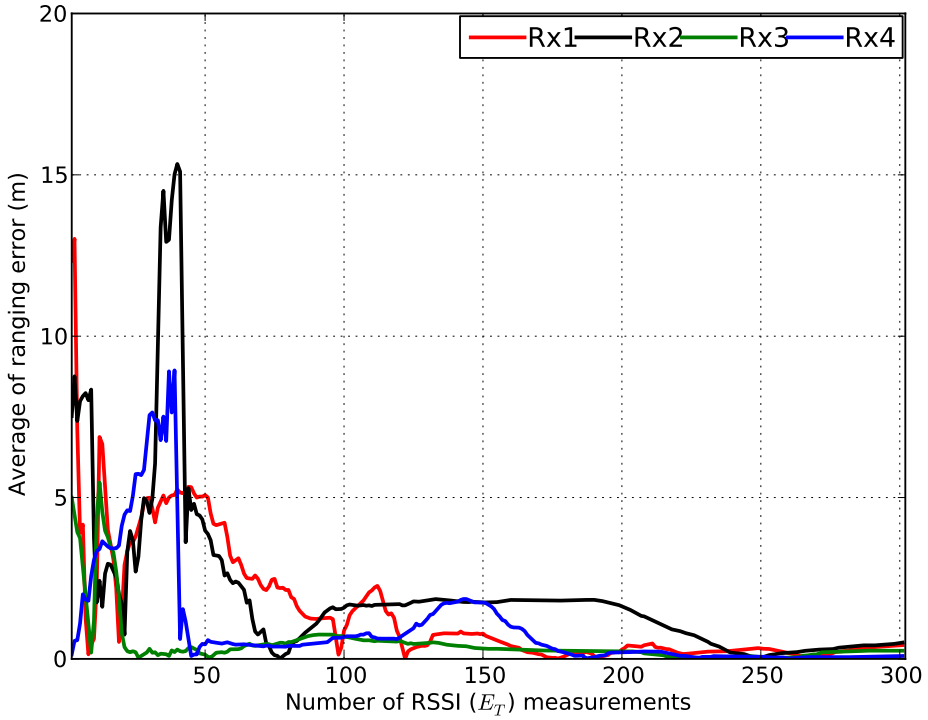

Figure 3.27: Evolution of ranging error with respect to the number of used RSSI using mode estimator and E_T.

While handovering from one BS coverage area to another, a MS goes through a special step where it is at once connected to both base stations. The scenario is depicted by Figure 3.25. In the first situation, the handovering MS is only connected to the first BS and it is exchanging RSSIs and APL models with BS1. In the second step, the MS enters in the coverage of the second BS but it is still connected to the first BS. At this step, the MS should get information about the PL model of the new BS. That is, it should send a PL request asking for PL parameters actually stocked in the second BS. This BS responds by giving a PL acknowledgment which contains the requested parameters. At this step, the mobile can use both APLs in order to localize itself. Once the MS leaves the coverage of the first BS, it becomes connected only to the second BS and should withdraw the first APL.

Figure 3.26 plots the evolution of estimated path loss parameters with respect to the number of used RSSI measurements. This figure shows that after a given amount of RSSIs the parameters E_0 and n_p become constant and independent of the number of new measured RSSIs. By contrast, the shadowing σ_{sh} is more susceptible to the amount of measured RSSIs. Actually, some very attenuated signals can drastically vary the value of σ_{sh}. This strong variation is mainly caused by metallic objects. As an example, the strong variation of σ_{sh} of Rx3 for RSSI values from 120 to 130 is caused by a set of metallic cabinets located between Rx3 and these points (see Figure 3.9).

The effect of on-line path loss model learning on the RSSI based ranging accuracy is given in Figure 3.27. The figure plots the average absolute ranging error as a function of the number of RSSI measurements used to estimate the PL parameters. In this figure, we used E_T as RSSI and the mode estimator. At each step (i.e. incremental number of RSSIs), we estimate the APL parameters of each receiver and we apply the mode estimator (see eq (3.33)) to estimate the different ranges. Then, the average of absolute values of these estimated ranges is plotted as a function of the number of RSSIs. This figure shows that the ranging error is reduced as more as new measurements are involved. Even when the shadowing becomes higher, the ranging accuracy is better. In fact, as the number of involved measurements increases, the APL models describe better and better the signal attenuation. Thus, these APL models become more sophisticated and representative of the channel. This may allow a good estimation of ranges and thus positions.

3.3.2 Modeling of TOA

In section 3.1.2.3, we have presented three different techniques of CIR-based ranging techniques, namely Stg-TOA, Th-TOA, and Cum-TOA. We have also defined for both Th-TOA and Cum-TOA techniques the appropriate thresholds chosen based on measurements database (see section 3.2.2). In this section, we propose to study the performances of these different techniques and to extract models to be used later in for evaluating the proposed positioning techniques.

In Figure 3.28, we plot the CDFs of absolute ranging error for the three studied techniques of CIR-based ranging. This figure reveals that the Th-TOA and Cum-TOA techniques give close ranging accuracies and widely outperforms the Stg-TOA technique which assumes that the strongest path is the first path. The difference between these techniques is also divulged by Figure 3.29 where we plot the estimated

TOA ranges versus the true distances d respectively for each CIR-based technique. This figure shows that the Stg-TOA technique usually overestimates ranges since the strongest path arrives usually later than the first path. This observation is marked on the third box in Figure 3.29 where the whole points are estimated above the linear line (range= d) which represents the ideal estimation of ranges (i.e. without any error).

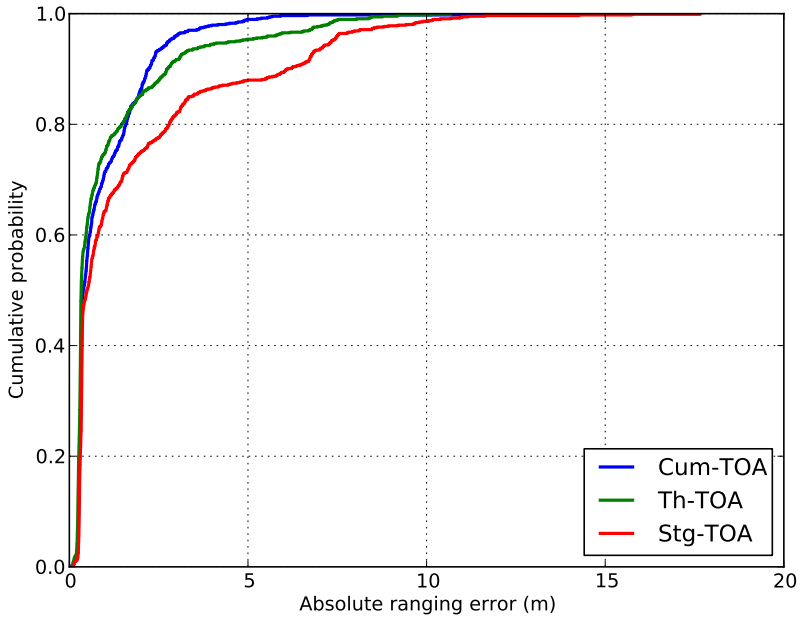

Figure 3.28: CDF of TOA-based ranging error using different TOA-ranging methods.

The statistical properties of TOA ranging error based on these different techniques are recapitulated in Table 3.5 where we give for each technique the mean, the standard deviation, and the extremum values.

Table 3.5: Statistical TOA ranging models extracted from UWB measurements.

Ranging Technique	Mean (m)	Std (m)	Min (m)	Max (m)
Stg-TOA	1.734	2.487	0.118	17.659
Th-TOA	1.050	1.608	0.082	10.680
Cum-TOA	0.931	1.142	0.016	13.964

This table reveals that the Cum-TOA ranging technique offers the best performances. Indeed, absolute ranging errors using this technique present the smallest standard deviation (i.e. 2.971 meters). The mean absolute error for Cum-TOA and Th-TOA are very close. Based on this table, we suggest to use Cum-TOA as the adequate ranging technique for UWB ranging in the rest of this document. We will assume that estimated ranges are Gaussian centered on the true value (i.e. d) with a standard deviation presented in Table 3.5 for each ranging technique.

In Figure 3.29, we also differentiated different visibility conditions using different colors. This figure shows that in LOS conditions it is very easy to accurately estimate

the TOA whatever the used ranging technique. As the strongest path is usually the first arriving path in LOS conditions, the Stg-TOA technique gives similar accuracy as the other advanced techniques. By contrast, this technique is not suitable for NLOS conditions. In addition, the figure reveals that in NLOS conditions it is more difficult to detect the first path especially in NLOS-DP where no direct path exists between the Tx and the Rx. Hence, the estimated range is quite different from the real distance. This is highlighted by the spreading of red points for all techniques.

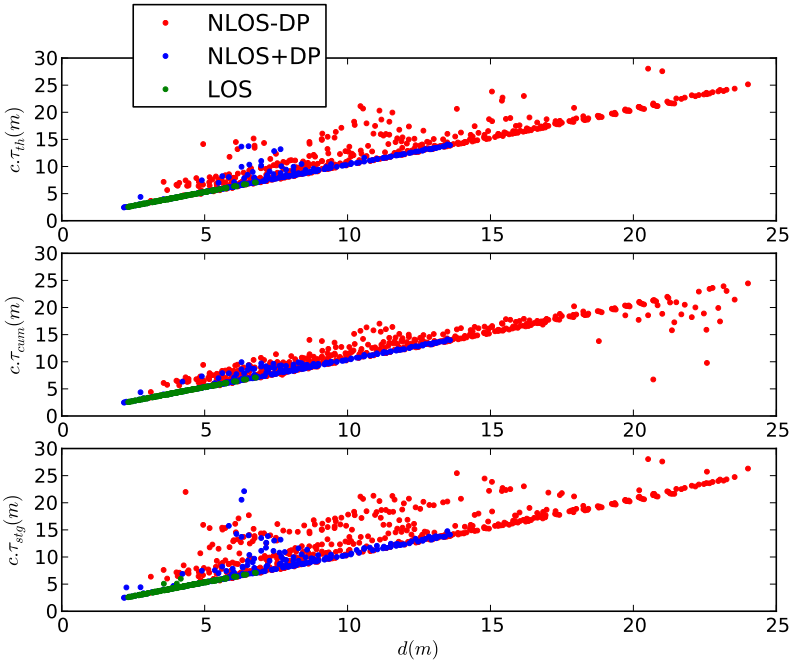

Figure 3.29: Estimated ranges versus true distances for different visibility conditions and different TOA-ranging methods.

3.3.3 Modeling of TDOA

Based on cross-correlation technique, we calculate TDOA between two signals. Without any loss of generality, we assume Rx1 as the reference receiver and all the TDOA are computed by cross-correlating the second signal with the signal received by Rx1. In Figure 3.30, we plot the CDF of obtained TDOA ranging error. Table 3.6 presents the statistical model of TDOA. The TDOA will be modeled by a Gaussian r.v centered in the true TDOA value with a standard deviation given by Table 3.6.

Table 3.6: Statistical TDOA ranging model extracted from UWB measurements.

Mean (m)	Std (m)	Min (m)	Max (m)
0.205	1.850	0.0019	14.954

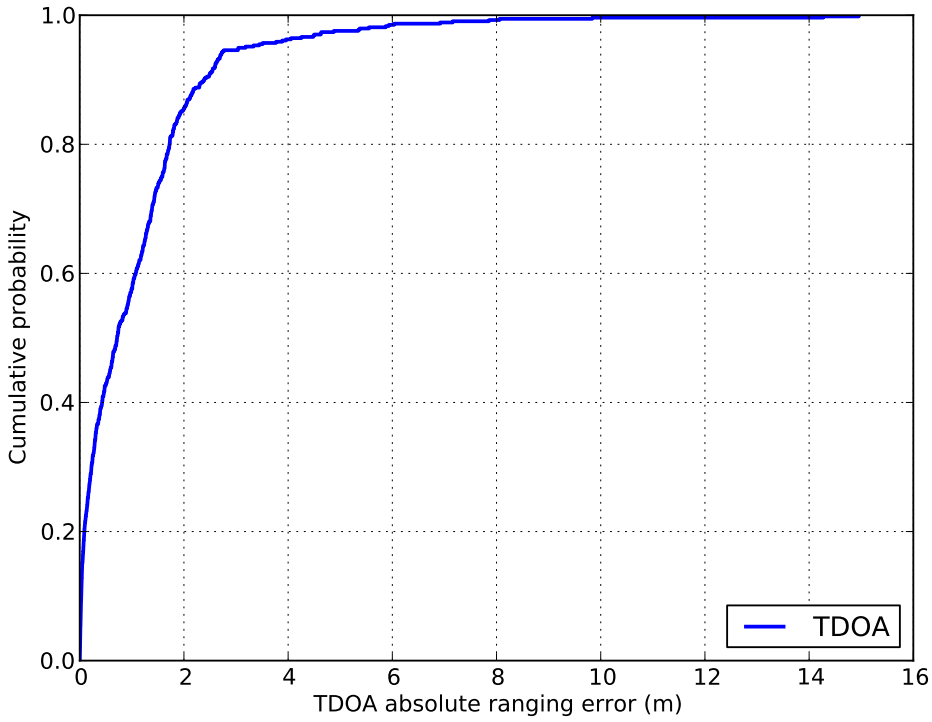

Figure 3.30: CDF of TDOA-based absolute ranging error.

3.4 Conclusion

This chapter has asked the following questions: how to measure, estimate, and model the location-dependent parameters (i.e. RSSI, TOA, and TDOA)?. In order to answer this question, we have started by giving an insight of the different techniques of LDP measurement defined in the different wireless standards and devices. Then, we have described the measurements campaign and the extracted LDP database. Based on this database, the questions of estimation and modeling of LDPs are answered. For TOA, we have studied two techniques of CIR-based ranging techniques which benefit from the high time precision of UWB signals. These two techniques are simple, low-cost, and can be implemented easily in UWB receivers. The TDOA has been estimated using cross-correlation techniques. For RSSI, we have extracted different path loss models. We have proposed to use a PL model per receiver in order to enhance the description of channel attenuation. Besides, novel techniques of RSSI-based ranging are proposed and evaluated and a scheme of joint localization and PL modeling is presented.

The effect of channel characteristics on the estimation and/or measurement of these LDPs is studied and evaluated based on the extracted database. These characteristics are mainly the visibility conditions and the radio link quality. We leave this chapter with a set of statistical models that describe the LDPs. These models will be used in order to evaluate both types of positioning techniques proposed during this thesis. We start in chapter 4 by algebraic techniques and we finish in chapter 5 by geometric techniques.

4

Algebraic Non-Hybrid and Hybrid Localization Techniques

After different techniques of estimation, measurement, and modeling of LDPs have been presented in the third chapter, this chapter will answer algebraically the question of how using these LDPs to estimate the unknown position of a device. The focus will be put on algebraic formulations of localization problems but also on how to fuse hybrid LDPs in order to enhance positioning accuracy. In a first short but important section 4.1, we define what a localization problem is and we present the parameters that go with. In order to facilitate the reading of this chapter, we recall the assumed statistical models already presented in chapter 3.

After this introductory first section, the second section 4.2 presents the algebraic localization techniques studied during this work. These techniques are based respectively on least-squares, maximum likelihood, and semidefinite programming. Application of these techniques on heterogeneous LDPs is proposed. The last section 4.3 presents the theoretical performances assessment of different non-hybrid and hybrid localization schemes. This assessment is based on Fisher information matrices (FIM), Cramer-Rao lower bounds (CRLB), and geometric dilution of precision (GDOP).

4.1 Localization problems: Notations and Assumptions

Before investigating any localization technique, we have chosen for clarity purposes to present in this section all the notations and assumptions which may be used in any localization problem. Some of these notations and assumptions are already been presented in the previous chapter and are recalled here. For convenience, we use bold font for vectors and matrices and regular font for scalers and expressions.

We define a localization problem as the issue of finding the position of a device, with

a given accuracy, using part of or all the available data. A localization problem can be localizable or unlocalizable. A localizable problem is a problem where a position can be given using the available data. Otherwise, the problem is called unlocalizable when the device position cannot be estimated using only available data. An unlocalizable problem can be transformed in a localizable problem if a new set of data becomes available and vice versa. In this report, we consider localizable problems.

A localization problem is defined by the following inevitable components:

- A targeted device to be localized. Its unknown true position is denoted in 2D by $\mathbf{X} = (x, y)$. Its estimated position is denoted in 2D by $\hat{\mathbf{X}} = (\hat{x}, \hat{y})$. The targeted device position is estimated with a positioning accuracy (PA) defined as the euclidean distance between $\mathbf{X}$ and $\hat{\mathbf{X}}$: $PA = \|\hat{\mathbf{X}} - \mathbf{X}\|_2$ where $\|.\|_2$ is the 2-norm operator. This device is able to support one or more radio access technologies (RATs).

- A set of K anchor devices with known positions $\mathbf{X}_k = (x_k, y_k)$ for k in $(1, 2, ..., K)$. We assume that $\mathbf{X}_k$ is well known without any error for each k. These anchors are necessary to the targeted device in order to perform location-dependent parameters measurements essential for localization. These measurements represent the third component of a localization problem.

- In this report, we consider especially RSSI, TOA, and TDOA as the possible location-dependent parameters that can be measured between two devices. These parameters are available after performing a measurement or an estimation. Each measurement has an accuracy which reflects how much reliable it is. The different models of considered LDPs have been extracted from the measurements campaign and presented in chapter 3. In the rest of this report, let us denote by E_k the RSSI of the k^{th} radio link. The TOA measured between the targeted device and the k^{th} anchor device is denoted τ_k. The TDOA measured between the targeted device and the k^{th} and j^{th} anchor devices is denoted τ_{kj}. In the case of TDOA, measurements are done with a reference anchor device. Without loss of generality, let j be the index of this reference device.

- Algorithms are needed for solving localization problem using the available data. A localization algorithm can be seen as a black-box able to estimate the position of the targeted device using only the available data (position of anchor devices and measurements). Different algorithms are proposed and will be investigated in this chapter.

A localization problem may be evaluated using different metrics. In this report, we consider the following metrics:

- The positioning accuracy (PA) of the targeted device's estimated position defined by $\text{PA} = \|\hat{\mathbf{X}} - \mathbf{X}\|_2$. Let $\text{PA}_{\min}$ be the best achievable positioning accuracy.

- The average positioning accuracy can be calculated as the average of PA of many targeted devices. This average PA reflects the overall positioning accuracy of a specific scenario or problem.

- The Cramer-Rao lower bound (CRLB) which represents the value of the best theoretical positioning accuracy that can be achieved by a specific localization problem. The CRLB is given in m^2 and it is equal to PA^2_{min}. Thus, we have $\sqrt{\text{CRLB}} = \text{PA}_{\text{min}}$. CRLB is investigated in section 4.3
- The Average CRLB (denoted by abuse of notation ACRLB) is calculated as the average of $\sqrt{\text{CRLB}}$ values of a set of targeted devices and gives an overall evaluation of theoretical achievable positioning accuracy.

A localization problem may be non-hybrid or hybrid depending on the nature of used LDPs. If only one type of these parameters (i.e. RSSI, TOA, or TDOA) is used, the problem is said to be non-hybrid. The problem is hybrid when more than one type of measurements are used. Considering RSSI, TOA, and TDOA, the possible hybrid localization problems are:

- TOA+ TDOA
- RSSI + TOA
- RSSI + TDOA
- RSSI + TOA + TDOA

Summary of statistical models extracted from the database

In chapter 3, we have extracted for each LDP some statistical models in order to describe their characteristics. In the rest of this report, we will consider Gaussian statistical models for these noisy measurements. For both TOA and TDOA, we assume that the measurement is centered on the true value (respectively the true TOA and TDOA) with a standard deviation σ_k and σ_{kj} for respectively the k^{th} TOA and the k^{th} TDOA:

$$c\tau_k \sim \mathcal{N}(d_k, \sigma_k^2) \tag{4.1}$$

$$c\tau_{kj} \sim \mathcal{N}(d_{kj}, \sigma_{kj}^2) \tag{4.2}$$

where d_k and d_{kj} are the actual range and difference-of-range respectively.

Moreover, RSSI is modeled using log-normal shadowing model described in 3.3.1. This model represents the k^{th} received energy E_k as a random variable centered on the mean received energy with a standard deviation of shadowing $\sigma_{sh\,k}$:

$$E_k \sim \mathcal{N}(E_0 - 10n_p log_{10}\left(\frac{d_k}{d_0}\right), \sigma_{sh\,k}^2) \tag{4.3}$$

After performing RSSI based ranging, the obtained ranges are assumed to be Gaussian centered on the true values with a standard deviation equal to $\sigma_{r\,k}$ for the k^{th} RSSI:

$$r_k \sim \mathcal{N}(d_k, \sigma_{r\,k}^2) \tag{4.4}$$

In the rest of the report we will consider E_T as the RSSI and the mode estimator as the RSSI ranging estimator. We will evaluate the performances of studied and proposed localization techniques using models extracted from the database. A summary of these models is given in Table 4.1:

Table 4.1: Statistical models extracted from the database and used for simulations.

RSSI	$E_0 = -36.029dB_{nJ}$, $n_p = 2.386$, $d_0 = 1m$, $\sigma_{sh\,k} = 3.98dB_{nJ}$
TOA	$\sigma_k = 1.142m$
TDOA	$\sigma_{kj} = 1.85m$

Definition of a Hybrid Localization Scenario

The assumed scenario here is a situation where the targeted mobile is connected to different anchor nodes and is able to get different LDPs from these anchor nodes. Let K be the total number of all anchor nodes implied in the scenario. Without any loss of generality, assume that the targeted MS can get:

- p RSSIs from anchor nodes with indexes $k \in (1, ..., p)$, $0 \leqslant p \leqslant K$
- $q - p$ TOAs from anchor nodes with indexes $k \in (p + 1, ..., q)$, $0 \leqslant p + q \leqslant K$
- $K - q - 1$ TDOAs from anchor nodes with indexes $k \in (q + 2, ..., K)$ obtained with respect to the $(q + 1)^{th}$ anchor node.

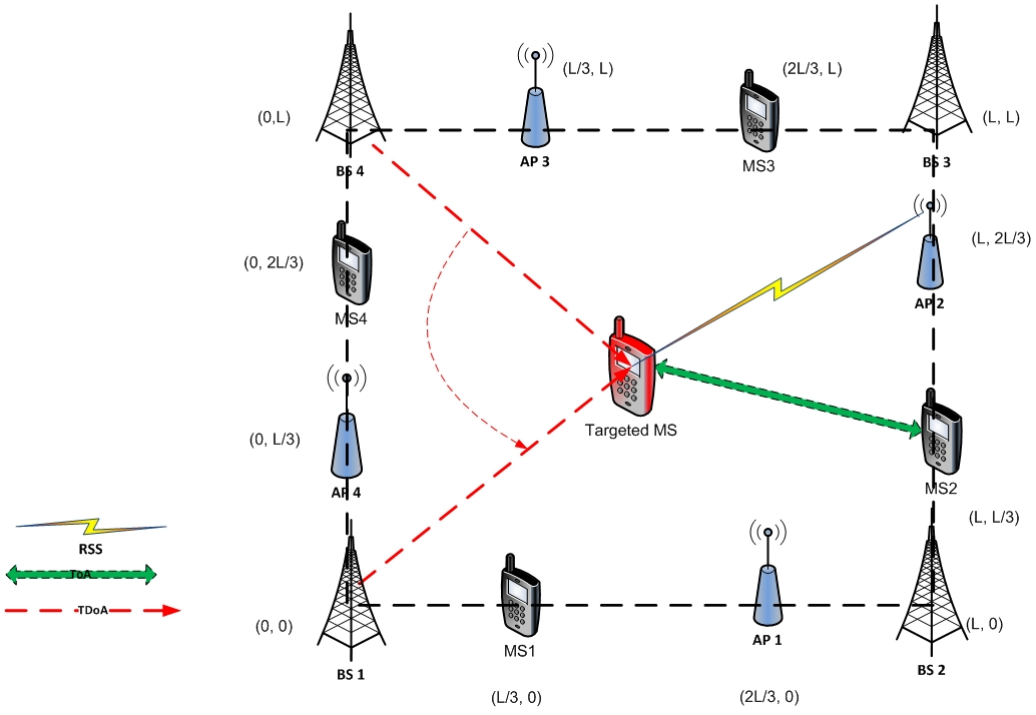

Figure 4.1: HDF scenario.

Figure 4.1 depicts an example of hybrid scenario where $p = 4$, $q = 8$, and $K = 12$. This plotted scenario will be used for simulations later in this chapter and in the next chapter. The targeted MS is supposed to lie in a $L - by - L$ squared area delimited by 4 base stations (or femtocells) from which the targeted MS can get three independent TDOAs measured with respect to the first base station located in $(0, 0)$, without any loss of generality. Besides of these four BSs, the scenario assumes that the targeted MS can get four independent TOA measurements from a set of ranging-capable MSs lying in the $L - by - L$ area. The RSSIs are finally measured within a set of access points chosen on the edges of the area. For all simulations L is taken equal to 20m.

4.2 Optimization techniques for localization purposes

In mathematics, optimization refers to choosing the best element from some set of available alternatives. In other words, this means solving problems in which one seeks to minimize or maximize an objective function by systematically choosing the values of variables from within an allowed set. An optimization problem can be written in its general formulation as follows [110]:

$$\begin{array}{ll} minimize & f_0(\mathbf{X}) \\ subject\ to & f_i(\mathbf{X}) \leqslant b_i, \quad i = 1, ..., n. \end{array} \tag{4.5}$$

Here the vector $\mathbf{X} = (x_1, ..., x_m)$ is the optimization variable of the problem, the function $f_0 : \mathbb{R}^m \to \mathbb{R}$ is the objective function, the functions $f_i : \mathbb{R}^m \to \mathbb{R}$, $i = 1, ..., n$, are the (inequality) constraint functions, and the constants $b_1, ..., b_n$ are the limits, or bounds, for the constraints. A vector $\hat{\mathbf{X}}$ is called optimal, or a solution of the problem (4.5), if it has the smallest objective value among all vectors that satisfy the constraints. An optimization problem is unconstrained if no constraints are defined on the solution. Respecting the notations in section 4.1, we get $m = 2$, $x_1 = x$, and $x_2 = y$.

In this section, we present different optimization algorithms applicable to localization problems. We start by two unconstrained optimization techniques which are least-squares (LS) and iterative maximum likelihood (ML) techniques. Then, we present the semidefinite programming technique which is based on constrained convex optimization.

4.2.1 Least-Squares Techniques

A least-squares problem is an unconstrained optimization problem with an objective which is a sum of squares of terms of the form $\mathbf{a}_i^T\mathbf{X} - b_i$:

$$minimize \quad f_0(\mathbf{X}) = \|\mathbf{AX} - \mathbf{b}\|_2^2 = \sum_{i=1}^{n} (\mathbf{a}_i^T\mathbf{X} - b_i)^2 \tag{4.6}$$

Here $\mathbf{A} \in \mathbb{R}^{n \times m}$ (with $n \geqslant m$), $\mathbf{a}_i^T$ are the rows of $\mathbf{A}$, and the vector $\mathbf{X} \in \mathbb{R}^m$ is the optimization variable. $\|.\|_2$ is the 2-norm (euclidean norm) [110]. After applying some linearizations, the solution of 4.6 can be reduced to solving a linear system [111]:

$$(\mathbf{A}^T\mathbf{A})\mathbf{X} = \mathbf{A}^T\mathbf{b} \tag{4.7}$$

The analytical solution is then given by $\mathbf{X} = (\mathbf{A}^T\mathbf{A})^{-1}\mathbf{A}^T\mathbf{b}$. For least-squares problems we have efficient algorithms (and software implementations) for solving the problem to high accuracy, with very high reliability. The least-squares problem can be solved in a time approximately proportional to m^2n. A current desktop computer can solve a least-squares problem with hundreds of variables, and thousands of terms, in a few seconds; more powerful computers, of course, can solve larger problems, or the same size problems, faster.

The least-squares problem is the basis of the linear regression. A least-squares based estimator is interpreted as the ML estimator for a vector $\mathbf{X}$ given linear measurements corrupted with Gaussian measurement errors [111]. A derivation of LS problem is the weighted least-squares problem (WLS). In WLS, the objective function $\sum_{i=1}^{n} w_i(\mathbf{a}_i^T\mathbf{X} - b_i)^2$ is minimized. The weights $w_1, ..., w_n$ are chosen positive to reflect differing levels of concern about the sizes of the terms $\mathbf{a}_i^T\mathbf{X} - b_i$, or simply to influence the solution. In a statistical setting, weighted least-squares arises in estimation of a vector $\mathbf{X}$, given linear measurements corrupted by errors with unequal variances. The weights are usually taken equal to measurement variances. The linear solution is given by:

$$\hat{\mathbf{X}} = (\mathbf{A}^T\mathbf{C}^{-1}\mathbf{A})^{-1}\mathbf{A}^T\mathbf{C}^{-1}\mathbf{b} \tag{4.8}$$

where $\mathbf{C}$ is a diagonal matrix with diagonal values equal to weights $w_1, ..., w_n$:

$$\mathbf{C} = \begin{bmatrix} w_1 & 0 & \cdots & 0 \\ 0 & w_2 & \cdots & 0 \\ \vdots & \vdots & \ddots & \vdots \\ 0 & 0 & \cdots & w_n \end{bmatrix} \tag{4.9}$$

The use of LS technique is quite different for RSSI, TOA, and TDOA. In the case of RSSI, the ranges are firstly estimated using techniques presented in section 3.3.1.3 and then LS techniques are applied on these ranges. In the case of TOA, the LS techniques are directly applied on ranges given by the TOAs multiplied by the speed of light c. The case of TDOA is quite different because the LS is applied on differences of ranges not on ranges. For each location-dependent parameter, different matrices $\mathbf{A}$, $\mathbf{b}$, and $\mathbf{C}$ are defined. Respecting the notations defined in section 4.1, $\mathbf{A}$ and $\mathbf{b}$ are given in Table 4.2 for 2D scenario where l_k is given by $l_k = x_k^2 + y_k^2$, $k \in (1, ..., K)$ and $c = 3.10^8 ms^{-1}$ is the speed of light. $\mathbf{C}$ is taken equal to $diag(\sigma_{r\,2}^2, ..., \sigma_{r\,p}^2)$ for RSSI, $diag(\sigma_{p+2}^2, ..., \sigma_q^2)$ for TOA, and $diag(\sigma_{(q+2)(q+1)}^2, ..., \sigma_{K(q+1)}^2)$ for TDOA. Notice that in the TDOA case, the vector $\mathbf{X}$ is of length $m + 1$ and estimates, in addition to the coordinates of the targeted MS, the range between the MS and the reference anchor.

Table 4.2: LS matrices for RSSI, TOA, and TDOA localization techniques.

LDP	Matrices	
RSSI	$\mathbf{A}_{\text{RSSI}}$	$\begin{pmatrix} x_2 - x_1 & y_2 - y_1 \\ x_3 - x_1 & y_3 - y_1 \\ \dots & \dots \\ x_p - x_1 & y_p - y_1 \end{pmatrix}$
	$\mathbf{b}_{\text{RSSI}}$	$\frac{1}{2}\begin{pmatrix} r_1^2 - r_2^2 + l_2 - l_1 \\ r_1^2 - r_3^2 + l_3 - l_1 \\ \dots \\ r_1^2 - r_p^2 + l_p - l_1 \end{pmatrix}$
TOA	$\mathbf{A}_{\text{TOA}}$	$\begin{pmatrix} x_{p+2} - x_{p+1} & y_{p+2} - y_{p+1} \\ x_{p+3} - x_{p+1} & y_{p+3} - y_{p+1} \\ \dots & \dots \\ x_q - x_{p+1} & y_q - y_{p+1} \end{pmatrix}$
	$\mathbf{b}_{\text{TOA}}$	$\frac{1}{2}\begin{pmatrix} c^2(\tau_{p+1}^2 - \tau_{p+2}^2) + l_{p+2} - l_{p+1} \\ c^2(\tau_{p+1}^2 - \tau_{p+3}^2) + l_{p+3} - l_{p+1} \\ \dots \\ c^2(\tau_{p+1}^2 - \tau_q^2) + l_q - l_{p+1} \end{pmatrix}$
TDOA	$\mathbf{A}_{\text{TDOA}}$	$\begin{pmatrix} x_{q+2} - x_{q+1} & y_{q+2} - y_{q+1} & c\tau_{(q+2)(q+1)} \\ x_{q+3} - x_{q+1} & y_{q+3} - y_{q+1} & c\tau_{(q+3)(q+1)} \\ \dots & \dots & \dots \\ x_K - x_{q+1} & y_K - y_{q+1} & c\tau_{K(q+1)} \end{pmatrix}$
	$\mathbf{b}_{\text{TDOA}}$	$\frac{1}{2}\begin{pmatrix} l_{q+2} - l_{q+1} - c^2\tau_{(q+2)(q+1)}^2 \\ l_{q+3} - l_{q+1} - c^2\tau_{(q+3)(q+1)}^2 \\ \dots \\ l_K - l_{q+1} - c^2\tau_{K(q+1)}^2 \end{pmatrix}$

Fusion of RSSI, TOA, and TDOA using least-squares

Applying WLS techniques to fuse different LDPs can be made easy since the used matrices (respectively $\mathbf{A}$,$\mathbf{b}$, and $\mathbf{C}$) for each LDP can be fused together and resulting in three new matrices which are denoted respectively $\mathbf{A}_{\text{HDF}}$,$\mathbf{b}_{\text{HDF}}$, and $\mathbf{C}_{\text{HDF}}$. Using the definition of assumed hybrid scenario in section 4.1, we construct $\mathbf{A}_{\text{HDF}}$,$\mathbf{b}_{\text{HDF}}$, and $\mathbf{C}_{\text{HDF}}$ respectively as follows [112]:

$$\mathbf{A}_{\text{HDF}} = \begin{bmatrix} x_2 - x_1 & y_2 - y_1 & 0 \\ & \dots & \\ x_p - x_1 & y_p - y_1 & 0 \\ x_{p+2} - x_{p+1} & y_{p+2} - y_{p+1} & 0 \\ & \dots & \\ x_q - x_{p+1} & y_q - y_{p+1} & 0 \\ x_{q+2} - x_{q+1} & y_{q+2} - y_{q+1} & c\tau_{(q+2)(q+1)} \\ & \dots & \\ x_K - x_{q+1} & y_K - y_{q+1} & c\tau_{K(q+1)} \end{bmatrix} \tag{4.10}$$

$$\mathbf{b}_{\text{HDF}} = \frac{1}{2}\begin{bmatrix} r_1^2 - r_2^2 + l_2 - l_1 \\ ... \\ r_1^2 - r_p^2 + l_p - l_1 \\ c^2\tau_{p+1}^2 - c^2\tau_{p+2}^2 + l_{p+2} - l_{p+1} \\ ... \\ c^2\tau_{p+1}^2 - c^2\tau_q^2 + l_q - l_{p+1} \\ l_{q+2} - l_{q+1} - c^2\tau_{(q+2)(q+1)}^2 \\ ... \\ l_K - l_{q+1} - c^2\tau_{K(q+1)}^2 \end{bmatrix} \tag{4.11}$$

$$\mathbf{C}_{\text{HDF}} = diag(\sigma_{r\,2}^2, ..., \sigma_{r\,p}^2, \sigma_{p+2}^2, ..., \sigma_q^2, \sigma_{(q+2)(q+1)}^2, ..., \sigma_{K(q+1)}^2) \tag{4.12}$$

Then, the solution will be given by: $\hat{\mathbf{X}} = (\mathbf{A}_{\text{HDF}}^T\mathbf{C}_{\text{HDF}}^{-1}\mathbf{A}_{\text{HDF}})^{-1}\mathbf{A}_{\text{HDF}}^T\mathbf{C}_{\text{HDF}}^{-1}\mathbf{b}_{\text{HDF}}$

Total Least squares enhancement

The major difficulty of using LS (respectively WLS) estimator is that $\mathbf{A}^T\mathbf{A}$ (respectively $\mathbf{A}^T\mathbf{C}^{-1}\mathbf{A}$) may be singular or ill-conditioned and thus cannot be exactly inverted. This fact may deteriorate the accuracy of positioning and give unacceptable solutions sometimes. In these cases, the Total Least Square (TLS) algorithm (respectively TWLS) may be of help. It is based on the Singular Value Decomposition (SVD) of $\mathbf{A}^T\mathbf{A}$ (respectively $\mathbf{A}^T\mathbf{C}^{-1}\mathbf{A}$) in order to eliminate singularities. The SVD states that there exists a factorization of any rectangular m-by-m matrix of the form $\mathbf{U}\mathbf{\Sigma}\mathbf{V}^T$ where $\mathbf{U}$ and $\mathbf{V}$ are m-by-m matrices. The matrix $\mathbf{\Sigma}$ is a m-by-m diagonal matrix with non-negative real numbers on the diagonal which contains the singular values of the rectangular initial matrix. This decomposition is very useful in statistical study of data. The vectors of $\mathbf{U}$ represent the directions of variation of the data. The diagonal values of $\mathbf{\Sigma}$ are similar to the energy or the importance which balances these directions of variation of the data. Thus, the SVD allows to construct an empiric model of the data which is as precise as the number of used energies is greater [113].

As the matrices $\mathbf{A}^T\mathbf{A}$ and $\mathbf{A}^T\mathbf{C}^{-1}\mathbf{A}$ are m-by-m rectangular ($m = 2$ in $2D$ and 3 in $3D$), a SVD can be made for them. After doing this decomposition, singular values should be eliminated based on the rank of the decomposed matrix. In fact, the number of non-zero singular values of any matrix is equal to its rank (denoted here as r). As rounding error may lead to small but non-zero singular values in a rank deficient matrix, we should eliminate these erroneous singular values from $\mathbf{\Sigma}$. Hence, the values to be replaced by zero are the $m - r$ smallest diagonal values of the matrix $\mathbf{\Sigma}$. Then, the inverse of the decomposed matrix is calculated simply by $\mathbf{V}\frac{1}{\mathbf{\Sigma}}\mathbf{U}^T$.

The condition number associated with a problem is a measure of that problem's amenability to digital computation, that is, how numerically well-conditioned the problem is. A problem with a low condition number is said to be well-conditioned, while a problem with a high condition number is said to be ill-conditioned [114]. In our study case, the condition number associated with the linear equations (4.7) and (4.8) gives a bound on how inaccurate the solution $\hat{\mathbf{X}}$ will be. Note that this is before the effects of round-off error are taken into account. Moreover, conditioning is a property of the

matrix, not the algorithm or floating point accuracy of the computer used to solve the corresponding system. The condition number of the linear systems given by (4.7) and (4.8) is then:

$$\kappa(\mathbf{A}) = \|\mathbf{A}\|\|\mathbf{A}^{-1}\| \tag{4.13}$$

where $\|\|$ is the norm operator.

Otherwise, $\kappa(\mathbf{A})$ can be defined as the quotient of the maximal by the minimal singular values of the matrix $\mathbf{A}$ [114]. Let's define $\kappa_{lim}(\mathbf{A})$ as the condition number threshold above which the problem is considered ill-conditioned and the SVD must be used. $\kappa_{lim}(\mathbf{A})$ is defined as the value of $\kappa(\mathbf{A})$ that satisfies the following equality: $\log_{10}(\kappa_{lim}(\mathbf{A})) \simeq$ the precision of matrix entries. The precision of matrix entries is simply the precision of LDP measurements (i.e. their standard deviations). The diagram in Figure 4.2 shows the proposed TWLS algorithm [115].

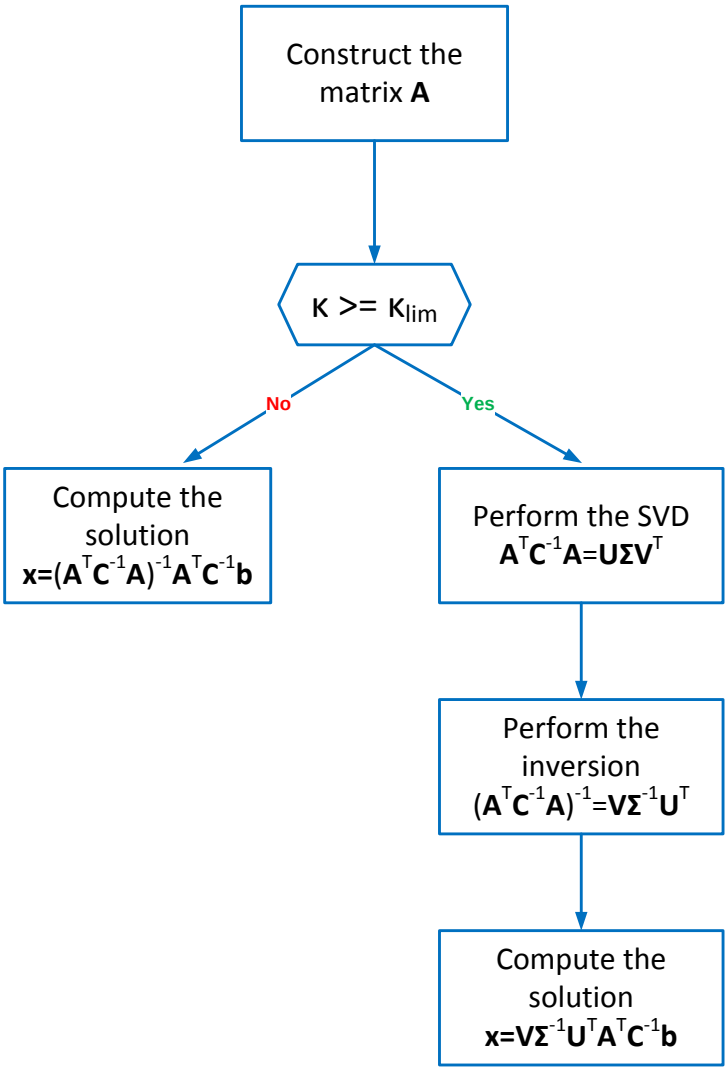

Figure 4.2: TWLS estimation scheme.

4.2.2 Iterative ML Techniques

In fact, LS and WLS techniques are suitable for linear (or linearized) optimization problems. In the case of non linear problems, solution can be obtained by maximizing the likelihood objective function. The maximum likelihood estimator is an alternative to the minimum variance unbiased estimator (MVUE) [111]. For many estimation problems, the MVUE does not exist. Moreover, when it does exist, there is no systematic procedure for finding it. In contrast, the ML estimator does not necessarily satisfy any optimality criterion, but it can almost always be computed, either through exact formulas or numerical techniques. For this reason, the ML estimator is one of the most common estimation procedures used in practice [111].

Suppose that the location dependent measurement vector (i.e. RSSI, TOA, or TDOA), denoted here $\mathcal{M}$, is distributed according to the density $p(\mathcal{M} \mid \mathbf{X})$ where $\mathbf{X}$ is the true position of targeted device. The likelihood function is defined by:

$$\mathbf{f}(\mathbf{X}, \mathcal{M}) = p(\mathcal{M} \mid \mathbf{X}) \tag{4.14}$$

The likelihood principle effectively states that all information we have about the unknown parameter $\mathbf{X}$ is contained in the likelihood function $\mathbf{f}(\mathbf{X}, \mathcal{M})$. The maximum likelihood estimate $\hat{\mathbf{X}}$ is defined by:

$$\hat{\mathbf{X}} = \underset{\mathbf{X}}{argmax}\, \mathbf{f}(\mathbf{X}, \mathcal{M}) \tag{4.15}$$

This means that we have chosen $\mathcal{M}$ that maximize the probability of occurrence of the observation of $\mathbf{X}$. If the likelihood function is differentiable, then $\hat{\mathbf{X}}$ is found by differentiating the likelihood (or log-likelihood), equating with zero, and solving:

$$\frac{\partial}{\partial \mathbf{X}}(log(\mathbf{f}(\mathbf{X}, \mathcal{M}))) = \mathbf{0} \tag{4.16}$$

Different iterative algorithms are proposed to resolve (4.16). The gradient descent method and the Newton method are widely used for resolving such problems [111]. These methods start in a given point $\mathbf{X}_0$ known as the initial guess and try to find the nearest local extrema which will be returned as the solution of the problem. This initial guess can be taken randomly or equal to the LS (or WLS) solution if available.

Assuming Gaussian models independence between considered LDP measurements, the likelihood functions are given receptively for RSSI, TOA, and TDOA by [116, 117]:

$$\begin{cases} \mathbf{f}_{\text{RSSI}}(\mathbf{X}, (E_k)_{1\leqslant k\leqslant p}) = \prod_{k=1}^{p} \frac{1}{\sqrt{2\pi} d_k S_k} e^{-\frac{(\ln d_k - M_k)^2}{2S_k^2}} & \text{for RSSI} \\ \mathbf{f}_{\text{TOA}}(\mathbf{X}, (\tau_k)_{p+1\leqslant k\leqslant q}) = \prod_{k=p+1}^{q} \frac{1}{\sqrt{2\pi}\sigma_k} e^{-\frac{(c\tau_k - d_k)^2}{2\sigma_k^2}} & \text{for TOA} \\ \mathbf{f}_{\text{TDOA}}(\mathbf{X}, (\tau_{k(q+1)})_{q+2\leqslant k\leqslant K}) = \prod_{k=q+2}^{K} \frac{1}{\sqrt{2\pi}\sigma_{k(q+1)}} e^{-\frac{(c\tau_{k(q+1)} - d_{k(q+1)})^2}{2\sigma_{k(q+1)}^2}} & \text{for TDOA} \end{cases} \tag{4.17}$$

where S_k and M_k are defined for each k respectively by (3.29) and (3.30).

Then, by applying (4.16) on these likelihood functions, we obtain easily the different ML estimators for respectively RSSI, TOA, and TDOA [116, 117].

$$\begin{cases} \nabla \mathbf{f}_{\text{RSSI}} = \sum_{k=1}^{p} \frac{1}{S_k^2} \frac{\left((M_k - S_k^2) - \ln d_k\right)}{{d_k}^2} (\hat{\mathbf{X}} - \mathbf{X}_k) = \mathbf{0} \text{ for RSSI} \\ \nabla \mathbf{f}_{\text{TOA}} = \sum_{k=p+1}^{q} \frac{1}{\sigma_k^2} \frac{(c\tau_k - d_k)}{d_k} \left(\hat{\mathbf{X}} - \mathbf{X_k}\right) = \mathbf{0} \text{ for TOA} \\ \nabla \mathbf{f}_{\text{TDOA}} = \sum_{k=q+2}^{K} \frac{\left(c\tau_{k(q+1)} - d_{k(q+1)}\right)}{\sigma_{k(q+1)}^2} \left(\frac{\mathbf{X} - \mathbf{X}_{q+1}}{d_{q+1}} - \frac{\mathbf{X} - \mathbf{X}_k}{d_k}\right) = \mathbf{0} \text{ for TDOA} \end{cases} \tag{4.18}$$

Fusion of RSSI, TOA, and TDOA using ML iterative techniques

When different measurements come from different receivers, the assumption of independence between these measurements can be made. For the hybrid scenario where different LDP are collected from different receivers, we can define the hybrid likelihood function as follows:

$$\nabla \mathbf{f}_{HDF} = \nabla \mathbf{f}_{RSSI} + \nabla \mathbf{f}_{TOA} + \nabla \mathbf{f}_{TDOA} \tag{4.19}$$

where $\nabla \mathbf{f}_{RSSI}$, $\nabla \mathbf{f}_{TOA}$, and $\nabla \mathbf{f}_{TDOA}$ are defined respectively in (4.17).

4.2.3 Convex optimization techniques: Semidefinite Programming

The matter within the ML iterative techniques is the non-convexity of the likelihood function. Indeed, when the likelihood function is not convex, the given solution can be different from the global extrema and thus leads to an erroneous estimate and a poor positioning accuracy. The solution for this problem consists mainly in using convex optimization techniques like the semidefinite programming (SDP) techniques. A fundamental property of convex optimization problems is that any locally optimal point is also globally optimal.

A semidefinite program is a convex problem which has the following form [110]:

$$\begin{aligned} &\textit{minimize} && \mathbf{c}^T \mathbf{x} \\ &\textit{subject to} && \mathbf{F}(\mathbf{x}) = x_1 \mathbf{F}_1 + ... + x_n \mathbf{F}_n + \mathbf{G} \leq 0 \\ & && \mathbf{A}\mathbf{x} = \mathbf{b} \end{aligned} \tag{4.20}$$

where $\mathbf{G}$, $\mathbf{F}_1$,...,$\mathbf{F}_n$ are symmetric matrices.

The inequality constraint represents a matrix inequality on the cone of positive semidefinite matrices, i.e. the eigenvalues of $\mathbf{F}(\mathbf{x})$ are constrained to be non-positive. This is known as a linear matrix inequality (LMI). The objective function must be linear for SDP. Constraints can be stacked in either method. This definition of SDP is used and is sufficient to solve RSSI, TOA, and TDOA localization problems.

To proceed, we propose to simplify the problem (4.15) in the form of a minimax approximation for respectively RSSI and TOA. These approximations are supported

by the so-called equivalence between both 2-norm and ∞-norm. The case of TDOA is more tricky and has not been investigated in this dissemination. The solutions for these two different problems are given respectively by:

$$\hat{\mathbf{X}} = \text{argmin} \max_{k=1,...,p} \frac{1}{\sigma_{sh\,k}} |E_k - E_0 + 10 n_p \log_{10} \frac{\|\mathbf{X} - \mathbf{X}_k\|}{d_0}| \tag{4.21}$$

$$\hat{\mathbf{X}} = \text{argmin} \max_{k=p+1,...,q} \frac{1}{\sigma_k} |(c\tau_k)^2 - \|\mathbf{X} - \mathbf{X}_k\|^2| \tag{4.22}$$

Let us define a $(m+1) \times 1$ vector $\overline{\mathbf{X}} = \begin{bmatrix} \mathbf{X}^T & 1 \end{bmatrix}^T$ and for each k in $(1, 2, ..., K)$ a matrix $\mathbf{Q}_k$ by:

$$\mathbf{Q}_k = \begin{bmatrix} \mathbf{I} & -\mathbf{X}_k \\ -\mathbf{X}_k^T & \mathbf{X}_k^T \mathbf{X}_k \end{bmatrix} \tag{4.23}$$

For RSSI cases, we define β_k by:

$$\beta_k = d_0^{-2} 10^{\frac{E_k - E_0}{5 n_p}} \tag{4.24}$$

Using $\overline{\mathbf{X}}$ and $\mathbf{Q}_k$, we express the minimax problems defined by (4.21) and (4.22) in the form of constrained SDP programs. Hence, we obtain:

$$\begin{array}{cc} \textit{minimize} & \|\mathbf{t}\|_2 \\ \textit{s.t.} & \overline{\mathbf{X}}(m+1) = 1 \\ & -\sigma_{sh\,k}\mathbf{t}[k] < \log_{10}(\beta_k \overline{\mathbf{X}}^T \mathbf{Q}_k \overline{\mathbf{X}}) < \sigma_{sh\,k}\mathbf{t}[k], k = 1, ..., p \end{array} \tag{4.25}$$

$$\begin{array}{cc} \textit{minimize} & \|\mathbf{t}\|_2 \\ \textit{s.t.} & \overline{\mathbf{X}}(m+1) = 1 \\ & -\sigma_k \mathbf{t}[k] < (c\tau_k)^2 - \overline{\mathbf{X}}^T \mathbf{Q}_k \overline{\mathbf{X}} < \sigma_k \mathbf{t}[k], k = p+1, ..., q \end{array} \tag{4.26}$$

$\mathbf{t}$ is a vector of length equal to the number of used LDPs. Now, let us denote $\chi = \overline{\mathbf{X}}\overline{\mathbf{X}}^T$. After applying semidefinite relaxation [110, 118–120], the problems can be reformulated into:

$$\begin{array}{cc} \textit{minimize} & \|\mathbf{t}\|_2 \\ \textit{s.t.} & \chi \succeq \mathbf{0} \\ & \chi(m+1, m+1) = 1 \\ & -\sigma_{sh\,k}\mathbf{t}[k] < \text{Trace}(\beta_k \mathbf{Q}_k \chi) - 1 < \sigma_{sh\,k}\mathbf{t}[k], k = 1, ..., p \end{array} \tag{4.27}$$

$$\begin{array}{cc} \textit{minimize} & \|\mathbf{t}\|_2 \\ \textit{s.t.} & \chi \succeq \mathbf{0} \\ & \chi(m+1, m+1) = 1 \\ & -\sigma_k \mathbf{t}[k] < (c\tau_k)^2 - \text{Trace}(\mathbf{Q}_k \chi) < \sigma_k \mathbf{t}[k], k = p+1, ..., q \end{array} \tag{4.28}$$

$\chi \succeq \mathbf{0}$ denotes symmetric positive semidefinite. Equations (4.27) and (4.28) are convex optimization problems. Their global optimal solutions can be found using

modern SDP solvers like *CVXOPT* and *CVXMOD* [110]. A semidefinite based solution for TDOA case is given in [121] but it does not match our objectives since we look for a minimax formulation similar to those of RSSI and TOA cases. This formulation is necessary in order to fuse TDOA with RSSI and TOA.

Fusion of RSSI and TOA using SDP techniques

The SDP program for the fusion of RSSI and TOA can be written as follows:

$$\begin{array}{cc} minimize & \|\mathbf{t}\|_2 \\ s.t. & \chi \succeq \mathbf{0} \\ & \chi(m+1,m+1) = 1 \\ & -\sigma_{sh\,k}\mathbf{t}[k] < \mathrm{Trace}(\beta_k \mathbf{Q}_k \chi) < \sigma_{sh\,k}\mathbf{t}[k], k = 1,...,p \\ & -\sigma_k \mathbf{t}[k] < (c\tau_k)^2 - \mathrm{Trace}(\mathbf{Q}_k \chi) < \sigma_k \mathbf{t}[k], k = p+1,...,q \end{array} \tag{4.29}$$

4.2.4 Simulations and Discussions

Simulations are carried out respecting the scenario and parameters defined above in section 4.1. The goal of these simulations is twofold : first, to compare the different algorithms of localization studied in this chapter and second to compare the different non-hybrid and hybrid localization schemes and evaluate the effect of fusion of hybrid LDPs on positioning accuracy. For all simulations, 1000 positions of the targeted MS are drawn randomly in the $L - by - L$ squared area with $L = 20$m. The presented results are obtained using these different positions and with applying statistical models presented in 4.1.

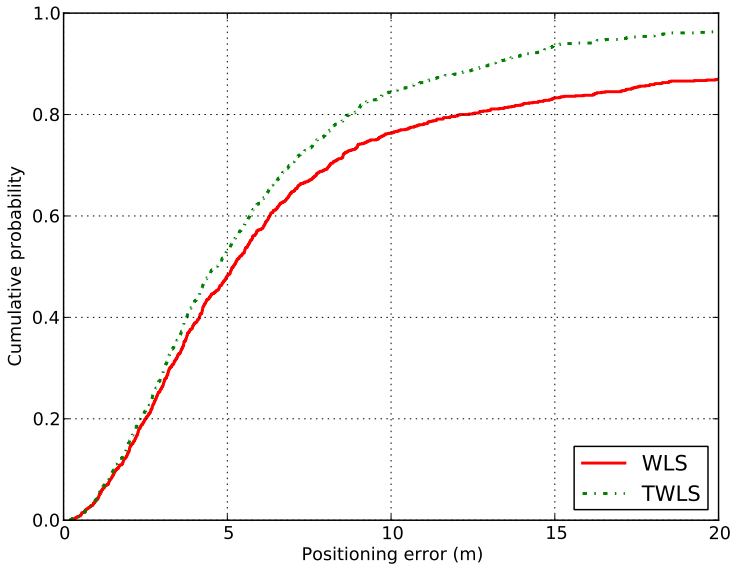

Figure 4.3: Comparison between TWLS and WLS algorithm for TDOA scheme.

First of all and in order to show the importance of the total (weighted) least-squares technique, we compare in Figure 4.3 the cumulative density functions (CDFs) of positioning error obtained respectively by WLS and TWLS techniques in the case of TDOA localization. The comparison between the two CDFs shows that the TWLS algorithm outperforms the typical WLS algorithm. For example, 80% of positioning errors are under 12.68m when using WLS technique. This error is reduced to 8.21m when using TWLS. This enhancement reveals that the TWLS algorithm avoids singularities in position computation and outperforms typical WLS algorithm.

Based on this result, we will consider and compare in the rest of this chapter the three following algorithms:

1. the Total Weighted Least-Squares algorithms : TWLS,
2. the Maximum Likelihood algorithms : ML,
3. and the Semidefinite Programming based algorithms: SDP.

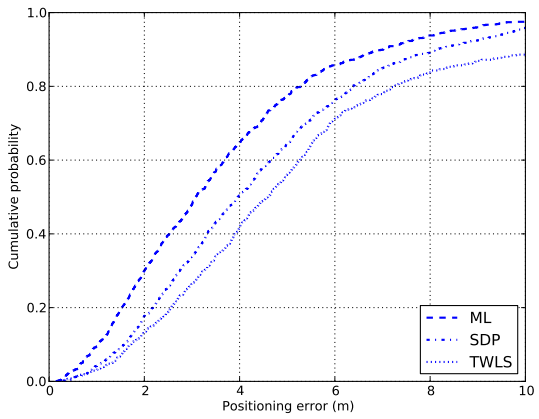

(a) RSSI

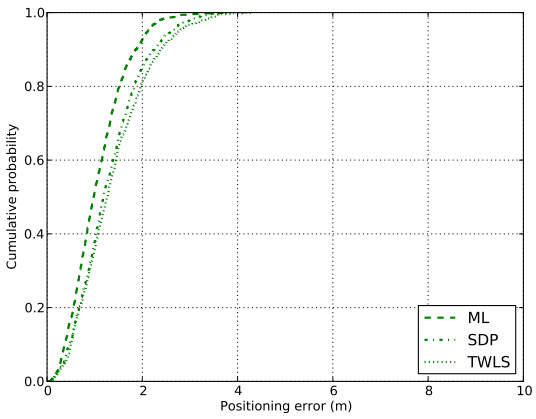

(b) TOA

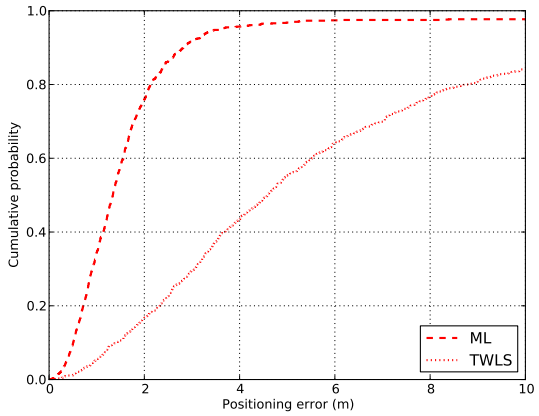

(c) TDOA

Figure 4.4: CDFs of positioning error using different estimators applied on non-hybrid localization problems.

The performances of these three algorithms applied on different non-hybrid and hybrid localization schemes are plotted respectively in Figure 4.4 and Figure 4.5. In

these figures, for each scheme the CDFs of absolute positioning error using different estimation techniques are plotted. Table 4.3 summaries these performances by giving the values of positioning error at respectively 67% and 95%. These two figures and the table reveals that different location estimators give different positioning accuracies. The ML technique outperforms the SDP technique which itself outperforms the TWLS technique. This classification of estimators is verified for all non-hybrid and hybrid localization schemes. The poor performances of the TWLS and the SDP, compared to the ML technique, are mainly due to respectively the linearization and the semidefinite approximation of the localization problem. When doing these operations, some informations are lost which affects the estimation result. In contrast, these informations are still considered by the ML non linearized objective function. Nevertheless, the ML technique may suffer from some singularities especially in the case of TDOA (see Figure 4.4-(c) where the CDF tends toward infinity because of the presence of singularities which result in large positioning errors). These singularities are due the non convexity of the ML objective functions.

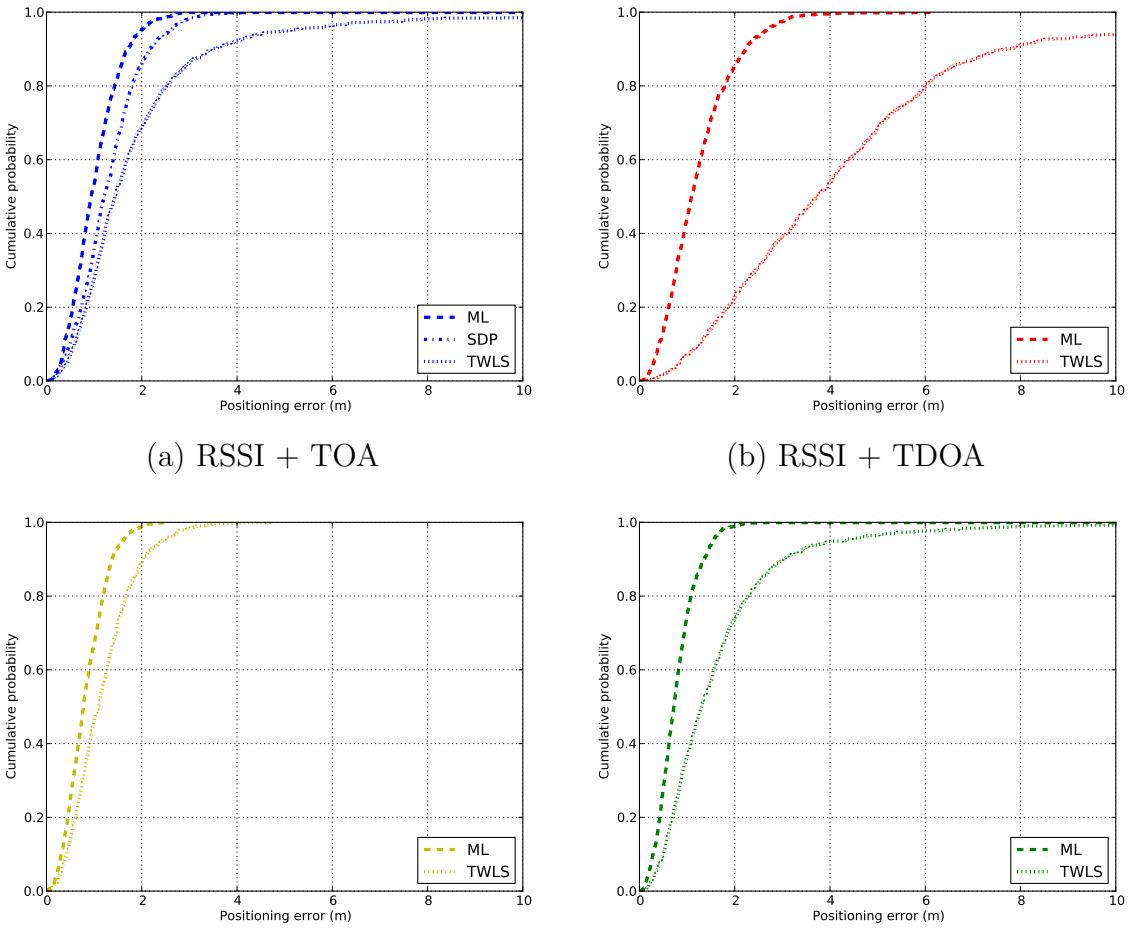

(a) RSSI + TOA (b) RSSI + TDOA

(c) TOA + TDOA (d) RSSI + TOA + TDOA

Figure 4.5: CDFs of positioning error using different estimators applied on the fusion of RSSI, TOA, and TDOA.

Table 4.3: Performances of different localization techniques applied on non-hybrid and hybrid localization problems.

LDP	Technique	Cumulative Probability	
		67%	95%
RSSI	TWLS	5.64m	14.25m
	SDP	5.13m	9.77m
	ML	4.15m	8.37m
TOA	TWLS	1.59m	2.76m
	SDP	1.51m	2.59m
	ML	1.25m	2.11m
TDOA	TWLS	6.40m	18.13m
	ML	1.69m	3.60m
RSSI + TOA	TWLS	1.88m	5.08m
	SDP	1.51m	2.56m
	ML	1.18m	1.98m
RSSI + TDOA	TWLS	4.88m	10.52m
	ML	1.42m	2.65m
TOA + TDOA	TWLS	1.37m	2.42m
	ML	1.00m	1.60m
RSSI + TOA + TDOA	TWLS	1.75m	4.26m
	ML	0.90m	1.55m

Since the ML gives the best performances among the studied estimators, we use it below in order to compare the different localization schemes and to study the effect of hybrid fusion of LDPS on positioning accuracy. That is, the performances of different non-hybrid and hybrid schemes using ML technique are depicted in Figure 4.6. This figure and Table 4.3 reveals the following points:

- Comparison between non-hybrid schemes shows that time-based LDPs give better accuracies than the power-based LDP (i.e. RSSI) which gives the worst positioning accuracy. Since localization with RSSI relies on path loss models which give an imperfect statistical representation of radio channel, the offered positioning accuracy cannot be very reliable. Moreover, the variation of shadowing is generally higher and makes the estimation of distance very inaccurate. In order to enhance the RSSI-based positioning accuracy, more sophisticated path loss models are needed.

- Adding TOA, TDOA, or both of them to RSSI drastically enhances the positioning accuracy. By contrast, adding RSSI to TOA, TDOA, or both results in minor enhancement of positioning accuracy. This is justified by the higher precision of time-based LDPs (especially in UWB networks) and the unreliability of RSSI measurements because of shadowing and radio propagation phenomena. This point has been expected at the beginning of the thesis and validates one of our objectives. Nevertheless, we will see later that the effect of additional LDPs depends not only on their precisions but also on the precision of already available

ones. For example, a RSSI measurement fused with a very imprecise TOA would enhance the positioning accuracy.

- Fusing all available LDPs is obviously the most accurate localization scheme. This is in line with the estimation theory stating that more are available informations better is the estimation accuracy.

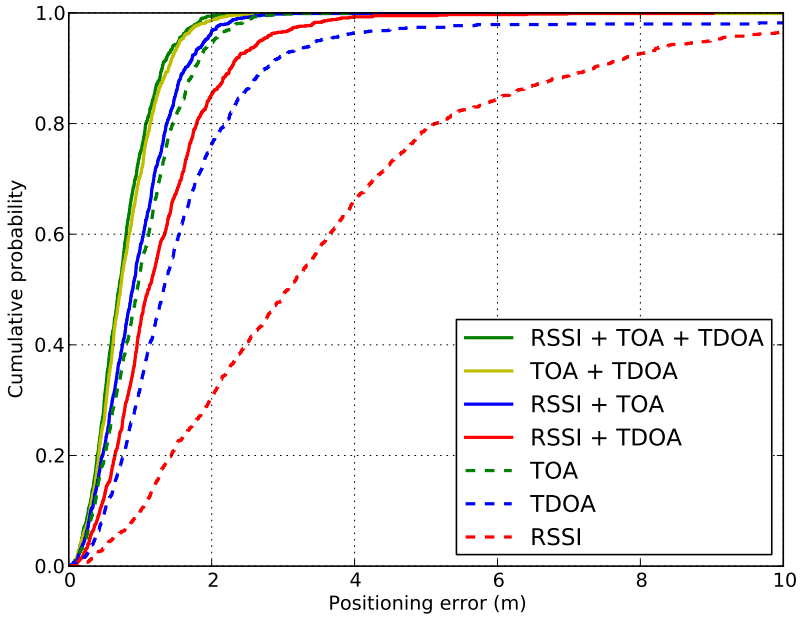

Figure 4.6: CDFs of positioning error for different non-hybrid and hybrid schemes using ML technique.

Since it is interesting for operators to reduce complexity and resources consumption, the use of ranging procedures must be reduced because such procedures consume much resources and cause overhead. Moreover, RSSIs are usually accessible without additional costs. That is, reaching the requested accuracy while using all available RSSIs and reducing the number of TOA and TDOA seems to be a very interesting scenario. In order to show the effect of adding TOA (respectively TDOA) to RSSI on positioning accuracy, let us consider the ML technique applied on the scheme (RSSI+TOA) (respectively (RSSI+TDOA)). Let us assume all four RSSIs available and gradually increase the number of additional TOAs (respectively TDOAs). Figure 4.7 plots first the CDFs of absolute positioning error and second the evolution of average absolute positioning error over the area with respect to the number of added TOAs. Figure 4.8 represents the same results in the TDOA case. These figures show a gradual enhancement provided by increasing the number of used TOA (respectively TDOA). Nevertheless, adding some LDPs may deteriorate the positioning accuracy. This can be explained by the fact that some LDPs are very imprecise or that they come from a device misplaced with respect to other devices. Hence, a localization system must be able to expect the effect of additional TOAs or TDOAs in order to perform the adequate number of ranging procedures with the adequate available devices. The Cramer-Rao Lower Bounds

seem to be the best candidate that allow the system expecting positioning accuracies.

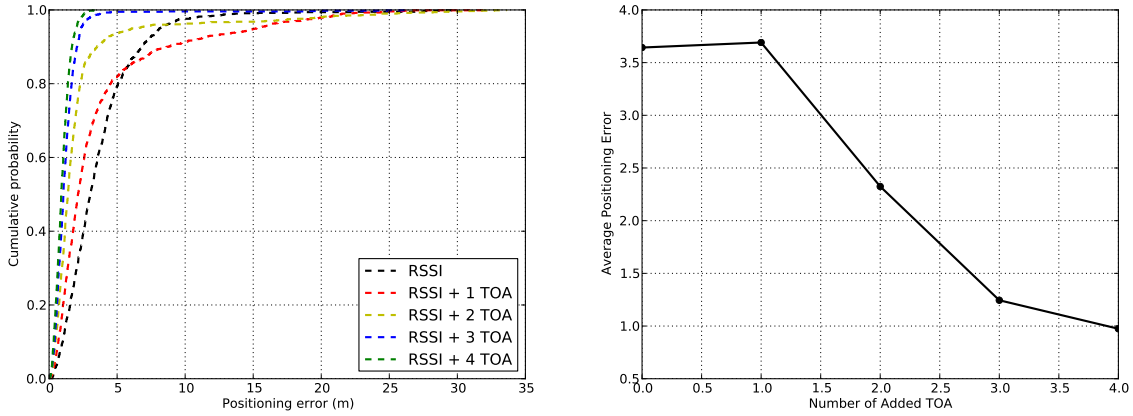

Figure 4.7: Effect of additional TOA on hybrid (RSSI+TOA) positioning accuracy using ML technique.

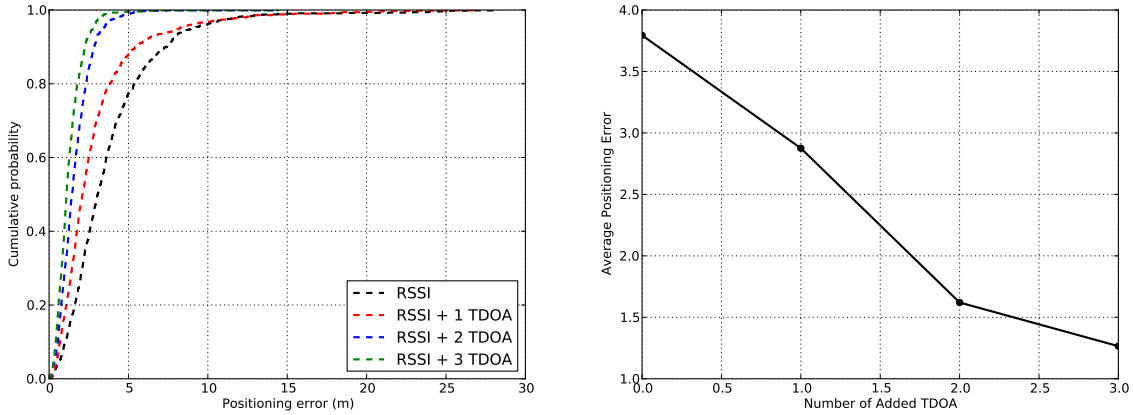

Figure 4.8: Effect of additional TDOA on hybrid (RSSI+TDOA) positioning accuracy using ML technique.

4.3 Performances assessment of Hybrid and Non-Hybrid Localization Schemes

4.3.1 Fisher Information and Cramer-Rao Lower Bound

In estimation theory and statistics, the Cramer-Rao bound (CRB) or Cramer-Rao lower bound (CRLB), named in honour of Harald Cramér and Calyampudi Radhakrishna Rao who were among the first to derive it, expresses a lower bound on the variance of estimators of a deterministic parameter. The bound is also known as the Cramer-Rao inequality or the information inequality [122]. In its simplest form, the bound states

that the variance of any unbiased estimator is at least as high as the inverse of the Fisher information (FI). An unbiased estimator which achieves this lower bound is said to be efficient. Such a solution achieves the lowest possible mean squared error among all unbiased methods, and is therefore the minimum variance unbiased estimator (MVUE). However, in some cases, no unbiased technique exists which achieves the bound. This may occur even when a MVUE exists [122].

The Fisher information is a way of measuring the amount of information that an observable random variable ($\mathcal{M}$ in our study) carries about an unknown parameter $\mathbf{X}$ upon which the likelihood function of $\mathbf{X}$, $\mathbf{f}(\mathbf{X}, \mathcal{M})$, depends. The likelihood function is the joint probability of the data, conditional on the value of $\mathbf{X}$, as a function of $\mathbf{X}$. The Fisher information is equal to the variance of the score. The score is the partial derivative, with respect to $\mathbf{X}$, of the logarithm (commonly the natural logarithm) of the likelihood function [123]. Since the expectation of the score is zero, the variance is simply the second moment of the score, the derivative of the log of the likelihood function with respect to $\mathbf{X}$. Consider position vectors, the FI takes the form of a $m - by - m$ matrix with m equal to 2 in 2D and 3 in 3D. This matrix is called the Fisher Information Matrix (FIM) and its typical element is defined by [123]:

$$\left(\mathbf{J}_{\mathcal{M}}(\mathbf{X})\right)_{ij} = E\left\{\frac{\partial}{\partial \mathbf{X}_i}\ln \mathbf{f}\left(\mathcal{M}, \mathbf{X}\right)\frac{\partial}{\partial \mathbf{X}_j}\ln \mathbf{f}\left(\mathcal{M}, \mathbf{X}\right)|\mathbf{X}\right\} \tag{4.30}$$

The Fisher information is thus the expectation of the squared score. A random variable carrying high Fisher information implies that the absolute value of the score is often high. Fisher information may thus be seen to be a measure of the "sharpness" of the support curve near the maximum likelihood estimate of $\mathbf{X}$. Besides, information is additive, in that the information yielded by two independent experiments is the sum of the information from each experiment separately:

$$\mathbf{J}_{\mathcal{M},\mathcal{N}}(\mathbf{x}) = \mathbf{J}_{\mathcal{M}}(\mathbf{X}) + \mathbf{J}_{\mathcal{N}}(\mathbf{X}) \tag{4.31}$$

The covariance matrix of any unbiased estimator $\hat{\mathbf{X}}$ of $\mathbf{X}$ is then bounded by the inverse of the Fisher information matrix:

$$var\left(\mathbf{X}\right) \geq \left(\mathbf{J}_{\mathcal{M}}\left(\mathbf{X}\right)\right)^{-1} \tag{4.32}$$

The Cramer-Rao Lower Bound is then defined as the trace of the inverse of the FIM [123]:

$$\mathrm{CRLB}\left(\mathbf{X}\right) = tr\left\{\left(\mathbf{J}\left(\mathbf{X}\right)\right)^{-1}\right\} \tag{4.33}$$

These theoretic results will be then applied for non-hybrid and hybrid localization problems in order to assess theoretic performances of different studied localization schemes.

4.3.2 Application to Non-Hybrid and Hybrid localization Techniques

Based on results presented in the previous section, we develop the expressions of FIMs and CRLBs for both non-hybrid and hybrid localization schemes. The FIM for respectively RSSI-, TOA-, and TDOA- based localization schemes are defined by:

$$\mathbf{J}_{\text{RSSI}} = E\left[\nabla \mathbf{f}_{RSSI} \cdot \nabla \mathbf{f}_{RSSI}^{T}\right] \tag{4.34}$$

$$\mathbf{J}_{\text{TOA}} = E\left[\nabla \mathbf{f}_{TOA} \cdot \nabla \mathbf{f}_{TOA}^{T}\right] \tag{4.35}$$

$$\mathbf{J}_{\text{TDOA}} = E\left[\nabla \mathbf{f}_{TDOA} \cdot \nabla \mathbf{f}_{TDOA}^{T}\right] \tag{4.36}$$

Since calculations are similar in the three cases, we will only present the case of TOA. The CRLB of RSSI and TDOA based localization schemes can be obtained similarly as in the TOA case. The detailed calculations are shown in the Appendix D.

Using the expression of $\nabla \mathbf{f}_{\text{TOA}}$ defined in (4.18) and assuming independence between TOA measurements, the FIM given by (4.35) can be written as [117]:

$$\mathbf{J}_{\text{TOA}} = E\left[\sum_{k=p+1}^{q} \frac{1}{\sigma_k^4} \frac{\left(c\tau_k - d_k\right)^2}{{d_k}^2} \left(\mathbf{X} - \mathbf{X}_k\right)\left(\mathbf{X} - \mathbf{X}_k\right)^T\right] \tag{4.37}$$

Developing this expression leads to:

$$\mathbf{J}_{\text{TOA}} = \sum_{k=p+1}^{q} \frac{\left(\mathbf{X} - \mathbf{X}_k\right)\left(\mathbf{X} - \mathbf{X}_k\right)^T}{\sigma_k^2} \tag{4.38}$$

and then to:

$$\mathbf{J}_{\text{TOA}} = \sum_{k=p+1}^{q} \frac{1}{\sigma_k^2} \begin{bmatrix} \frac{(x-x_k)^2}{{d_k}^2} & \frac{(x-x_k)(y-y_k)}{{d_k}^2} \\ \frac{(x-x_k)(y-y_k)}{{d_k}^2} & \frac{(y-y_k)^2}{{d_k}^2} \end{bmatrix} \tag{4.39}$$

The CRLB is then computed using (4.33) and it is given by:

$$\sigma^2_{\text{TOA}} = \frac{\sum_{k=p+1}^{q} \frac{1}{\sigma_k^2}}{\sum_{k=p+1}^{q} \frac{(x-x_k)^2}{\sigma_k^2 d_k^2} \sum_{k=p+1}^{q} \frac{(y-y_k)^2}{\sigma_k^2 d_k^2} - \left(\sum_{k=p+1}^{q} \frac{(x-x_k)(y-y_k)}{\sigma_k^2 d_k^2}\right)^2} \tag{4.40}$$

After simplifications, (4.40) can be written as:

$$\sigma^2_{\text{TOA}} = \frac{\sum_{k=p+1}^{q} \frac{1}{\sigma_k^2}}{\frac{1}{2} \sum_{k=p+1}^{q} \sum_{l=p+1}^{q} \frac{((x-x_k)(y-y_l)-(x-x_l)(y-y_k))^2}{\sigma_k^2 \sigma_l^2 d_k^2 d_l^2}} \tag{4.41}$$

Let φ_k be the angle between the d_k and the line $(y = 0)$. We get $\cos(\varphi_k) = \frac{x-x_k}{d_k}$ and $\sin(\varphi_k) = \frac{y-y_k}{d_k}$. Introducing that in (4.41), using the trigonometric equality

$\cos(\varphi_k)\sin(\varphi_l) - \cos(\varphi_l)\sin(\varphi_k) = \sin(\varphi_l - \varphi_k)$, and defining $\varphi_{lk} = \varphi_l - \varphi_k$ the angle between d_k and d_l lead to the simplified expression of the CRLB.

$$\sigma^2_{\text{TOA}} = \frac{\sum_{k=p+1}^{q} \frac{1}{\sigma_k^2}}{\sum_{k=p+1}^{q}\sum_{l=p+1}^{q} \frac{sin^2(\varphi_{lk})}{2\sigma_k^2\sigma_l^2}} \tag{4.42}$$

Similarly to (4.42), the CRLBs of RSSI and TDOA cases are given respectively by:

$$\sigma^2_{\text{RSSI}} = \frac{\sum_{k=1}^{p} \frac{(1+S_k^2)}{S_k^2 d_k^2}}{\sum_{k=1}^{p}\sum_{l=1}^{p} \frac{(1+S_k^2)(1+S_l^2)sin^2(\varphi_{lk})}{2S_k^2 S_l^2 d_k^2 d_l^2}} \tag{4.43}$$

$$\sigma^2_{\text{TDOA}} = \frac{\sum_{k=q+2}^{K} \frac{1-\cos(\varphi_{k(q+1)})}{\sigma^2_{k(q+1)}}}{\sum_{k=q+2}^{K}\sum_{l=q+2}^{K} \frac{(sin(\varphi_{lk})-(sin(\varphi_{l(q+1)})-sin(\varphi_{k(q+1)})))^2}{4\sigma^2_{k(q+1)}\sigma^2_{l(q+1)}}} \tag{4.44}$$

In the case of heterogeneous scenario and assuming independence between all measurements, the FIM can be defined as the sum of the FIMs of different LDP implied in the scenario. That is, for a scenario that implies RSSI, TOA, and TDOA:

$$\mathbf{J}_{\text{HDF}} = \mathbf{J}_{\text{RSSI}} + \mathbf{J}_{\text{TOA}} + \mathbf{J}_{\text{TDOA}} \tag{4.45}$$

Consequently, the CRLB is given by :

$$\sigma^2_{\text{HDF}} = tr\left\{(\mathbf{J}_{\text{HDF}})^{-1}\right\} \tag{4.46}$$

These CRLBs give a theoretical prior information about the best positioning accuracy that can be achieved for a given localization problem. These expressions of different CRLBs show that the positioning accuracy depends on different parameters:

- The nature of used LDPs (RSSI, TOA, or TDOA): for each LDP or combination of LDPs a different expression of the CRLB is defined. Hence, the achieved positioning accuracy depends strongly on the implied LDP (or combination of LDPs).

- The number of used LDP: depending on the values of K, the positioning accuracy may increase or decrease. Nevertheless, using more LDPs does not mean automatically a better positioning accuracy. For example, 4 cellular RSSIs may not perform better than 3 UWB based TOAs. In fact, this depends mainly on the two next parameters.

- The precision of the used LDP: given by $\sigma_{sh\,k}$, σ_k, and $\sigma_{k(q+1)}$ for repectively RSSI, TOA, and TDOA. Their values depend on different parameters (RAT, radio channel, propagation phenomena, etc) as shown in chapter 3.

- The position of the targeted device with respect to anchor nodes: i.e. the relative geometry of the localization problem. The position of an additional anchor node should be properly chosen in order to enhance the positioning accuracy. In fact, this parameter is represented in the CRLB expressions by $\sin(\varphi_{lk})$. For fixed $\sigma_{sh\,k}$, σ_k, and $\sigma_{k(q+1)}$, the best configuration of anchor nodes is the configuration which minimizes $\sum_k \sum_l \sin(\varphi_{lk})$ (i.e. which minimizes the CRLB). This is very interesting when the system has to choose an additional LDP in order to enhance the positioning accuracy. It should choose the LDP that minimizes the CRLB.

4.3.3 Simulations and Discussions

4.3.3.1 Geometric Distribution of CRLBs for Both Non Hybrid and Hybrid Localization Schemes

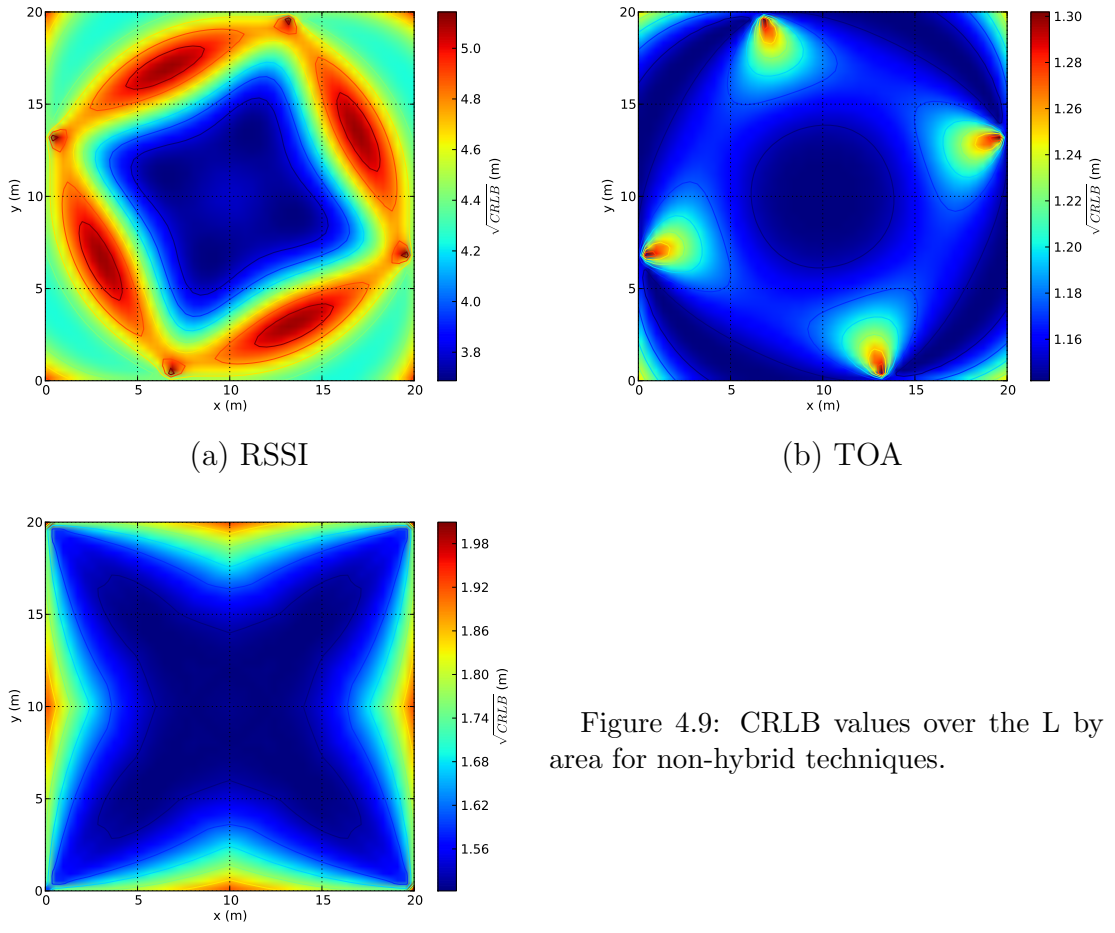

(a) RSSI

(b) TOA

(c) TDOA

Figure 4.9: CRLB values over the L by L area for non-hybrid techniques.

The CRLBs for RSSI, TOA, and TDOA are shown respectively in Figure 4.9 (a), (b), and (c). These figures are obtained using the same precision parameters (i.e. S_k, σ_k, and $\sigma_{k(q+1)}$) for all anchor devices. Hence, these figures show the geometric distribution of the CRLB over the assumed area. The comparison between these three figures

obviously reveals that time based techniques (i.e. TOA and TDOA) have better overall localization accuracy than power based technique (RSSI). In addition, comparison between Figure 4.9-(b) and Figure 4.9-(c) shows that the TOA technique outperforms the TDOA technique. Moreover, these three figures show that the CRLB depends on the position of targeted MS with respect to the configuration of anchor nodes. This dependency is quite different from one LDP to another. In the RSSI case, the positioning accuracy is degraded as the MS approaches an anchor node or an edge of the considered squared area. In the case of TOA, the difficulties of localization are located around the anchor nodes and the positioning accuracy is as better as the MS moves toward the center of the area (i.e. equidistant to all ANs). In the TDOA case, the difficulties of localization are mainly located around the edges of the assumed squared area.

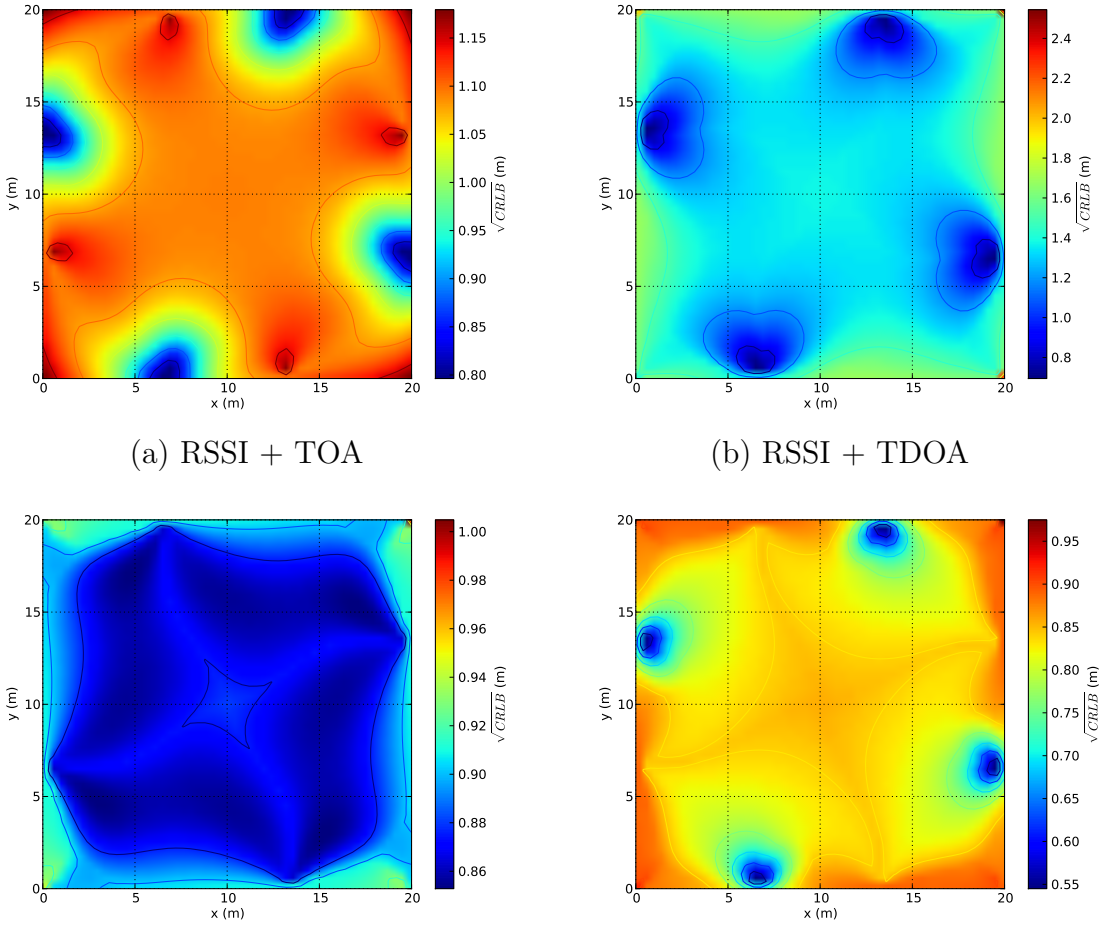

(a) RSSI + TOA

(b) RSSI + TDOA

(c) TOA + TDOA

(d) RSSI + TOA + TDOA

Figure 4.10: CDFs of positioning error using different estimators applied on the fusion of RSSI, TOA, and TDOA.

In order to theoretically evaluate the effect of fusion of different LDP on positioning accuracy, we plot in Figure 4.10 from (a) to (d) the values of CRLBs over the simulated area for respectively (RSSI+TOA), (RSSI+TDOA), (TOA+TDOA), and

(RSSI+TOA+TDOA) hybrid schemes. These figures show that the overall positioning accuracy is enhanced when fusing LDPs. The comparison between these figures reveals that the fusion of the three parameters is the scheme that offers the best accuracy. The fusion of time-based parameters (TOA and TDOA) itself offers a better accuracy than the two schemes (RSSI+TOA) and (RSSI+TDOA) which offer close performances. The enhancement is more drastic when time based parameters are fused with RSSI. Table 4.4 gives the ACRLB values for each localization schemes.

Table 4.4: ACRLB values over the L-by-L area for non hybrid and hybrid schemes.

LDP	ACRLB (m)
RSSI	4.378
TDOA	1.600
TOA	1.165
RSSI+TDOA	1.334
RSSI+TOA	1.065
TOA+TDOA	0.875
RSSI+TOA+TDOA	0.824

For given $S_k = S$, $\sigma_k = \sigma$, and $\sigma_{k(q+1)} = \sigma_{q+1}$, (4.43), (4.42), and (4.44) become respectively:

$$\sigma^2_{\text{TOA}} = \frac{2(q-p)\sigma^2}{\sum\limits_{k=p+1}^{q}\sum\limits_{l=p+1}^{q} sin^2(\varphi_{lk})} \tag{4.47}$$

$$\sigma^2_{\text{RSSI}} = \frac{\frac{2S^2}{1+S^2}\sum\limits_{k=1}^{p}\frac{1}{d_k^2}}{\sum\limits_{k=1}^{p}\sum\limits_{l=1}^{p}\frac{sin^2(\varphi_{lk})}{d_k^2 d_l^2}} \tag{4.48}$$

$$\sigma^2_{\text{TDOA}} = \frac{4\sigma^2_{(q+1)}\sum\limits_{k=q+2}^{K}(1-\cos(\varphi_{k(q+1)}))}{\sum\limits_{k=q+2}^{K}\sum\limits_{l=q+2}^{K}(sin(\varphi_{lk}) - (sin(\varphi_{l(q+1)}) - sin(\varphi_{k(q+1)})))^2} \tag{4.49}$$

Hence, we obtain three purely geometric quantities respectively for RSSI, TOA, and TDOA as follows:

$$g^2_{\text{TOA}} = \frac{1}{\sum\limits_{k=p+1}^{q}\sum\limits_{l=p+1}^{q} sin^2(\varphi_{lk})} \tag{4.50}$$

$$g^2_{\text{RSSI}} = \frac{\sum\limits_{k=1}^{p}\frac{1}{d_k^2}}{\sum\limits_{k=1}^{p}\sum\limits_{l=1}^{p}\frac{sin^2(\varphi_{lk})}{d_k^2 d_l^2}} \tag{4.51}$$

$$g^2_{\text{TDOA}} = \frac{\sum_{k=q+2}^{K} (1 - \cos(\varphi_{k(q+1)}))}{\sum_{k=q+2}^{K} \sum_{l=q+2}^{K} (sin(\varphi_{lk}) - (sin(\varphi_{l(q+1)}) - sin(\varphi_{k(q+1)})))^2} \tag{4.52}$$

These quantities define the geometric dilution of precision (GDOP) for respectively RSSI, TOA, and TDOA. Similarly and using (4.45) and (4.46) the GDOP for hybrid schemes can be obtained. The GDOP is commonly defined as the term associated with errors in position caused by the relative location of anchor nodes with which LDP measurements are performed [124]. Moreover, the GDOP matrix is defined as the unweighted FIM [50]. In the case of TOA, this GDOP matrix is given by:

$$\mathbf{G}_{\text{TOA}} = \sum_{k=p+1}^{q} \begin{bmatrix} \frac{(x-x_k)^2}{{d_k}^2} & \frac{(x-x_k)(y-y_k)}{{d_k}^2} \\ \frac{(x-x_k)(y-y_k)}{{d_k}^2} & \frac{(y-y_k)^2}{{d_k}^2} \end{bmatrix} \tag{4.53}$$

Thus, all distributions shown in Figure 4.9 and Figure 4.10 are proportional to the distribution over the area of the GDOP. The GDOP can be used as a criteria to choose the right configuration of anchor nodes. The lower value of this term is measured, the better geometric conditions we have. Equations (4.50), (4.51), and (4.52) reveals that GDOP is as higher as φ_{lk} approaches zero. Hence, bad geometry occurs when anchor nodes are placed along a line or very close to each other.

4.3.3.2 Effect of LDPs

In this section, effect of precisions of LDPs on positioning accuracy are theoretically assessed using the definition of Average CRLB (ACRLB). Three parameters are considered: the RSSI shadowing given by $\sigma_{sh\,k}$, the TOA ranging error given by σ_k and the TDOA ranging error given by $\sigma_{k(q+1)}$.

Effect of the RSSI shadowing
For each hybrid scheme that involve RSSI, Figure 4.11 plots the evolution of ACRLB over the area ($L = 20\,m$) with respect to the standard deviation of RSSI shadowing ($\sigma_{sh\,k}$). Obviously, when $\sigma_{sh\,k}$ increases the accuracy of RSSI-based localization scheme decreases. By contrast, when fusing RSSI with other time-based LDPs the effect of shadowing (i.e. $\sigma_{sh\,k}$) is attenuated. For $\sigma_{sh\,k} = 6dB_{nJ}$, a gain of 5.3m and 4.9m is performed when adding TOA or TDOA to RSSI respectively. This gain passes to 5.6m when fusing both TOA and TDOA with RSSI.

Effect of the TOA ranging error
Figure 4.12 plots the evolution of ACRLB with respect to the TOA ranging error (σ_k) for techniques involving TOA. The figure shows obviously that the accuracy of non-hybrid TOA localization scheme deteriorates as σ_k increases. The adding of RSSI measurements enhances this accuracy and reduce the effect of ranging error. This enhancement provided by RSSI is as important as the TOA are less precise (a gain of 0.21m at $\sigma_k = 2m$ and 2.9m at $\sigma_k = 6m$). Moreover, the curves of both (TOA+TDOA) and (RSSI+TOA+TDOA) techniques reveal that fusing TOA with TDOA or both

TDOA and RSSI drastically attenuate the effect of TOA ranging error on positioning accuracy. When adding RSSI and TDOA, a gain of 4.9m is performed for $\sigma_k = 6m$.

Effect of the TDOA ranging error

The effects of TDOA ranging error ($\sigma_{k(q+1)}$) on localization techniques involving TDOA parameters are plotted in Figure 4.13. This figure reveals similar remarks like in the TOA and RSSI cases. Indeed, as $\sigma_{k(q+1)}$ increases the accuracy of TDOA technique deteriorates. The RSSI reduces the ACRLB by 2.5m at $\sigma_{k(q+1)} = 6m$. But adding TOA or both RSSI and TOA enhances deeply the positioning accuracy and compensates the effect of TDOA ranging error.

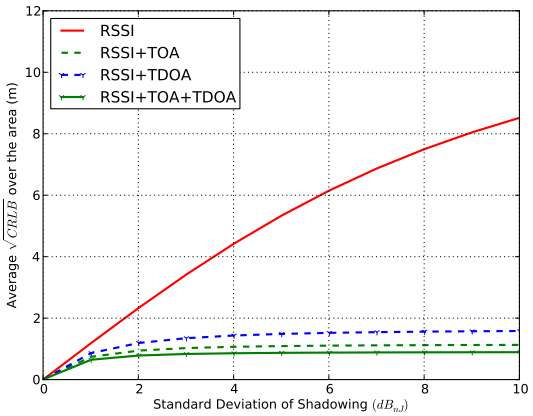

Figure 4.11: ACRLB of different techniques with respect to the RSSI shadowing

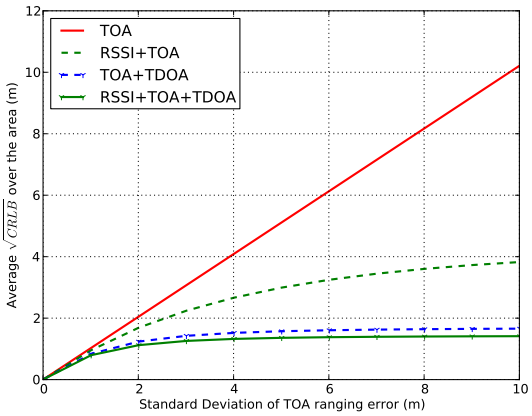

Figure 4.12: ACRLB of different techniques with respect to TOA ranging error

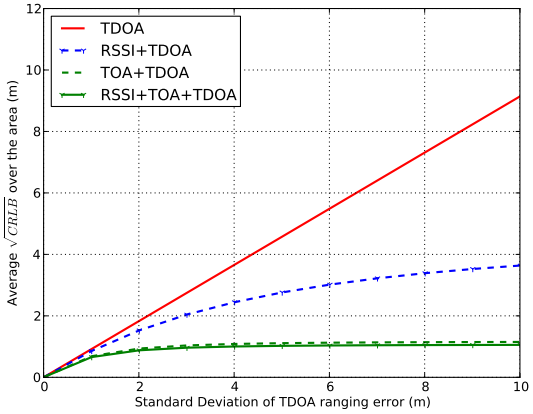

Figure 4.13: ACRLB of different techniques with respect to TDOA ranging error

4.3.3.3 Choice of localization techniques based on CRLB

The theoretical and simulated results presented till now in section 4.3 emphasize the fact that CRLB can be used as a criteria for the choice of the right localization scheme

(i.e. LDPs) and the planning of localization systems. Because of its theoretical nature, the CRLB can be calculated before performing localization task. Hence, it can offer a prior information about the accuracy level reachable by the system using its available resources (anchor nodes, measurements techniques, etc) while considering accuracies of performed measurements. The CRLB can be presented as a criterion for choosing additional (LDPs) to enhance the actual positioning accuracy of the system. This is shown by the different steps in Figure 4.14.

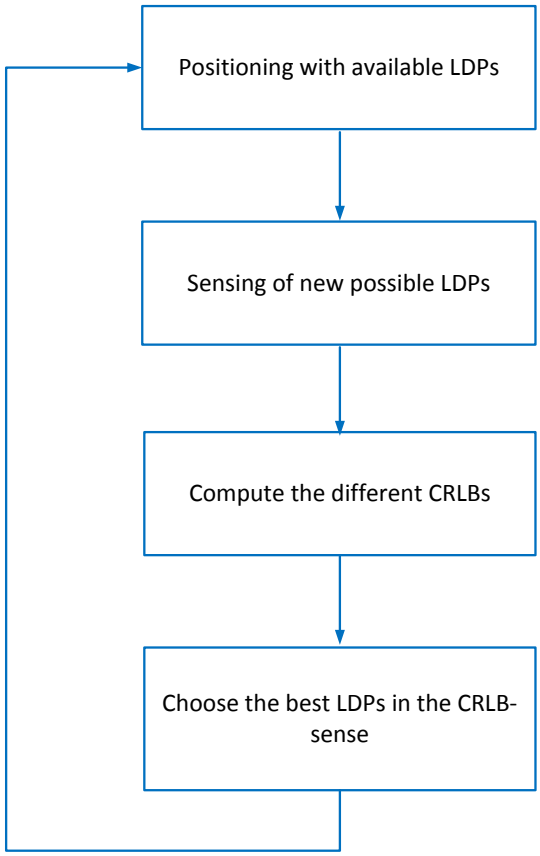

Figure 4.14: The CRLB as a criterion for choosing additional LDPs.

Since localization systems cannot be disassociated from communication systems already installed in different area, the available number of anchor nodes may be known and fixed. In this case, the accuracy of positioning technique depends only on the nature (RSSI, TOA, or TDOA), the number, and the accuracies of performed measurements. We are mainly interested in the scenario where the MS is using all available RSSI measurements and is trying to add some TOAs or TDOAs in order to reach the requested accuracy. Here, we assume that the targeted MS communicates first to discover all available ranging-capable devices. Then, the MS uses CRLB, computed using available estimation of its position, in order to choose the best set of these devices in order to perform ranging with them and then localization. As explained in section 2.3.3 in the second chapter, this scenario is justified by rational facts:

1. RSSI measurements are usually available with no additional costs in all RATs.

2. TOA and TDOAs measurements are more precise than RSSI especially in UWB standard.

3. TOAs or TDOAs are measured through ranging techniques which demand additional resources and costs.

4. These ranging procedures may cause network congestion and reduce network throughput. Hence, ranging attempts should be reduced as much as possible.

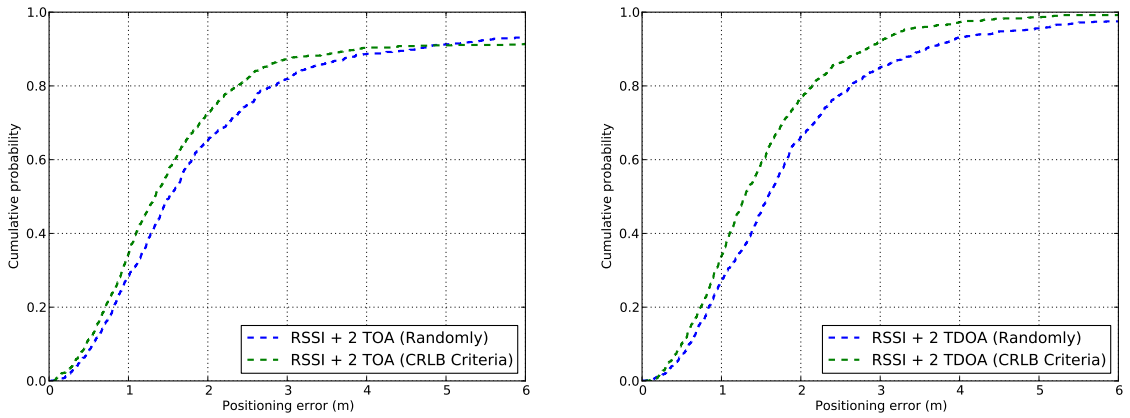

(a) (b)

Figure 4.15: CDF of positioning error for the hybrid scheme (4 RSSI + 2 TOA (TDOA)) with TOA (TDOA) chosen first randomly and then based on CRLB.

The steps presented in Figure 4.14 are applied on respectively the two hybrid schemes (RSSI+TOA) and (RSSI+TDOA). We assume the targeted MS has access to all available RSSIs and seeks to enhance its positioning accuracy using two additional TOAs or TDOAs. These additional measurements can be taken randomly or using the CRLB as a criteria. For respectively (RSSI+TOA) and (RSSI+TDOA), Figure 4.15-(a) and (b) plot the CDFs of positioning errors for both random and CRLB-based cases. In the first case, the two additional time-based LDPs are chosen randomly from the possible LDPs (see Figure 4.1). The second scenario chooses the couple of additional LDPs based on the calculation of CRLB of all possible couples (in the assumed scenario: 6 couples of TOAs and 3 couples of TDOAs). At each iteration, the couple that offers the lowest CRLB value is chosen and localization is performed by ML technique using the four available RSSIs and the two chosen TOAs (respectively TDOAs). Figure 4.15 shows that the second scenario outperforms the first one for both (RSSI+TOA) and (RSSI+TDOA) schemes. This result justifies the hypothesis that CRLB can be used as a criteria to enhance localization accuracy.

4.4 Conclusion

This chapter has been dedicated to algebraic localization techniques. These techniques aim to use available LDPs to perform the task of finding a position of a targeted device.

The focus has been first put on defining clearly what a localization problem is and on explaining the difference between non-hybrid and hybrid problems. The second section has presented the most used algebraic estimators which are all based on optimization techniques. We have started by least-squares based techniques and proposed a total least-squares enhancement. Then, we have presented maximum-likelihood techniques and semidefinite-programming based techniques. For each of these techniques, we have presented the expressions of estimators for both non-hybrid and hybrid problems. The performances of these estimators have been then evaluated within a generic scenario. These simulations have shown that different estimators give different performances and that the ML and SDP techniques outperform the TWLS technique. Moreover, simulations have revealed that the fusion of RSSI with TOA or/and TDOA clearly enhances the non-hybrid RSSI based localization scheme which confirms the assumptions done in the second chapter.

The third and last section of this chapter has been dedicated to the theoretical performances assessment of different non-hybrid and hybrid localization problems. This has been done using two theoretical tools: the Fisher Information and the Cramer-Rao Lower Bound. These tools give us a prior information about the reachable positioning accuracy that a localization scenario can achieve. From the CRLB formulas, the GDOP terms have been deduced. These terms give us measure of geometric configuration badness. The lower is the GDOP the best is the reachable positioning accuracy. After the evaluation of theoretical performances of non-hybrid and hybrid schemes, the effects of radio parameters on CRLB have been investigated. Finally, an example of using CRLB as a criteria for choosing LDPs has been defined and evaluated using the hybrid schemes (RSSI+TOA) and (RSSI+TDOA). It has been shown that the CRLB can enhance the performances of positioning systems with the prior information that it offers. After this "algebraic" chapter, we will focus now in a generic geometric algorithm of localization based mainly on the exchange of constraints.

5

Geometric Non-Hybrid and Hybrid Localization Techniques

Like in chapter 4, non-hybrid and hybrid localization techniques are investigated in this fifth chapter but in a geometric manner. In this chapter, the problem of localization presented in section 4.1 of the previous chapter is modeled using geometry. A generic algorithm is defined and presented below and it is called Robust Geometric Positioning Algorithm (RGPA). The RGPA is based mainly on the geometric representation of LDPs in a Cartesian coordinates system. We start in section 5.1 by giving the necessary definitions and assumptions which support the proposed geometric algorithm. The second section (5.2) is mainly dedicated to the representation of LDPs in the form of geometric constraints. The technique of fusion of geometric constraints aiming to compute position is also presented in this section. The last section (5.3) presents the whole algorithm flow. Furthermore, carried simulations assuming the scenario defined in previous chapter are presented and discussed in order to evaluate the proposed algorithm and to compare it to algebraic techniques and to the CRLB.

5.1 Geometric Localization Problems: Definitions and Assumptions

A geometric localization problem is based on the concept of constraints. In geometric problems, the meaning of a LDP (i.e. RSSI, TOA, TDOA, and others) is different from both algebraic vision (in which a LDP is a random variable characterized by some uncertainty) and network vision (in which a LDP is a measured value). From the geometric vision, a LDP is seen as a geometric constraint. More explicitly, LDP is seen as a set of points in space that satisfy this geometric constraint. In order to clearly explain this concept, we start in this section by giving some definitions. The concept of constraints will be presented in section 5.2.

5.1.1 Voxel

Like a "pixel" in 2D, a voxel represents a volume element in 3D space (see Figure 5.1). It is the smallest addressable space element; it is the smallest unit of a volume that can be controlled. Voxels are good at representing regularly-sampled spaces that are non-homogeneously filled. Common uses of voxels include volumetric imaging in medicine [125] and representation of terrain in games and simulations [126]. This concept of voxel is the basis of geometric representation of constraints of the proposed algorithm.

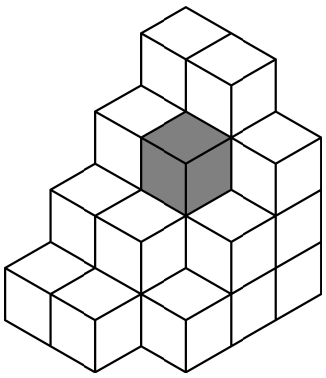

Figure 5.1: A set of voxels in stack. Only one voxel is highlighted.

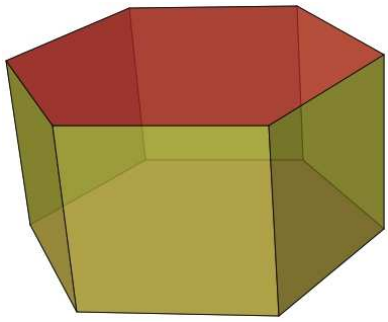

Figure 5.2: A 5-sided prism.

5.1.2 Prism

In geometry, a n-sided prism is a polyhedron made of a n-sided polygonal base, a translated copy, and n faces joining corresponding sides. Thus, these joining faces are parallelograms. All cross-sections parallel to the base faces are the same shape (see Figure 5.2) [127]. In particular, a room is generally a 4-sided prism with two congruent polygonal faces. The polygonal contour of the room constitutes the two congruent polygonal faces and the other sides are the vertical walls.

5.1.3 Cartesian Coordinate System

An important point which affects the algorithm functioning is the choice of the coordinate system able to address each voxel alone. The proposed RGPA algorithm presented in this chapter is based on the world geodetic system (WGS) used for GPS. The WGS is a standard for use in cartography, geodesy, and navigation. It comprises a standard coordinate frame for the Earth, a standard spheroidal reference surface (the datum or reference ellipsoid) for raw altitude data, and a gravitational equipotential surface (the geoid) that defines the nominal sea level. The latest revision is WGS 84 (dating from 1984 and last revised in 2004) [128]. This coordinate system is the most suitable because it would facilitate the recursive computation of intersections between convex volumes and because it is already tested and verified within GPS systems.

For practical implementations on embedded systems, it is very important to use an indexing technique based on integers encoded on 32 bits. The choice of integers is only related to the purposes of simplicity and embeddability of algorithms. For a cubic voxel with an edge $q = 5$mm, each axis of the Cartesian coordinate system can be discretized on an interval $\pm D = \pm 2^{31} q = \pm 10737.418$km when using only integers encoded on 32 bits. Since the earth radius measures 6370km, this discretization is largely sufficient to localize the targeted MS until an altitude of 4367.418km. That is, the voxel can be defined with a shorter edge. Nevertheless, satellites positions cannot be addressed with this altitude of 4367.418km. A simple calculation reveals that a voxel with an edge of 20cm allows us to address satellites. This is very interesting for hybrid scenarios which include observables coming from satellites. For this type of hybrid scenarios, an encoding on 64 bits can drastically enhance the positioning precision by reducing the voxel volume.

The major advantage that has prevailed in choosing a global coordinate system is the easiness it can offer when devices exchange constraints. Indeed, the constraints available to a newcomer MS in an area can be directly mobilized by the neighbor devices without implementing a special conversion process. Furthermore, the algorithm RGPA can be also implemented properly in a different Cartesian coordinate system with a different origin and voxel size, or even without defining voxel at all if the code is implemented in "floating point". For illustration, we present below a numerical example which compares the distances between two points obtained respectively by the GPS coordinates and the proposed encoding.

$$iP1 - iP2 = [2210, -3788, -2078]q$$

$$(ip1 - ip2)^2 = [4884100, 14348944, 4318084]q$$

$$\sum (ip1 - ip2)^2 = 235151128$$

$$\sqrt{235151128} = 4852.95$$

$$d = 4853q = \mathbf{24.26m}$$

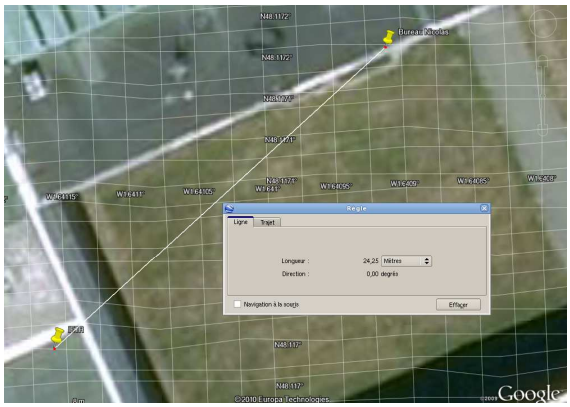

Figure 5.3: Distance between the two points as calculated by Google Earth (**d = 24.25m).**

Numerical Example

The GPS coordinates of the chosen points are:

P1: Latitude $48,117023$, Longitude -1.641160, Altitude 120m

P2: Latitude $48,117163$, Longitude -1.640910, Altitude 120m

Using a voxel with $q = 5$mm, we obtain the two integer coordinates as follows:

iP1=$[852880570, -24436292, 945113018]q$ (12 Bytes)

iP2=$[852878360, -24432504, 945115096]q$ (12 Bytes)

The difference between these integers can be exploited to compute the distance d

between these two points. The most complex algebraic operation involved in this calculation is the square root. This can easily be implemented by simple dichotomous algorithms. The calculation of the distance with the proposed technique is presented above. Figure 5.3 shows the two points and the distance that separates them on Google Earth. The comparison between the two values reveals a high accuracy performed by the proposed technique of encoding.

5.1.4 Intervals and Boxes

A real interval, denoted $[x] = [\underline{x}, \overline{x}]$, is defined as a closed and connected subset of $\mathbb{R}$. The basic operations on intervals are defined as follows [129]:

$$\begin{cases} [x] + [y] = \left[\underline{x} + \underline{y}, \overline{x} + \overline{y}\right] \\ [x] - [y] = \left[\underline{x} - \underline{y}, \overline{x} - \overline{y}\right] \\ [x] \times [y] = \left[min\{\underline{x}\underline{y}, \underline{x}\overline{y}, \overline{x}\underline{y}, \overline{x}\overline{y}\}, max\{\underline{x}\underline{y}, \underline{x}\overline{y}, \overline{x}\underline{y}, \overline{x}\overline{y}\}\right] \\ 1/[y] = \left[1/\underline{y}, 1/\overline{y}\right] \text{ (provided that } 0 \notin [y]) \\ [x]/[y] = [x] \times 1/[y] \end{cases} \tag{5.1}$$

All continuous basic functions (e.g. *sin*, *cos*, *sqrt*, etc) can be used with intervals. Let f be one of these functions, we define $f([x])$ as follows:

$$f([x]) = \{f(x) \mid x \in [x]\} \tag{5.2}$$

A n-dimensional box $[\mathbf{x}]$ of $\mathbb{R}^n$ is defined as a Cartesian product of n intervals $[\mathbf{x}] = \bigotimes_{k=1,\ldots,n} [x_k]$ [129]. In $3D$ and using the Cartesian coordinate system, a box $[\mathbf{x}]$ is denoted $[\mathbf{x}] = \{[x], [y], [z]\}$ where $[x]$, $[y]$, and $[z]$ are respectively the intervals following the three system axes.

5.2 The Concept of Geometric Constraints

5.2.1 Definition

A geometric constraint is a set of points which satisfy a radio LDP or a location dependent information (LDI) (e.g. inclusion in a room or a building, etc). Possible radio LDPs are RSSI, TOA, TDOA, AOA, and AOD. In this dissertation, we are interested only in RSSI, TOA, and TDOA. For both RSSI and TOA, the geometric constraint takes the form of a spherical shell which is the volume lying between two concentric spheres in 3D and the form of an annulus in 2D. The geometric constraint for TDOA takes the form of a hyperboloid in 3D and a hyperbola in 2D. The 2D forms of these geometric constraints are shown in Figure 5.4. The thickness of these geometric constraints is defined by the LDP uncertainty. Assuming Gaussian error, this thickness is equal to six times the standard deviation of the error (σ) taken of both sides of the true value of the LDP. The choice of six σ is justified by the 3-sigma rule stating that for a normal distribution, nearly all values lie within 3 standard deviations of the mean. The geometric constraint becomes as thick as the LDP is less precise (i.e. as σ is higher). The set of points which satisfy the k^{th} constraint is called the "feasible set of the constraint" and denoted $\mathbb{S}_k$. We define also the "feasible set of the problem"

$\mathbb{S}$ as the intersection of feasible sets of all the constraints (i.e. $\mathbb{S} = \bigcap_k \mathbb{S}_k$). Both $\mathbb{S}_k$ and $\mathbb{S}$ can be convex or non convex volumes. The feasible set of a constraint is always continuous for all considered LDPs by contrast to the feasible set of the problem which can be discontinuous. When a geometric problem presents contradictory constraints, $\mathbb{S}$ can be empty and the problem cannot be resolved. In this case, an additional constraint (or a set of constraints) may be necessary to resolve the problem.

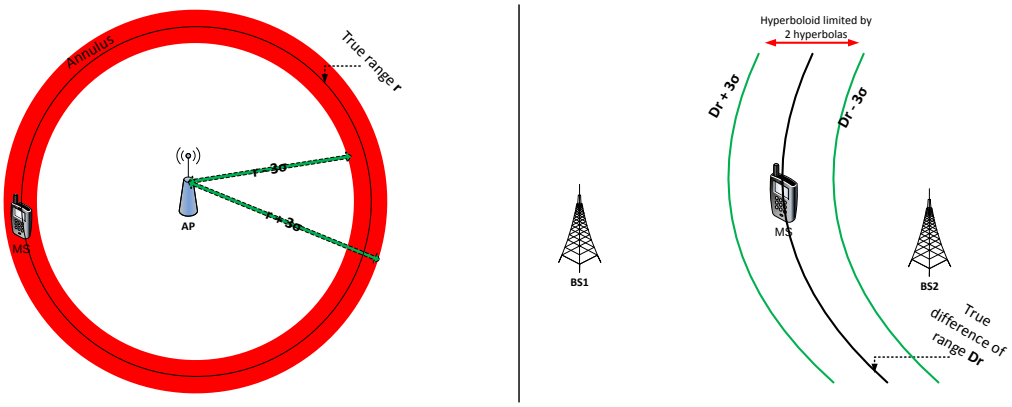

Figure 5.4: The annulus (RSSI or TOA) and the hyperbola (TDOA).

To simplify the representation and the use of a constraint, we define the feasible box of the constraint $[\mathbb{S}_k]$ which is a cuboid encompassing the feasible set $\mathbb{S}_k$ of the constraint. It is easily defined by an interval on each axis of the coordinate system. This approximation makes easier the use of the constraints. Indeed, the storage and the sharing of the constraint can be performed by only saving the endpoints of three (respectively two) intervals in 3D (repectively in 2D). Besides, the fusing and the intersection of the constraints become easier when adopting this box-based presentation. For both TOA and RSSI, where the constraint takes the form of a spherical shell, the constraint box is defined as the circumscribed cuboid that encompasses this spherical shell. The case of TDOA is more specific because the constraint is infinite. To deal with this specificity, we use the fact that the actual absolute value of the difference of range cannot exceed the distance between the two reference devices with which the TDOA is measured. This property allows us to define the feasible box of the TDOA constraint.

5.2.2 Classification of Geometric Constraints

Geometric constraints can be classified using different criteria. Most important ones are presented below.

Radio vs. Non-Radio Constraints

Radio constraints are constraints which result from a LDP. Possible LDPs are RSSI, TOA, and TDOA. As we said before, other LDPs can be considered such as AOA and AOD. Moreover, some additional radio constraints can be derived from GPS measurements for example. Non-radio constraints are mainly constraints resulting from LDIs.

LDIs are data which are location-dependent but do not result from radio measurements. These informations are usually very precise and firm. The inclusion/exclusion of a device in/of an area are examples of LDIs.

Soft vs. Hard Constraints
A geometric constraint can be either soft or hard regarding the device inclusion in the feasible set defined by this constraint. The constraint is said to be hard when the inclusion of the device in the feasible set is certain (i.e. the probability of inclusion is equal to 1). This is usually the case of LDIs. In this case, it is known for example that the device (user) has entered in the room and hasn't left. Unlike hard constraints, soft constraints are uncertain (i.e. the probability of inclusion is inferior to 1). This is the case of LDPs where the device inclusion in the feasible set is characterized by an uncertainty resulting from the imprecision of measurements.

Shared vs. Dedicated Constraints
This criteria is decided with respect to the number of devices (i.e. MS, BS, AP, etc) concerned by the constraint. A constraint which is defined for only one device is a dedicated constraint. LDIs (e.g. an inclusion in an area or a room) is usually a dedicated constraint. The RSSI and TOA constraints are shared between two devices. The TDOA constraint is shared between three devices. While a dedicated constraint can only be used by the considered device, shared constraints can be used in localization of more than one device (i.e. all the devices implied in the constraint).

5.2.3 Fusion of Heterogeneous Geometric Constraints

In order to obtain the feasible set of a localization problem, all available constraints should be fused. The fusion of constraints aims to intersect their feasible sets to obtain the feasible set $\mathbb{S}$ of the problem. $\mathbb{S}$ will then give the solution of the problem and its associated accuracy. As constraints are now presented with their feasible boxes, the intersection will be performed between these boxes. The resulting box will contain $\mathbb{S}$ and it is called the feasible box of the problem (denoted $[\mathbb{S}]$).

5.2.3.1 Box Based Intersection

Let K be the number of constraints (i.e. the number of LDPs and LDIs). Three scenarios may occur:

1. Scenario 1 ($s1$): All K constraints intersect. In this case, $[\mathbb{S}] = \bigcap_{k=1,\dots,K} [\mathbb{S}_k]$.

2. Scenario 2 ($s2$): Only a number N of constraints intersect with $0 < N < K$. In this case, the feasible set of the problem can be defined as the union of intersections obtained with N constraints $[\mathbb{S}] = \bigcup_N \bigcap_{k=1,\dots,N} [\mathbb{S}_k]$.

3. Scenario 3 ($s3$): All K constraints do not intersect. This case gives $[\mathbb{S}] = \emptyset$. A preliminary conclusion is to say that such a problem has no solution and the problem is not localizable.

Figure 5.5 presents an example of these different scenarios using three constraints. While in $(s1)$, the solution is given by the centroid of the obtained $[\mathbb{S}]$, in $(s2)$ and $(s3)$ the solution is ambiguous. A technique of constraint widening (CW) is applied in order to get the intersection of all constraints. This technique transforms scenarios $(s2)$ and $(s3)$ into a $(s1)$ scenario. The CW applies a multiplicative factor on each radio constraint to enlarge its feasible set $\mathbb{S}_k$. In order to keep the same ratio between constraints, this multiplicative factor should be proportional to the standard deviation of each LDP. This multiplicative factor is increased gradually until finding an intersection between all feasible boxes. The CW technique is only applied on LDPs and does not concern the LDIs which are firm constraints and cannot be modified. Once the intersection is obtained, the next step is to approximate the feasible set of the problem. The objective is to keep, from the resulting feasible box of the problem, only the set where all constraints are verified (see Figure 5.5-(a)).

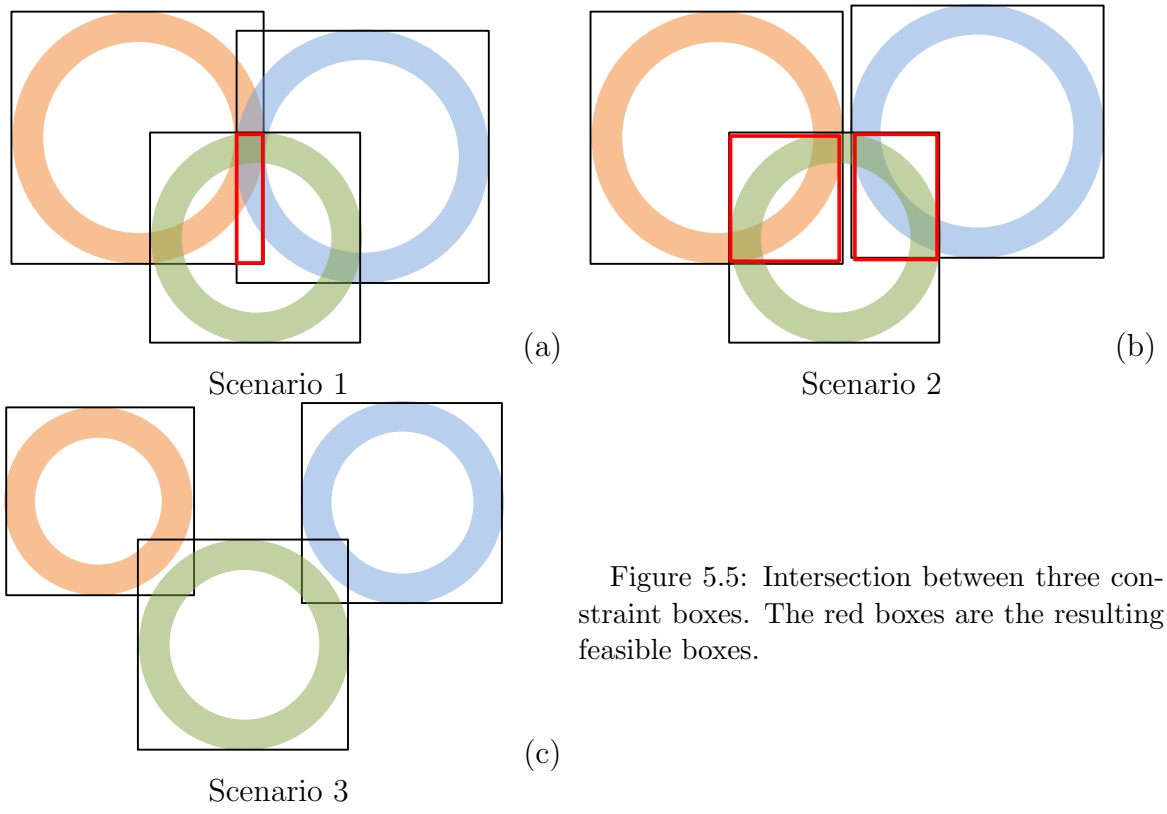

Figure 5.5: Intersection between three constraint boxes. The red boxes are the resulting feasible boxes.

5.2.3.2 Characterization of the feasible set of the problem

Once the feasible box $[\mathbb{S}]$ of the problem is obtained, it is essential to get the feasible set $\mathbb{S}$ itself. In fact, $\mathbb{S}$ is usually smaller than $[\mathbb{S}]$ and the centroid of $\mathbb{S}$ is different from the centroid of $[\mathbb{S}]$. This difference may be important and hence the use of $[\mathbb{S}]$ centroid may result in a large positioning error. In order to get $\mathbb{S}$ from $[\mathbb{S}]$ the set inversion via interval analysis (SIVIA) technique is applied. The principle of SIVIA is to split the initial problem of characterizing $\mathbb{S}$ into a sequence of more manageable tasks [130, 131].

The SIVIA starts by dividing $[\mathbb{S}]$ into 8 (4 in 2D) identical smaller boxes $\left[\mathbb{S}^{(1)}_{j=1,\ldots,8}\right]$. This is done by dividing all three (two in 2D) intervals into two equal smaller intervals.

Then, the constraints will be evaluated conjointly in each of obtained boxes. If a common intersection is found, the box is kept else it is discarded. The obtained boxes can be totally or partially included in $\mathbb{S}$. Let $[\mathbb{S}_t]$ denotes the union of all boxes which are totally included in $\mathbb{S}$. These steps result in a new feasible box of the problem which is denoted $[\mathbb{S}]^{(1)}$. Recursively, we obtain $[\mathbb{S}]^{(i)}$, $i = 2, 3, ...$ [130, 131]. The stop criteria will be the percentage of $[\mathbb{S}_t]$ with respect to $[\mathbb{S}]^{(i)}$. Let this percentage be 95%. When reaching this ratio, the resulting $[\mathbb{S}_t]$ is taken as the approximation of $\mathbb{S}$. The technique is described by Algorithm 1. An illustration example is also given in Figure 5.6.

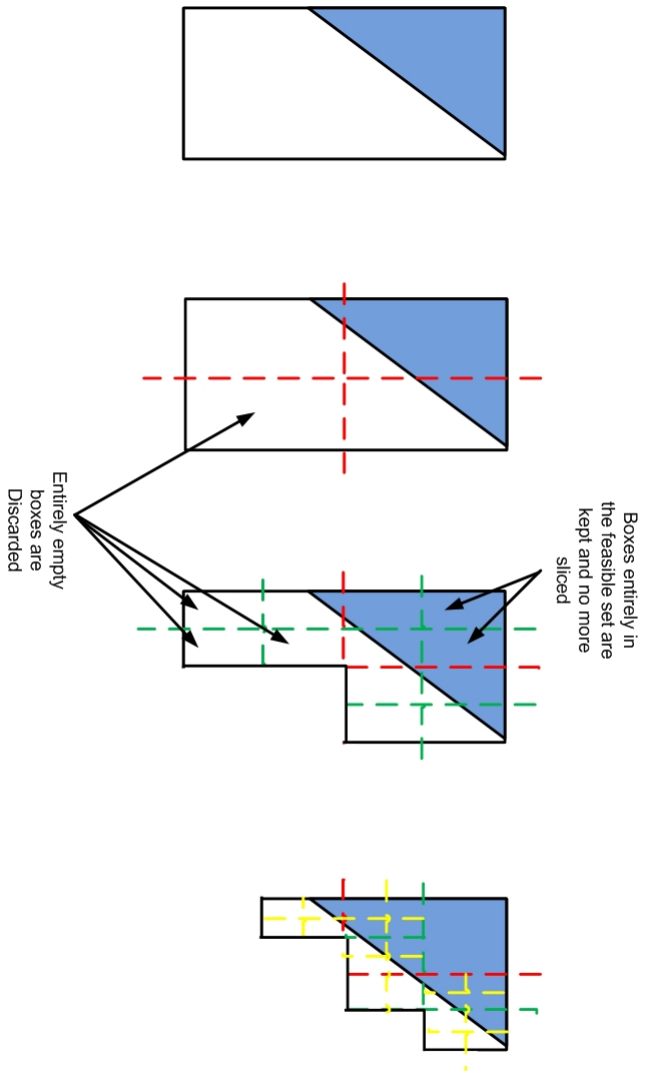

Figure 5.6: Illustration example of SIVIA technique.

Algorithm 1 Set Inversion Via Interval Analysis

$[\mathbb{S}_t] \leftarrow \emptyset$
$i \leftarrow 0$
$\varepsilon \leftarrow 0.95$
if $[\mathbb{S}] \subseteq \mathbb{S}$ **then**
  $\mathbb{S} \leftarrow [\mathbb{S}]$
else
  while $\frac{size([\mathbb{S}_t])}{size([\mathbb{S}]^{(i)})} < \varepsilon$ **do**
    for $j = 1$ to 8 **do**
      compute $\left[\mathbb{S}_j^{(i+1)}\right]$
      if $\left[\mathbb{S}_j^{(i+1)}\right] \subset \mathbb{S}$ **then**
        $[\mathbb{S}_t] \leftarrow [\mathbb{S}_t] \cup \left[\mathbb{S}_j^{(i+1)}\right]$
      end if
    end for
    $i \leftarrow i + 1$
  end while
  $\mathbb{S} \leftarrow [\mathbb{S}_t]$
end if

5.2.4 Use of Constraints in a Network

In order to use and share constraints between different devices present in a network, we define the constraint layer array (CLA) concept. The CLA of a device is an array which contains all geometric constraints associated with the device. The number of constraints saved in the CLA is not fixed but it depends on the memory size of the CLA. Each constraint is represented by the following entries:

- Timestamp: The timestamp is the time at which the constraint is recorded by the device. It allows to track the constraint and to remove it in case of expiry. This timestamp is necessary to manage dynamic localization techniques.

- Type: This entry indicates the nature of the constraint (i.e. RSSI, TOA, TDOA, or LDI).

- Parameters: The parameters of the constraint depend mainly on the type of the constraint. In the case of LDI constraint, the parameters are the 6 indexes which delimit the volume of the constraint. In the case of LDPs we save, in addition to the 6 indexes which delimit the feasible box of the constraint, the positions of anchors, the measurement, and its precision (i.e. the variance of measurement).

- Order: The order of a constraint informs about the number of elementary constraints implied. The fusion of constraints of order 1 gives a constraint of order 2. This fusion is necessary when the memory size is not sufficient to save all available constraints. When different constraints are fused, the timestamp, the type, and parameters of each constraint are kept.

- Size: the size of the constraint is saved to facilitate the management of available memory.

These entries take the form of arrays. Let C_k be the k^{th} constraint of the targeted device. C_k is represented by an array as follows:

$$C_k = [Timestamp|Type|Parameters|Order|Size] \tag{5.3}$$

The CLA is hence defined by the concatenation of all C_k for $k = 1, ..., K$:

$$CLA = [C_1|C_2|...|C_K] \tag{5.4}$$

5.3 Simulation and Evaluation of The RGPA technique

5.3.1 RGPA Flow

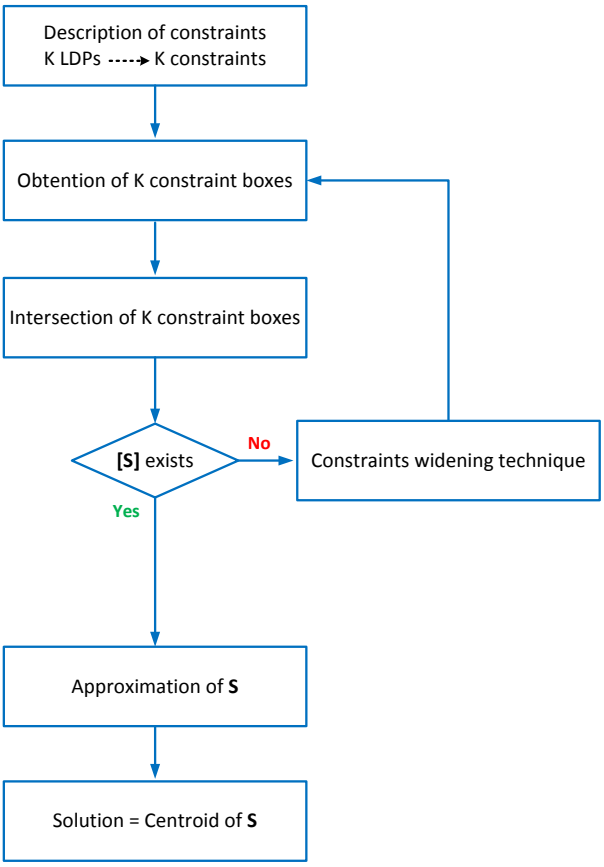

Figure 5.7: Different steps of RGPA algorithm.

The RGPA technique consists in a sequence of simple geometrical calculations aiming to obtain the position of the targeted device. The main steps are presented in Figure 5.7. These steps are described as follows:

1. Description in the form of geometric constraints of all radio LDPs or LDIs. As a result of this step, we obtain for each constraint a feasible set $\mathbb{S}_k$, $k = 1, ..., K$ with K the number of constraints.

2. Definition of the feasible box $[\mathbb{S}_k]$ which circumvents the feasible set of each constraint.

3. Fusion of available constraints by intersecting all $[\mathbb{S}_k]$: the result of this fusion is a box denoted $[\mathbb{S}]$.

4. If all constraints are checked in at least one point of $[\mathbb{S}]$, we say that $[\mathbb{S}]$ exists and we perform step 5. Else, we perform the constraint widening technique until $[\mathbb{S}]$ exists.

5. The feasible set $\mathbb{S}$ is approximated using SIVIA technique applied on $[\mathbb{S}]$.

6. The solution is obtained as the centroid of the approximated $\mathbb{S}$.

5.3.2 Simulations and Discussions

Table 5.1: Performances of RGPA, ML, and CRLB applied on non-hybrid localization schemes.

LDP	Technique	Cumulative Probability	
		67%	95%
RSSI	ML	4.034m	8.614m
	RGPA	4.109m	7.653m
	CRLB	2.902m	5.137m
TOA	ML	1.251m	2.081m
	RGPA	1.264m	2.086m
	CRLB	0.836m	1.357m
TDOA	ML	1.805m	3.490m
	RGPA	1.584m	2.743m
	CRLB	1.386m	2.304m
RSSI + TOA	ML	1.096m	1.882m
	RGPA	1.015m	1.836m
	CRLB	0.594m	1.005m
RSSI + TDOA	ML	1.458m	2.705m
	RGPA	1.282m	2.267m
	CRLB	0.842m	1.415m
TOA + TDOA	ML	0.936m	1.622m
	RGPA	0.770m	1.404m
	CRLB	0.476m	0.821m
RSSI + TOA + TDOA	ML	0.913m	1.492m
	RGPA	0.780m	1.366m
	CRLB	0.392m	0.639m

In order to compare the proposed geometric technique to the ML technique which is the most accurate algebraic technique, we consider the same scenario as in chapter 4 (see Figure 4.1 and section 4.1). For each localization scheme, we compare the RGPA technique to the maximum likelihood technique initialized randomly. These two techniques are also compared to the CRLB. To perform these comparisons, we plot in Figure 5.8 and Figure 5.9 the CDFs of absolute localization errors and CRLB for respectively different non hybrid and hybrid schemes. Table 5.1 summarizes these CDFs for non-hybrid and hybrid schemes.

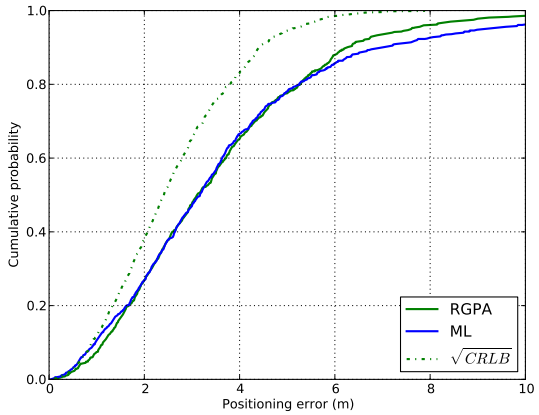

(a) RSSI

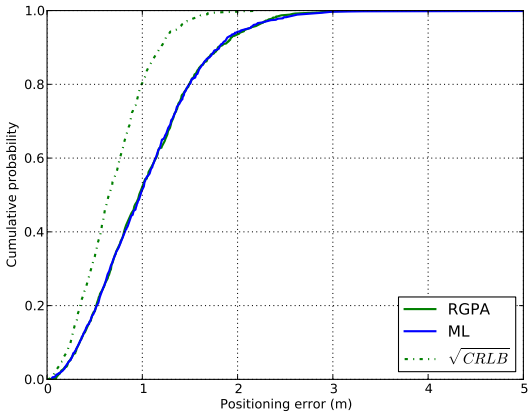

(b) TOA

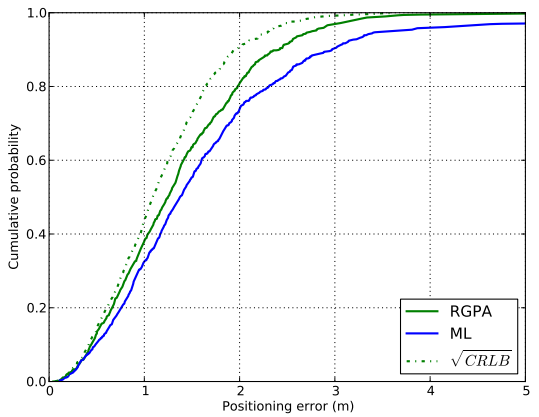

(c) TDOA

Figure 5.8: CDFs of positioning error using RGPA, ML, and CRLB applied on non-hybrid localization schemes.

These figures and tables show that the proposed RGPA technique outperforms the ML technique randomly initialized (and thus, all algebraic techniques) except in the case of TOA scheme where it gives the same performances as the ML technique and in the case of the scheme (RSSI+TOA) where ML and RGPA gives very close performances. The highest gains are performed in schemes involving TDOA. The comparison between the CDFs of the ML and RGPA techniques and the CDFs of the CRLB shows that RGPA is closer to the CRLB than the ML technique.

Figure 5.10 plots the CDFs of all localization schemes using RGPA technique. This figure shows, like in Chapter 4, that TOA and TDOA outperform the RSSI. Moreover, the figure highlights that the fusion of hybrid LDPs enhances the positioning accuracy. According to this figure, the schemes (RSSI+TOA+TDOA) and (TOA+TDOA) offer the best positioning accuracy among all schemes. Furthermore, the adding of TDOA or TOA to RSSI widely enhances the performances of positioning accuracy when comparing to the positioning accuracy performed by the non-hybrid RSSI scheme. These enhancements validate one of the objectives of this thesis which consists in demonstrating that available RSSIs must be aided by time based LDPs in order to reach the requested positioning accuracy.

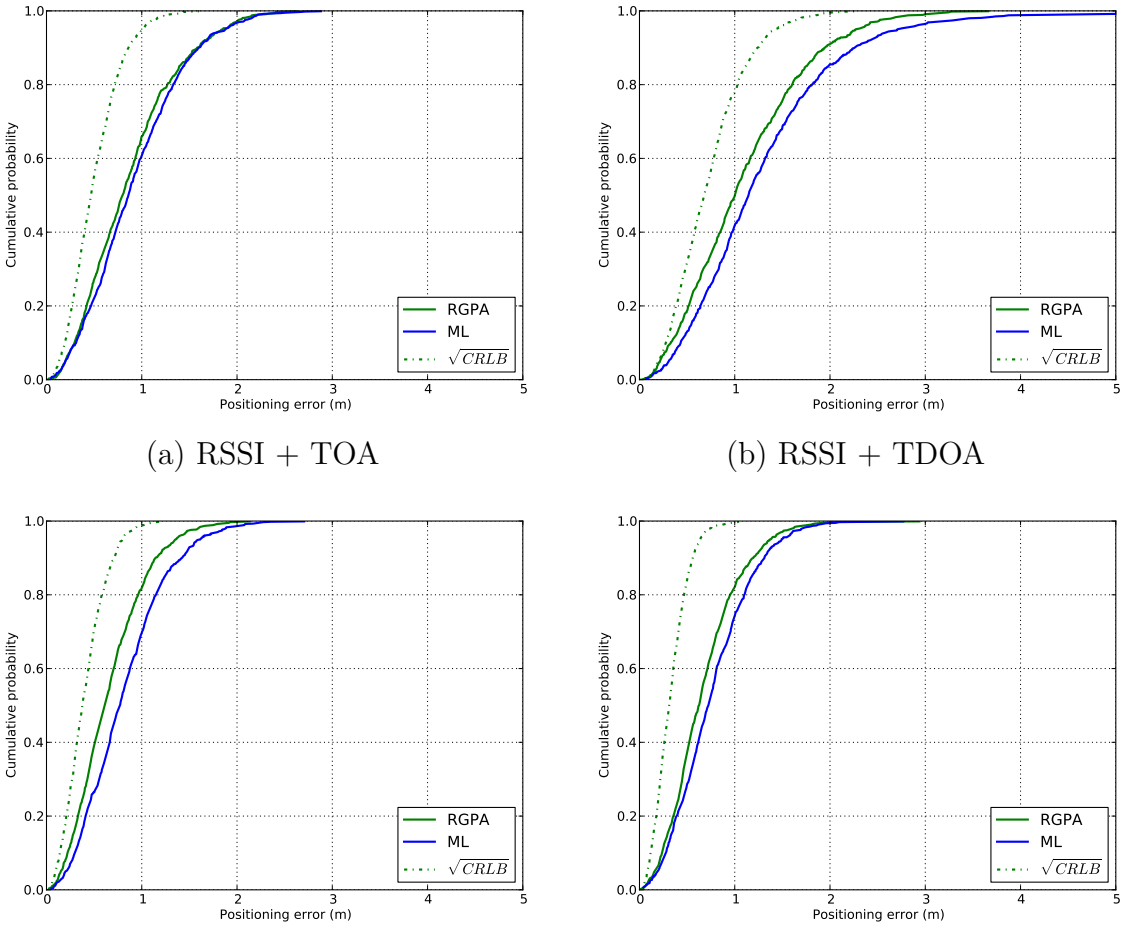

(a) RSSI + TOA

(b) RSSI + TDOA

(c) TOA + TDOA

(d) RSSI + TOA + TDOA

Figure 5.9: CDFs of positioning error using RGPA, ML, and CRLB applied on the fusion of RSSI, TOA, and TDOA.

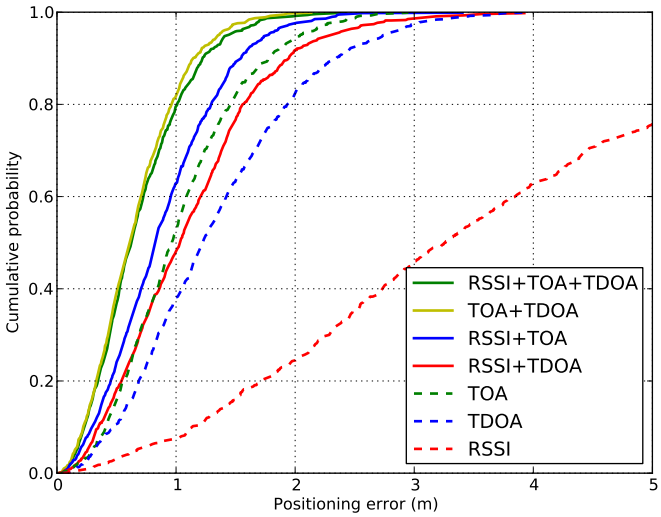

Figure 5.10: Comparison between different localization schemes using the RGPA technique.

5.4 Conclusion

In this chapter, we have geometrically investigated the localization problem. A generic algorithm RGPA is proposed for resolving localization problems. The basis of RGPA is the geometric representation of LDPs and LDIs in the form of sets of points (feasible sets). This representation is based on interval analysis theory. In order to simplify the computation, a feasible box is defined to encompass each constraint. The intersection between all feasible boxes of a problem give the feasible box of constraints where the solution lies. This box contains the feasible set of the problem. In order to approximate this feasible set, the SIVIA algorithm is applied. Once the feasible set of the problem is obtained, its centroid gives the estimate of the targeted location. The problem of non-intersection between constraints is resolved using a constraint widening technique which consists in conjointly enlarging the feasible sets of all constraints proportionally to their precisions until finding an intersection between them.

The proposed algorithm is promising compared to algebraic techniques. The carried simulations have shown that the RGPA outperforms all algebraic algorithms especially in the case of TDOA where it overcomes singularities occurring when using iterative optimization. Besides, this algorithm may be enhanced to involve tracking and cooperative based localization. Furthermore, the algorithm is easily embeddable in devices and would not consume much resources because it is based only on simple mathematical operations.

6 Conclusions and Future Work

Two years and eight months haven't been sufficient to explore all the wider area of localization. Nevertheless, this period has been very worthwhile. Many results has been obtained including estimation techniques of location-dependent parameters (LDPs) and localization techniques using these LDPs. The focus has been mainly put on localization techniques. Nevertheless, some investigations of LDPs estimation and measurement techniques have been necessary to get more complete understanding of localization field. In this chapter, we summarize the obtained results and the reached conclusions and we give some directions for intended future work.

6.1 Conclusions

- The heterogeneity of present and future wireless networks motivates the fusion of different LDPs to perform localization but at the same time imposes new challenges to localization systems. On the one hand, in a heterogeneous network, the amount of available LDPs is usually sufficient to make the localization problem localizable. Moreover, the presence of ranging capable standards like UWB and WLAN made available the time-based LDPs (i.e. TOA and TDOA) which are usually accurate and can drastically enhance localization accuracy when being fused with RSSI. On the other hand, the fusion of LDPs different in nature and precision must be done carefully and smartly in order to obtain better performances. Moreover, algorithms become more and more complex and computation resources are more and more used. Nevertheless, the evolution of mobile devices and their computation capacities allows the implementation of such algorithms.

- RSSI is usually available in each standard and in each radio link. The use of RSSI does not require any additional cost. RSSI is usually said to be a "free" LDP. By contrast, TOA and TDOA cannot be obtained without an additional cost. These time-based LDPs necessitate ranging procedures to be measured.

Usually synchronization between radio link sides is required to perform ranging. Nevertheless, the synchronization can be avoided. In the case of TDOA, when the MS transmits, anchors receive synchronized signals. In the case of TOA, TWR and RTT ranging techniques does not require synchronization between devices. However, the TWR consumes more resources than OWR which need synchronization to be performed.

- For RSSI, we have considered log-normal shadowing model because it offers a linear relation between the path loss and the distance and hence the position. We have shown that different path loss models can be deduced from measurements. A general path loss model (GPL) is a model obtained using all available RSSIs in a given environment. For each anchor (i.e. BS, AP, or femtocell) an anchor path loss model (APL) can be defined. We have shown that this model is different from one anchor to another. Each anchor has a particular vision of radio channel. Moreover, each anchor can gradually construct its APL by adding available RSSIs. In this way, each anchor keeps an updated APL and tracks channel variations.

- Ranging techniques have been studied for both TOA and RSSI. Since UWB standard benefits from high time precision, separation of rays is made possible. This separation allows to identify the time of arrival and the carried energy by the strongest path. The proposed TOA-ranging techniques are threshold-based. While the first studied method (Th-TOA) is classic, the second (Cum-TOA) is novel and use the cumulative impulse response. Different thresholds can be used and are function of energies carried by all rays and the strongest ray respectively. For RSSI, ranging can be made using three different estimators of distance (the mean, the median, and the mode of the distance distribution). Indeed, assuming the log-normal shadowing model for RSSI, the distribution of distance is developed and different estimators are proposed. The mode estimator is the most accurate. Furthermore, the use of APL enhances RSSI-based ranging and positioning accuracies.

- The positioning accuracy is factor of used LDPs and their precisions. RSSI is usually less accurate than time-based LDPs. This is justified by the effect of shadowing. Simulations have shown that adding accurate time-based LDPs to RSSI drastically enhances the positioning accuracy. In a matter of reducing the cost of localization systems, the use of the scheme (RSSI+TOA) is justified. The "free" availability of RSSI and the accurate ranging techniques defined by UWB and WLAN standards are the main motivations of this choice. We can also use TDOA in place or with TOA but TDOA needs more resources than TOA since it implies two anchors and requires synchronization.

- The positioning accuracy is also factor of used location estimation technique. Different estimation techniques result in different levels of accuracy and also different levels of complexity. Comparison of algebraic techniques has revealed that the ML estimator is usually the most accurate and that SDP technique is more reliable than TWLS technique. The use of ML and SDP which are iterative techniques is still more expensive than TWLS which is a very quick and cheap

technique. The RGPA technique presented in chapter 5 is a generic technique which can be applied for each localization scheme and which is able to fuse all kinds of LDPs coming from different sources. RGPA outperforms all algebraic techniques and offers better positioning accuracy. Besides, RGPA is very simple and can be easily embedded in small devices. This simplicity results mainly from the Cartesian representation of LDPs. This suggests the introduction of a Cartesian representation of position in wireless devices.

- CRLB and GDOP offer a prior information about the reachable positioning accuracy of a given scenario. In addition, these terms can be computed promptly and with minor resources. Thus, they can be used as criteria for choosing LDPs in order to enhance positioning accuracy. While the GDOP informs only about geometric configuration conditions, the CRLB add an information about the precisions of used LDPs.

6.2 Future work

- More sophisticated statistical models may be used in the place of Gaussian models. These models must also take into account biased measurements and correlation between different LDPs. Biases are mainly introduced by NLOS situations in the case of TOA and TDOA ranging. Correlation between LDPs occurs when these LDPs come from close anchors. By contrast to Gaussian models, with these models the development of location estimators will be more difficult and tricky. This will be the cost of having better evaluation of positioning techniques and schemes.

- More sophisticated path loss models may be used in order to better describe the attenuation of signal when it propagates in radio channel. One of these interesting models is the Motley-Keenan model which is based on log-normal shadowing model for which it adds two additional terms: the first represents attenuations caused by walls and the second represents those caused by floors. This model assumes the knowledge of environment layout and the characteristics of the materials of all walls and floors. This model can be implemented using ray tracing tools.

- The effects of visibility conditions on LDPs has been partially addressed in chapter 3. These effects have to be more investigated.

- Evaluation on other measurements (e.g. cellular and WLAN) should bring more accurate conclusions about non-hybrid and hybrid localization performances. This necessitates to carry out measurements from these different standards at the same time and in the same environment. Since we haven't had access to such heterogeneous measurements, the evaluation of heterogeneity has been performed only by varying the precision of LDPs.

- SDP algorithm should be developed and evaluated in the case of TDOA. In order to allow fusion with SDP, this algorithm must take the same form of those developed in TOA and RSSI cases.

- The geometric algorithm has to be improved in order to accelerate the intersection of constraints and the computation of position. A weighted version of the centroid calculation would be more interesting. The goal would be to make a trade-off between the rapidity of the algorithm and its performances in order to be embedded in small devices while guaranteeing a higher positioning accuracy. Besides, it would be interesting to apply the ML algorithm only on the intersection of constraints obtained by RGPA.

- The validation and evaluation of RGPA technique on a real wireless device after being embedded in it would be a very interesting task.

- It would be interesting to use other LDPs and mainly angle based LDPs such as angle of arrival and angle of departure.

- It would be interesting to include LDIs (e.g. inclusion in a room) in both algebraic and geometric techniques in order to asses their effects on the positioning accuracy.

- The most important future work will be to extend both algebraic and geometric techniques to deal with cooperative and dynamic scenarios. This is in line with the objectives of *WHERE2* European FP7 project.

A

RSSI Monitoring Application for Bluetooth, WLAN, and GSM

In this appendix, we present a Master II project carried out during this thesis and aimed to develop an embedded application on Pocket-PC able to monitor various informations (mainly RSSI and SSID) about wireless networks to those the Pocket-PC is connected. We consider Bluetooth, WLAN, and GSM networks. This work is done in collaboration with Hana Harrath from ETSI (École Supérieure de Technologie et d 'Informatique). Some screen-shots are presented in Figure A.1.

This application has been developed using C# language on Visual Studio 2010. The screen-shots are obtained using an emulator of Pocket-PC available within Visual Studio 2010. The developed application still present some bugs and needs some more enhancements before being implemented on a real Pocket-PC. Nevertheless, the application would facilitate the real-time measurements of RSSI, the construction of RSSI database of a given environment when it is associated with GPS capability of the Pocket-PC.

(a) User Authentication (b) Application Choice (c) WiFi Monitoring

(c) WiFi Informations (c) GSM Monitoring (c) Bluetooth Monitoring

Figure A.1: Screen-shots of RSSI monitoring developed application using a Pocket-PC emulator.

B

RSSI monitoring in a Zigbee based network: Texas Instruments CC2431 System-on-Chip

The CC2431 from Texas Instruments is the first SoC with a hardware location engine targeting low-power ZigBee wireless sensor networking applications, such as asset tracking, patient monitoring, inventory control, security and commissioning networks. The device features a powerful RSSI-based location engine, which reduces network traffic compared to centralized location systems, and is supported by Z-Stack protocol stack from TI. The CC2431 is based on the industry's first available SoC solution for low-power RF applications, the CC2430. Both devices combine the excellent performance of the industry-leading CC2420 RF transceiver core with an enhanced 8051 microcontroller, up to 128kB flash memory, 8kB of RAM and many additional features all in a small $7mmx7mm$ package (see Figure B.1).

The Location Engine is used to estimate the position of nodes in an ad-hoc wireless network. Reference nodes exist with known coordinates, typically because they are part of an installed infrastructure. Other nodes are blind nodes, whose coordinates need to be estimated (see Figure B.2). These blind nodes are often mobile and attached to assets that need to be tracked. The Location Engine implements a distributed computation algorithm that uses received signal strength indicator (RSSI) values from known reference nodes. Nevertheless, the Location Engine does not allow us to monitor all gathered RSSIs. It gives only information about the best RSSI. Hence, the objective is to develop an application able to monitor all RSSIs in real time and stock them in a file. The goal of this application is to be able to construct Zigbee RSSI databases for given environments. This work is done in collaboration with Mr Ahmed Cheikhrouhou and Mr Lotfi Ben Taher in the framework of a mater II project at the IFSIC (Institut de Formation Supérieure en Informatique et Communication).

The idea is to exploit the format of messages exchanged between network elements and customize the frames they contain. The customized frame is the message "*Blind Node Find Response*" which represents the cyclic response (in AUTO mode) of the

blind node informing about its current position estimate. The message "*Blind Node Find Response*" carries only a single value of RSSI (the best one among many). We have therefore decided to remove non-essential informations (Statute, Xpos, Ypos, Number of Reference Node, Closest Xpos, Closest Ypos) and recover instead of them the other RSSI values. An interface is developed in order to show the evolution of RSSIs which are also saved in an accessible database. The interface is given in FGIURE B.3.

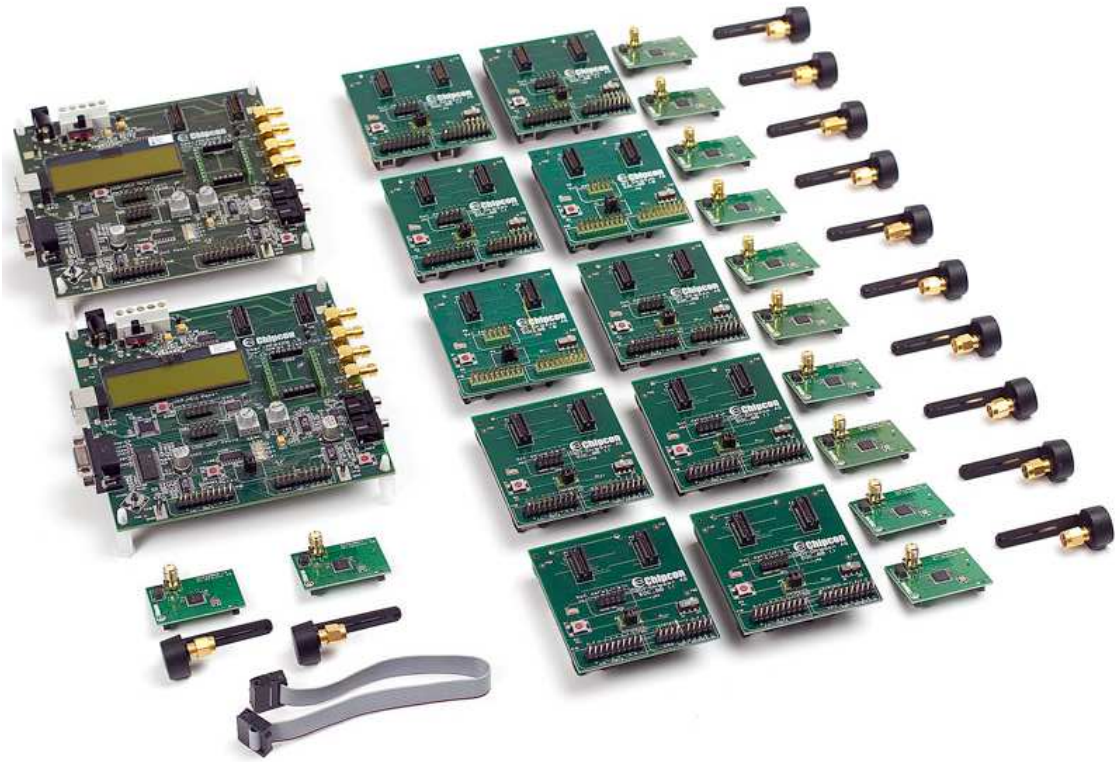

Figure B.1: CC2431DK development kit.

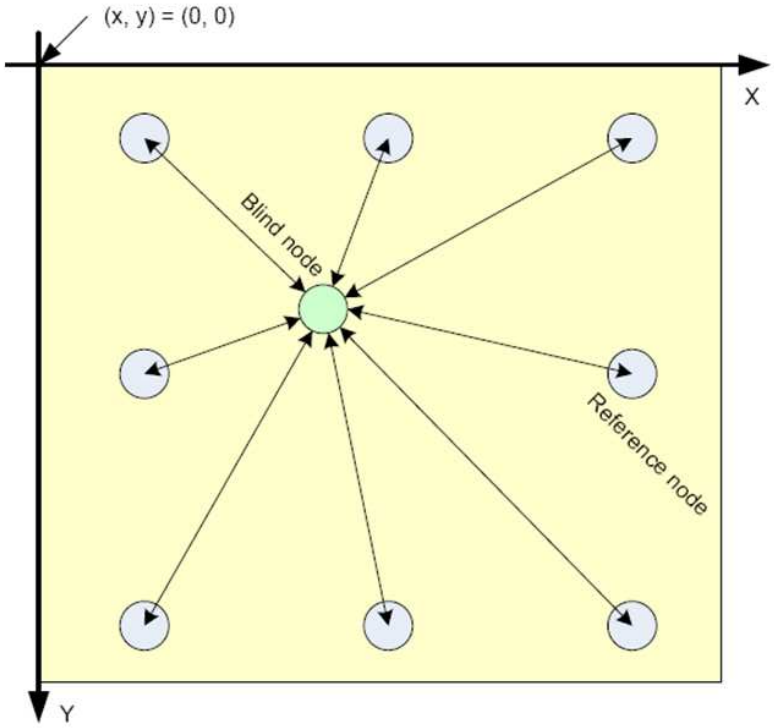

Figure B.2: Reference and blind nodes in the interface of the Location Engine.

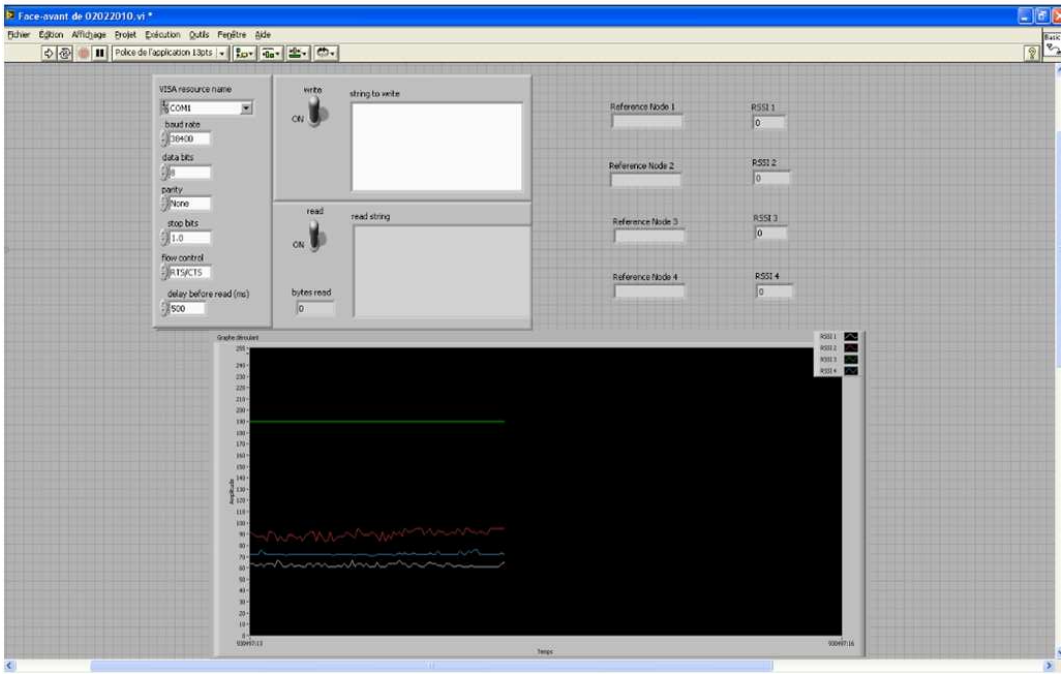

Figure B.3: RSSI monitoring application interface.

C

Calculation of RSSI-based ranging estimators variances

The developed RSSI-based ranging estimators are:

$$\hat{d}_{mean} = e^{M+\frac{S^2}{2}} \tag{C.1}$$

$$\hat{d}_{median} = e^{M} \tag{C.2}$$

$$\hat{d}_{mode} = e^{M-S^2} \tag{C.3}$$

Since $\hat{d}_{mean} = \hat{d}_{median} e^{\frac{S^2}{2}}$ and $\hat{d}_{mode} = \hat{d}_{median} e^{-S^2}$, we develop the moments for median estimator and then we deduce those of mode and mean estimators.

First moments

$$E(\hat{d}_{median}) = \frac{d_0}{\sqrt{2\pi}\sigma_{sh}} \int 10^{\frac{L-L_0}{10n_p}} e^{-\frac{(L-(L_0+10n_p log_{10}(\frac{d}{d_0})))^2}{2\sigma_{sh}^2}} dL \tag{C.4}$$

Let u be:

$$u = \frac{(L-(L_0+10n_p log_{10}(\frac{d}{d_0})))^2}{\sqrt{2}\sigma_{sh}} \tag{C.5}$$

Thus, using $\frac{L-L_0}{10n_p} = \frac{\sqrt{2}\sigma_{sh}u}{10n_p} + log_{10}(\frac{d}{d_0})$ and $\sqrt{2}\sigma_{sh}du = dL$, C.4 becomes:

$$E(\hat{d}_{median}) = \frac{d}{\sqrt{\pi}} \int 10^{\frac{\sqrt{2}\sigma_{sh}u}{10n_p}} e^{-u^2} du \tag{C.6}$$

which becomes after development:

$$E(\hat{d}_{median}) = \frac{d}{\sqrt{\pi}} e^{\frac{(\ln(10))^2\sigma_{sh}^2}{200n_p^2}} \int e^{-v^2} dv \tag{C.7}$$

with $v = u - \frac{\sqrt{2}\sigma_{sh}}{20n_p}\ln(10)$ Developing C.7 gives the first moment of median estimator:

$$E(\hat{d}_{median}) = de^{\frac{S^2}{2}} \tag{C.8}$$

The first moments of mean and mode estimators are given by:

$$E(\hat{d}_{mean}) = e^{\frac{S^2}{2}}E(\hat{d}_{median}) = de^{S^2} \tag{C.9}$$

$$E(\hat{d}_{mode}) = e^{-S^2}E(\hat{d}_{median}) = de^{-\frac{S^2}{2}} \tag{C.10}$$

Second moments

$$E(\hat{d}^2_{median}) = \frac{d_0^2}{\sqrt{2\pi}\sigma_{sh}}\int 10^{2\frac{L-L_0}{10n_p}} e^{-\frac{(L-(L_0+10n_p log_{10}(\frac{d}{d_0})))^2}{2\sigma^2_{sh}}} dL \tag{C.11}$$

Like in the first moment and using the same definitions of u and v we get:

$$E(\hat{d}^2_{median}) = d^2e^{2S^2} \tag{C.12}$$

The first moments of mean and mode estimators are given by:

$$E(\hat{d}^2_{mean}) = e^{S^2}E(\hat{d}^2_{median}) = d^2e^{3S^2} \tag{C.13}$$

$$E(\hat{d}^2_{mode}) = e^{-2S^2}E(\hat{d}^2_{median}) = d^2 \tag{C.14}$$

Variances

Using the definition of variance, we get:

$$\hat{\sigma}^2_{mean} = E(\hat{d}^2_{mean}) - (E(\hat{d}_{mean}))^2 = e^{2M+3S^2}(e^{S^2} - 1) \tag{C.15}$$

$$\hat{\sigma}^2_{median} = E(\hat{d}^2_{median}) - (E(\hat{d}_{median}))^2 = e^{2M+S^2}(e^{S^2} - 1) \tag{C.16}$$

$$\hat{\sigma}^2_{mode} = E(\hat{d}^2_{mode}) - (E(\hat{d}_{mode}))^2 = e^{2M-2S^2}(1 - e^{-S^2}) \tag{C.17}$$

D

Development of Fisher information matrices for RSSI and TDOA

FIM of RSSI

We have the definition of the FIM of RSSI localization scheme:

$$\mathbf{J}_{\text{RSSI}} = E\left[\nabla \mathbf{f}_{\text{RSSI}} \cdot \nabla \mathbf{f}_{\text{RSSI}}^{T}\right] \tag{D.1}$$

Using the expression of $\nabla \mathbf{f}_{\text{RSSI}}$ defined in (4.18) and assuming independence between RSSI measurements, the FIM given by (D.1) can be written as:

$$\mathbf{J}_{\text{RSSI}} = E\left[\sum_{k=1}^{p} \frac{1}{S_k^4} \frac{\left((M_k - {S_k}^2) - \ln\left(d_k\right)\right)^2}{{d_k}^4} \left(\mathbf{X} - \mathbf{X}_k\right)\left(\mathbf{X} - \mathbf{X}_k\right)^T\right] \tag{D.2}$$

Developing this expression leads to:

$$\mathbf{J}_{\text{RSSI}} = \sum_{k=1}^{p} \frac{\left(1 + {S_k}^2\right)}{S_k^2 {d_k}^4} \left(\mathbf{X} - \mathbf{X}_k\right)\left(\mathbf{X} - \mathbf{X}_k\right)^T \tag{D.3}$$

because $E[((M_k - {S_k}^2) - \ln(d_k))^2] = {S_k}^2(1 + {S_k}^2)$. Then, we obtain:

$$\mathbf{J}_{\text{RSSI}} = \sum_{k=1}^{p} \frac{\left(1 + {S_k}^2\right)}{S_k^2} \begin{bmatrix} \frac{(x-x_k)^2}{{d_k}^4} & \frac{(x-x_k)(y-y_k)}{{d_k}^4} \\ \frac{(x-x_k)(y-y_k)}{{d_k}^4} & \frac{(y-y_k)^2}{{d_k}^4} \end{bmatrix} \tag{D.4}$$

FIM of TDOA

We have the definition of the FIM of TDOA localization scheme:

$$\mathbf{J}_{\text{TDOA}} = E\left[\nabla \mathbf{f}_{\text{TDOA}} \cdot \nabla \mathbf{f}_{\text{TDOA}}^{T}\right] \tag{D.5}$$

Using the expression of $\nabla \mathbf{f}_{\text{TDOA}}$ defined in (4.18) and assuming independence between TDOA measurements, the FIM given by (D.5) can be written as:

$$\mathbf{J}_{\text{TDOA}} = E\left[\sum_{k=q+2}^{K} \frac{\left(c\tau_{k(q+1)} - d_{k(q+1)}\right)^2}{\sigma^4_{k(q+1)}} \left(\frac{\mathbf{X}-\mathbf{X}_k}{d_k} - \frac{\mathbf{X}-\mathbf{X}_{q+1}}{d_{q+1}}\right)\left(\frac{\mathbf{X}-\mathbf{X}_k}{d_k} - \frac{\mathbf{X}-\mathbf{X}_{q+1}}{d_{q+1}}\right)^T\right] \tag{D.6}$$

Developing this expression leads to:

$$\mathbf{J}_{\text{TDOA}} = \sum_{k=q+2}^{K} \frac{1}{\sigma^2_{k(q+1)}} \left(\frac{\mathbf{X}-\mathbf{X}_k}{d_k} - \frac{\mathbf{X}-\mathbf{X}_{q+1}}{d_{q+1}}\right)\left(\frac{\mathbf{X}-\mathbf{X}_k}{d_k} - \frac{\mathbf{X}-\mathbf{X}_{q+1}}{d_{q+1}}\right)^T \tag{D.7}$$

and then to:

$$\mathbf{J}_{\text{TDOA}} = \sum_{k=q+2}^{K} \frac{1}{\sigma^2_{k(q+1)}} \begin{bmatrix} \left(\frac{x-x_k}{d_k} - \frac{x-x_{q+1}}{d_{q+1}}\right)^2 & \left(\frac{x-x_k}{d_k} - \frac{x-x_{q+1}}{d_{q+1}}\right)\left(\frac{y-y_k}{d_k} - \frac{y-y_{q+1}}{d_{q+1}}\right) \\ \left(\frac{x-x_k}{d_k} - \frac{x-x_{q+1}}{d_{q+1}}\right)\left(\frac{y-y_k}{d_k} - \frac{y-y_{q+1}}{d_{q+1}}\right) & \left(\frac{y-y_k}{d_k} - \frac{y-y_{q+1}}{d_{q+1}}\right)^2 \end{bmatrix} \tag{D.8}$$

References

[1] K. Virrantaus, J. Markkula, A. Garmash, and Y.V. Terziyan. Developing GIS-supported location- based services. *Proceedings of the Second International Conference on Web Information Systems Engineering, 2001*, 2:423432, August 2001.

[2] F. Espinoza, P. Persson, A. Sandin, H. Nyström, E. Cacciatore, and M. Bylund. Geonotes: Social and navigational aspects of location-based information systems. *Ubiquitous Computing International Conference: Ubicomp2001*, Springer 2201/2001:2–17, January 2001.

[3] L. G. Canton. *Emergency Management: Concepts and Strategies for Effective Programs.* Wiley-Interscience, January 2007.

[4] Federal Communications Commission. Guidelines for testing and verifying the accuracy of wireless E911 location systems. *FCC Reports and Carrier Data*, April 2000.

[5] A. Aloudat, K. Michael, and J. Yan. Location-based services in emergency management- from government to citizens: Global case studies. *Recent Advances in Security Technology*, Ed. P. Mendis, 1st Ed, September 2007. Available at: http://works.bepress.com/kmichael/14.

[6] ICT-217033 WHERE Project. Deliverable 3.1: Physical layer enhancements using localisation data, January 2009.

[7] ICT-217033 WHERE Project. Deliverable 1.1: Definition of the where framework and scenarios, March 2009.

[8] ICT-217033 WHERE Project. Deliverable 3.4: Location based optimisation for PHY algorithms/protocols, May 2010.

[9] S. Majhi, Y. Nasser, R. Raulefs, and A. Dammann. Geo-location aided cooperative communications. *Proceedings of WPNC Conference*, March 2010.

[10] C. Oestges and B. Clerckx. *MIMO Wireless Communications: From Real-world Propagation to Space-time Code Design.* Academic Press Inc, March 2007.

[11] L. Brunel, M. Plainchault, and N. Gresset. Inter-cell interference coordination and synchronization based on location information. *Proceedings of WPNC Conference*, March 2010.

[12] M. Hildebrand, G. Cristache, K. David, and F. Fechter. Location-based radio resource management in multi standard wireless network environments. *Proceedings of the IST Mobile and Wireless Communications Summit*, June 2002.

[13] S. K. Jayaweera. Virtual MIMO-based cooperative communications for energy-constraint wireless sensor networks. *IEEE Transactions on wireless communications*, 5(5):984–989, May 2006.

[14] ICT-217033 WHERE Project. Deliverable 3.5: Location based cross-layer optimisation for PHY/MAC, May 2010.

[15] Y. Zhang, Y. Ma, and R. Tafazolli. Power allocation for bidirectional AF relaying over rayleigh fading channels. *IEEE Communications Letters*, 14(2):145–147, 2010.

[16] J. J. Nielsen, T. K. Madsen, and H.-P. Schwefe. Location-based mobile relay selection and impact of inaccurate path loss model parameters. *Proceedings of IEEE Wireless Communications and Networking Conference*, pages 1–6, April 2010.

[17] ICT-217033 WHERE Project. Deliverable 3.6: Relaying and cooperative communications enhancements based on positioning data, May 2010.

[18] L. Doherty, L. E. Ghaoui, and K. Pister. Convex position estimation in wireless sensor networks. *Proceedings of IEEE INFOCOM 2001*, 3:1655–1663, 2001.

[19] P. Biswas and Y. Ye. Semidefinite programming for ad hoc wireless sensor network localization. *Proceedings of the 3rd international symposium on Information processing in sensor networks*, pages 46–54, 2004.

[20] C. Savarese, J. M. Rabaey, and J. Beutel. Locationing in distributed ad-hoc wireless sensor networks. *Proceedings of IEEE International Conference on Acoustics, Speech and Signal Processing*, 4:2037–2040, 2001.

[21] K. K. Chintalapudi, A. Dhariwal, R. Govindan, and G. Sukhatme. Ad-hoc localization using ranging and sectoring. *Proceedings of IEEE INFOCOM 2004*, 4: 2662–2672, 2004.

[22] E. D. Kaplan. *Understanding* GPS*: Principles and Applications.* Artech House Publishers, February 2006.

[23] J. J. Spilker. *Chapter 3:* GPS *Signal Structure and Theoretical Performance, From Global Positioning System: Theory and Applications, Volume I.* B. W. Parkinson and J. J. Spilker Editions, American Institute of Aeronautics and Astronautics, 1996.

[24] J. J. Caffery and G. L. Stuber. Overview of radiolocation in CDMA cellular systems. *IEEE Communications Magazine*, 36(4):38–45, April 1998.

[25] S. Gezici. A survey on wireless position estimation. *Wireless Personal Communications (Springer Netherlands)*, 44(3):263–282, February 2008.

[26] H. Liu, H. Darabi, P. Banerjee, and J. Liu. Survey of wireless indoor positioning techniques and systems. *IEEE Transactions on Systems, Man, and Cybernetics*, 37(6):10671080, November 2007.

[27] S. Gezici and H. V. Poor. Position estimation via ultra-wideband signals. *Proceedings of the IEEE (Special Issue on UWB Technology and Emerging Applications)*, 97(2):386–403, February 2008.

[28] T. Pavani, G. Costa, M. Mazzotti, D. Dardari, and A. Conti. Experimental results on indoor localization technique through wireless sensors network. *Proceedings of the IEEE Vehicular Technology Conference (VTC 2006-Spring)*, May 2006.

[29] F. Sottile and M. A. Spirito. Robust localization for wireless sensor networks. *Proceedings of the IEEE Conference on Sensor and Ad Hoc Communications and Networks (SECON)*, 1(1):5061, June 2008.

[30] J. Vidal and M. Nájar. Kalman tracking for mobile location in NLOS situations. *Proceedings of the IEEE Conference on Personal, Indoor and Mobile Radio Communications (PIMRC)*, 3:2203–2207, September 2003.

[31] M. Nájar, J. M. Huerta, J. Vidal, and J. A. Castro. Mobile location with bias tracking in non-line-of-sight. *Proceedings of the IEEE International Conference on Acoustics, Speech and Signal Processing*, 3:956959, May 2004.

[32] E.A. Wan and R. Van Der Merwe. The unscented Kalman filter for nonlinear estimation. *Proceedings of the IEEE Symposium on Adaptive Systems for Signal Processing, Communications, and Control*, page 956959, October 2000.

[33] N. Gordon, T. Clapp, S. Arulampalam, and S. Maskell. A tutorial on particle filters for on-line nonlinear/non-gaussian bayesian tracking. *IEEE Transactions on Signal Processing*, 50(2):174188, February 2002.

[34] N. Bergman, U. Forsell, J. Jansson, R. Karlsson, P. J. Nordlund, F. Gustafsson, and F. Gunnarsson. Particle filters for positioning, navigation and tracking. *IEEE Transactions on Signal Processing*, 50(2), February 2002.

[35] P. Rong and M. L. Sichitiu. Angle of arrival localization for wireless sensor networks. *Proceedings of 3rd Annual IEEE Communications Society on Sensor and Ad Hoc Communications and Networks*, 1:374–382, September 2006.

[36] E. Grosicki and K. Abed-Meraim. An efficient low-complexity method to mitigate the impact of some non line-of-sight errors in aoa measurements for mobile localization. *Proceedings of IEEE 5th Workshop on Signal Processing Advances in Wireless Communications*, pages 566–570, July 2004.

[37] Q. H. Spencer, B. D. Jeffs, M. A. Jensen, and A. L. Swindlehurst. Modeling the statistical time and angle of arrival characteristics of an indoor multipath channel. *IEEE Journal on Selected Areas in Communications*, 18(3):347–360, March 2000.

[38] K. Abed-Meraim. Mobile localization techniques. *Proceedings of IEEE International Conference on Signal Processing and Communications ICSPC*, pages xlvi–xlvii, November 2007.

[39] M. Triki, D. T. M. Slock, V. Rigal, and P. Francois. Mobile terminal positioning via power delay profile fingerprinting: Reproducible validation simulations. *Proceedings of the IEEE Vehicular Technology Conference (VTC-Fall 2006)*, pages 1–5, September 2006.

[40] F. Althaus, F. Troesch, and A. Wittneben. UWB geo-regioning in rich multipath environment. *Proceedings of the IEEE Vehicular Technology Conference (VTC-Fall 2005)*, 2(2):1001–1005, September 2005.

[41] H. Laitinen, S. Juurakko, T. Lahti, R. Korhonen, and J. Lahteenmaki. Experimental evaluation of location methods based on signal-strength measurements. *IEEE Transactions on Vehicular Technology*, 56(1):287–296, January 2007.

[42] T. Roos, P. Myllymaki, and H. Tirri. A statistical modeling approach to location estimation. *IEEE Transactions on Mobile Computing*, 1:59–69, January-March 2002.

[43] H. Laitinen, J. Lahteenmaki, and T. Nordstrom. Database correlation method for GSM location. *Proceedings of the IEEE Vehicular Technology Conference (VTC-Spring 2001)*, 4:2504–2508, May 2001.

[44] A.J. Weiss. On the accuracy of a cellular location system based on RSS measurements. *IEEE transactions on vehicular technology*, 52(6):1508–1518, 2003.

[45] B. Li, Y. Wang, H. K. Lee, A. G. Dempster, and C. Rizos. Method for yielding a database of location fingerprints in WLAN. *IEE proceedings on Communications*, 152(5):580–586, October 2005.

[46] M. Laaraiedh. Implementation of Kalman filter with python language. *Python Papers Journal*, 4, 2009.

[47] D. B. Jourdan, J. J. Jr. Deyst, M. Z. Win, and N. Roy. Monte carlo localization in dense multipath environments using UWB ranging. *IEE proceedings on Communications*, pages 314–319, September 2005.

[48] Z. Sahinoglu, S. Gezici, and I. Guvenc. *Ultra-Wideband Positioning Systems: Theoretical Limits, Ranging Algorithms, and Protocols*. Cambridge University Press, October 2008.

[49] F. Barceló, J. Paradells, E. Zola, F. Izquierdo, and M. Ciurana. Performance evaluation of a TOA-based trilateration method to locate terminals in WLAN. *Proceedings of International Symposium on Wireless Pervasive Computing*, pages 1–6, January 2006.

[50] J. Chaffee and J. Abel. GDOP and the cramer-rao bound. *Proceedings of IEEE Position Location and Navigation Symposium*, pages 663–668, April 2002.

[51] Y. Gwon, R. Jain, and T. Kawahara. Robust indoor location estimation of stationary and mobile users. *Proceedings of IEEE INFOCOM conference*, 2: 1032–1043, March 2004.

[52] D. B. Faria and D. R. Cheriton. No long-term secrets: Location-based security in over-provisioned wireless LANs. *Proceedings of ACM Conference*, November 2004.

[53] F. Anjum, S. Pandey, B. Kim, and P. Agrawal. Secure localization in sensor networks using transmission range variation. *Proceedings of IEEE International Conference on Mobile Ad-hoc and Sensor Systems*, pages 195–203, November 2005.

[54] S. Capkun and J. Hubaux. Secure positioning of wireless devices with application to sensor networks. *Proceedings of IEEE INFOCOM*, 3:1917–1928, 2005.

[55] P. Misra and P. Enge. *Global Positioning System. Signal Measurements and Performance*. Ganga-Jamuna Press, 2006.

[56] A. Michalski and J. Czajewski. The accuracy of the global positioning systems. *IEEE Instrumentation & Measurement Magazine*, 7(1):56–60, March 2004.

[57] J. Rife. GNSS solutions: WAAS functions and differential biases. *Inside GNSS GNSS Solutions*, page 1822, May-June 2008.

[58] P. Kemmpi. Next generation satellite navigation systems. *VTT research notes 2408, VTT Technical Research Centre of Finland*, 2007. Available at: http://www.vtt.fi/inf/pdf/tiedotteet/2007/T2408.pdf.

[59] M. O. Kanli. Limitations of pseudolite systems using off-the-shelf GPS receivers. *Journal of Global Positioning Systems*, 3:154166, December 2004.

[60] B. A. Stein and W. L. Tsang. Pseudolite-aided GPS: a comparison. *PLANS '88 - IEEE Position Location and Navigation Symposium*, pages 329–333, December 1988.

[61] S. Riley, N. Talbot, and G. Kirk. A new system for RTK performance evaluation. *IEEE Position Location and Navigation Symposium*, pages 231–236, March 2000.

[62] L. Wanninger. Introduction to network RTK. *IAG Working Group 4.5.1: Network RTK, 2004*, June 2008. Available at: http://www.network-rtk.info/intro/introduction.html.

[63] R. Taylor and J. Sennott. Navigation system and method, May 1981. US Patent 4445118.

[64] G. M. Djuknic and R.E. Richton. Geolocation and assisted GPS. *IEEE Computer Society Press*, 34(2):123–125, February 2001.

[65] European Commission Galileo Website. Galileo: Applications, December 2009. Available at: http://ec.europa.eu/transport/galileo/applications/applications_en.htm.

[66] J. Benedicto, S. E. Dinwiddy, G. Gatti, R. Lucas, and M. Lugert. Technical overview of Galileo. November 2000. Available at: http://esamultimedia.esa.int/docs/galileo_world_paper_Dec_2000.pdf.

[67] Russian Space Agency Glonass Website, December 2009. Available at: http://www.glonass-ianc.rsa.ru.

[68] M. L. Tsai, Y. S. Huang, K. W. Chiang, and M. Yang. The impact of Compass/BeiDou-2 on future GNSS: A perspective from Asia. *Proceedings of 4th Asian Space Conference*, October 2008.

[69] G. M. Nair. Satellites for navigation. *Press Information Bureau Government of India Bangalore*, August 2006.

[70] First IRNSS satellite by December. *Asian Surveying and Mapping*, May 2009.

[71] Qzss in 2010. A*sian Surveying and Mapping*, May 2009.

[72] J. H. Reed, K. J. Krizman, B. D. Woerner, and T. S. Rappaport. An overview of the challenges and progress in meeting the E-911 requirement for location services. *IEEE Communication Magazine*, 36(4):3037, April 1998.

[73] F. Viquez, A. L. Dragon, and T. Archdeacon. Location based services, a strategic analysis of wireless technologies, markets, and trends. *Technical report, Allied Business Intelligence, 1Q*, 2001.

[74] P. C. Mason, J. M. Cullen, and N. C. Lobley. UMTS architectures. *IEE Colloquium on Mobile Communications Towards the Next Millenium and Beyond*, pages 4/1–411, May 1996.

[75] M. Aatique. Evaluation of TDOA techniques for position location in CDMA systems. *PhD thesis, Falculty of the Virginia Polytechnic Institute and State University*, September 1997.

[76] G. Shen, R. Zetik, and R.S. Thomä. Performance comparison of TOA and TDOA based location estimation algorithms in LOS environment. *Proceedings of the 5th Workshop on Positioning, Navigation and Communication: WPNC'08*, pages 71–78, March 2008.

[77] Aeroscout website. Aeroscout MobileView data sheet. 2010. Available at: http://www.aeroscout.com/content/mobileview.

[78] Ekahau website. Ekahau EPE data sheet. 2010. Available at: http://www.ekahau.com/products/real-time-location-system/overview.html.

[79] Navizon technical paper: Bringing WiFi and cellular positioning to mobile devices and to the web. *Technical White Paper*, July 2007. Available at: http://www.navizon.com.

[80] Wi-Fi positioning system: Accuracy, availability, and time to fix performance. *Technical White Paper*, 2008. Available at: http://www.skyhookwireless.com.

[81] S. Roy, J. R. Foerster, V. S. Somayazulu, and D. G. Leeper. Ultrawideband radio design: the promise of high-speed, short-range wireless connectivity. *Proceedings of the IEEE*, 92(2):295–311, February 2004.

[82] A. F. Molisch, P. Orlik, Z. Sahinoglu, and J. Zhang. UWB-based sensor networks and the IEEE 802.15.4a standard - a tutorial. *Proceedings of the IEEE First International Conference on Communications and Networking ChinaCom'06*, pages 1–6, October 2006.

[83] S. Gezici, Z. Tian, G. B. Giannakis, H. Kobayashi, A. F. Molisch, H. V. Poor, and Z. Sahinoglu. Localization via ultra-wideband radios: a look at positioning aspects for future sensor networks. *IEEE Signal Processing Magazine*, 22(4): 70–84, 2005.

[84] Y. C. Liang, S. Sun, X. Peng, and F. Chin. Emerging wireless standards for WRAN, WiFi, WiMedia and ZigBee- Tutorial 2. *Proceedings of the 10th IEEE Singapore International Conference on Communication systems, ICCS 2006*, pages 27–29, October 2006.

[85] R. Verdone, D. Dardari, G. Mazzini, and A. Conti. *Wireless Sensor and Actuator Networks: Technologies, Analysis and Design*. Academic Press, January 2008.

[86] IEEE P802.15.4a/D4 (Amendment of IEEE Std 802.15.4). Part 15.4: Wireless medium access control (MAC) and physical layer (PHY) specifications for low-rate wireless personal area networks (LRWPANs). July 2006.

[87] M. Maroti, P. Völgyesi, S. Dora, B. Kusy, A. Nadas, A. Ledeczi, G. Balogh, and K. Molnar. Radio interferometric geolocation. *Proceedings of the ACM Conference on Embedded Networked Sensor Systems*, pages 1–12, November 2005.

[88] B. Didier and T. Rahim. Beyond 3G/4G radioaccess technologies (RATs)and standards roadmaps. *eMobility Technology Platform, White Paper*, December 2007.

[89] C. Mannweiler, R. Raulefs, J. Schneider, B. Denis, A. Klein, B. Uguen, M. Laaraiedh, and H. Schotten. A robust management platform for multi-sensor location data interpretation. *Proceedings of ICT mobile summit*, June 2010.

[90] W. G. Figel, N. H. Shepherd, and W. F. Trammel. Vehicle location by a signal attenuation method. *IEEE Transactions on Vehicular Technology*, 18:245–251, November 1969.

[91] T. S. Rappaport. *Wireless Communications: Principles and practice*. Prentice Hall, January 2002.

[92] M. Z. Win and R. A. Scholtz. Impluse radio: How it works. *IEEE Communications Letters*, 2(2):36–38, February 1998.

[93] Z. Sahinoglu and S. Gezici. Ranging in the IEEE 802.15.4a standard. *Proceedings of IEEE Wireless and Microwave Technology Conference (WAMICON)*, December 2006.

[94] D. Dardari, C. C. Chong, and M. Z. Win. Analysis of threshold-based TOA estimators in UWB channels. *Proceedings of 14th European Signal Processing Conference (EUSIPCO '06)*, September 2006.

[95] C. Mazzucco, U. Spagnolini, and G. Mulas. A ranging technique for UWB indoor channel based on power delay profile analysis. *Proceedings of IEEE Vehicular Technology Conference VTC 2004-Spring*, 5:2595–2599, May 2004.

[96] C. Falsi, D. Dardari, L. Mucchi, and M. Z. Win. Time of arrival estimation for UWB localizers in realistic environments. *EURASIP Journal on Applied Signal Processing*, 2006, 2006.

[97] I. Guvenc and Z. Sahinoglu. Threshold-based TOA estimation for impulse radio UWB systems. *Proceedings of IEEE International Conference on Ultra-Wideband (ICU05)*, pages 420–425, September 2005.

[98] D. Dardari, A. Conti, U. Ferner, A. Giorgetti, and M. Z. Win. Ranging with ultrawide bandwidth signals in multipath environments. *Proceedings of the IEEE*, 97(2):404–426, February 2009.

[99] J. Lee and R.A. Scholtz. Ranging in a dense multipath environment using an UWB radio link. *IEEE Journal on Selected Areas in Communications*, 20(9): 1677–1683, December 2002.

[100] J. Caffery. *Wireless Location in* CDMA *Cellular Radio Systems*. Springer, October 1999.

[101] M. Ylianttila, X. Li, K. Pahlavan, and M. Latva-aho. Comparison of indoor geolocation methods in DSSS and OFDM wireless LAN systems. *Proceedings of IEEE VTS-Fall VTC 2000*, 6:30153020, September 2000.

[102] B. Yan, L. Xiao-chun, X. Jing-song, and W. Jin. Research on uwb indoor positioning based on TDOA technique. *Proceedings of IEEE International Conference on Electronic Measurement & Instruments (ICEMI'09)*, pages 167–170, August 2009.

[103] ICT-217033 WHERE Project. Deliverable 4.1: Measurements of location-dependent channel features, October 2008.

[104] J. Keignart, C. Abou Rjeily, N. Daniele, and C. Delaveaud. UWB SIMO channel measurements and simulations. *IEEE Transactions on Microwave Theory and Techniques, Special Issue on Ultra-Wideband*, 54(4):1812–1819, April 2006.

[105] B. Denis and J. Keignart. Post-processing framework for enhanced UWB channel modeling from band-limited measurements. *Proceedings of IEEE UWBST Conference, Reston, VA*, pages 260–264, November 2003.

[106] A. Goldsmith. *Wireless Communications*. Cambridge University Press, August 2005.

[107] V. Abhayawardhana, W. Crosby, M. Sellars, and M. Brown. Comparison of empirical propagation path loss models for fixed wireless access systems. *Proceedings of IEEE Vehicular Technology Conference, VTC 2005 spring*, 1:73–77, 2005.

[108] M. Van Hauwermeiren and D. Vose. *A Compendium of Distributions [ebook]*. Vose Software, Ghent, Belgium, 2009. Available from www.vosesoftware.com. Accessed 27/04/2010.

[109] M. Laaraiedh, S. Avrillon, and B. Uguen. Enhancing positioning accuracy through RSS based ranging and weighted least square approximation. *Proceedings of POCA conference*, June 2009.

[110] S. Boyd and L. Vandenberghe. *Convex Optimization*. Cambridge University press, 2009.

[111] Y. Bar-Shalom and X. R. Li. *Estimation and Tracking:: Principles, Techniques, and Software*. Ybs Publishing, Ringbound edition, February 1998.

[112] M. Laaraiedh, S. Avrillon, and B. Uguen. Hybrid data fusion techniques for localization in UWB networks. *Proceedings of WPNC09*, pages 51–57, March 2009.

[113] S. Van Huffel and P. Lemmerling. *Total Least Squares and Errors-in-Variables Modeling: Analysis, Algorithms and Applications*. Springer, February 2002.

[114] L. N. Trefethen and D. Bau III. *Numerical Linear Algebra*. SIAM: Society for Industrial and Applied Mathematics, June 1997.

[115] M. Laaraiedh, S. Avrillon, and B. Uguen. Overcoming singularities in TDoA based location estimation using total least square. *Proceedings of the International Conference on Signals, Circuits and Systems (SCS09)*, pages 1–4, November 2009.

[116] M. Laaraiedh, S. Avrillon, and B. Uguen. Enhancing positioning accuracy through direct position estimators based on hybrid RSS data fusion. *Proceedings of VTC spring 2009*, pages 1–5, April 2009.

[117] M. Laaraiedh, S. Avrillon, and B. Uguen. A maximum likelihood TOA based estimator for localization in heterogeneous networks. *International Journal on Communication, Network and System Sciences (IJCNS)*, 3(1):38–42, January 2010.

[118] L. Vandenberghe and S. Boyd. Semidefinite programming. *SIAM Rev*, 38(1): 49–95, March 1996.

[119] N. D. Sidiropoulos and L. Zhi-Quan. A semidefinite relaxation approach to MIMO detection for high-order QAM constellations. *IEEE signal processing letters*, 13(9):525–528, September 2006.

[120] C. Meng, Z. Ding, and S. Dasgupta. A semidefinite programming approach to source localization in wireless sensor networks. *IEEE signal processing letters*, 15:253–256, September 2008.

[121] K. Yang, G. Wang, and Z. Q. Luo. Efficient convex relaxation methods for robust target localization by a sensor network using time differences of arrivals. *IEEE transactions on signal processing*, 57(7):2775–2784, July 2009.

[122] M. Steven. *Fundamentals of Statistical Signal Processing: Estimation Theory*. Prentice-Hall, May 1993.

[123] J. Shao. *Mathematical Statistics, 2nd edition*. Springer, October 2007.

[124] G. Frenkel. Geometric dilution of position (GDOP) in position determination through radio signals. *Proceedings of the IEEE*, 61(4):496–497, April 1973.

[125] R. A. Novelline and L. F. Squire. *Squire's fundamentals of radiology*. Cambridge, Mass. : Harvard University Press, 1997.

[126] A. S. Glassner. Space subdivision for fast ray tracing. *Proceedings of IEEE Computer Graphics and Applications*, 4:15–22, October 1984.

[127] R. Hartshorne. *Geometry:* E*uclid and Beyond*. Springer, June 2000.

[128] C. D. Ghilani and P. R. Wolf. *Elementary Surveying: An Introduction to Geomatics*. Prentice Hall, 11th Edition, May 2005.

[129] L. Jaulin, M. Kieffer, O.Didrit, and E. Walter. *Applied interval analysis*. Springer Verlag, September 2001.

[130] L. Jaulin and E. Walter. Set inversion via interval analysis for nonlinear bounded-error estimation. *Automatica (Journal of IFAC)*, 29(4):1053–1064, July 1993.

[131] V. Drevelle and P. Bonnifait. High integrity GNSS location zone characterization using interval analysis. *Proceedings of ION GNSS 2009*, pages 2178–2187, 2009.

Abstract Recent advancement in wireless networks and systems has seen the rise of localization techniques as a worthwhile and cost-effective basis for novel services. These location based services have been more and more beneficial and money-making for telecommunications operators and companies. Various LBSs can be offered to the user such as tracking, advertisement, security, and management. Wireless networks themselves may benefit from localization information to enhance the performances of the different network layers. Location based routing, synchronization, interference cancellation are some examples of fields where location information can be fruitful. Two main tasks a localization system must be able to do: measurement of location-dependent parameters (RSSI, TOA, and TDOA) and estimation of position using location estimation techniques. The main goal of this dissertation is the study of different location estimation techniques: algebraic and geometric. Studied algebraic techniques are least-squares, maximum likelihood, and semidefinite programming. The proposed geometric technique RGPA is based on interval analysis and geometric representation of location-dependent parameters. The focus is put on the fusion of different location-dependent parameters on the positioning accuracy. Estimation and measurement of location-dependent parameters are also investigated using a provided UWB measurements campaign in order to have a complete understanding of localization field.

Résumé Les avancements récents dans les technologies sans fil ont vu l'émergence de techniques de localisation qui constitue une base utile et rentable pour offrir des nouveaux services. Ces services topo-dépendants ont été de plus en plus bénéfiques pour les opérateurs et les entreprises de télécommunications. Divers services topo-dépendants peuvent être offerts à l'utilisateur tels que le suivi, la publicité, la sécurité, et la gestion. Les réseaux sans fil eux-mêmes peuvent bénéficier de l'information de localisation pour améliorer les performances de leurs différentes couches. Le routage, la synchronisation et l'annulation d'interférences sont quelques exemples où l'information de localisation peut être fructueuse. Un système de localisation doit être capable d'exécuter deux tâches principales : la mesure des paramètres topo-dépendants (RSSI, TOA, et TDOA) et l'estimation de la position en utilisant des estimateurs appropriés. L'objectif principal de cette thèse est l'étude de différentes techniques d'estimation de la position: algébriques et géométriques. Les techniques algébriques étudiées sont les moindres carrés, le maximum de vraisemblance, et la programmation semi-définie. La technique géométrique RGPA proposée est basée sur l'analyse par intervalles et la représentation géométrique des paramètres topo-dépendants. L'accent est mis sur la fusion de différents paramètres topo-dépendants et son influence sur la précision de positionnement. L'estimation et la mesure des paramètres topo-dépendants sont également étudiées en utilisant une campagne de mesures ULB afin d'avoir une compréhension complète du domaine de localisation.

Keywords Localization, Wireless Networks, Hybrid Data Fusion, Location Dependent Parameters, Cramer Rao Lower Bound.